UNIVERSITÉ DE MONTRÉAL

ERBIUM-YTTERBIUM CO-DOPPED ION-EXCHANGED WAVEGUIDE AMPLIFIERS

Peyman MESHKINFAM

DÉPARTEMENT DE GÉNIE PHYSIQUE ET
DE GÉNIE DES MATÉRIAUX

ÉCOLE POLYTECHNIQUE DE MONTRÉAL

MÉMOIRE PRÉSENTÉ EN VUE DE L'OBTENTION

DU DIPLÔME DE MAÎTRISE ÈS SCIENCES APPLIQUÉES

(GÉNIE PHYSIQUE)

NOVEMBER 1998

UNIVERSITÉ DE MONTRÉAL

ÉCOLE POLYTECHNIQUE DE MONTRÉAL

Ce mémoire intitulé:

ERBIUM-YTTERBIUM CO-DOPPED ION-EXCHANGED WAVEGUIDE AMPLIFIERS

Présenté par: MESHKINFAM Peyman

En vue de l'obtention du diplôme de: Maîtrise ès scienses appliquées

a été dûment accepté par le jury d'examen consisté de:

M. WU, KE, Ph.D., président et membre

M. NAJAFI, S. Iraj, Ph.D., membre et directeur de recherche

M. MARTINU, L, Ph.D., membre

Dedicated to My mother Parvin Azimzadeh
And my father Gholamali Meshkinfam

Acknowledgement

I would like to express my sincere gratitude to my research director Professor S.I. Najafi whose guidance and continuous support helped me enormously in carrying out my research works.

I would like to extend my special thanks to Dr. Mark P. Andrews and the chemistry department of McGill University who helped me through the process of fabrication. I also owe my gratitude to Dr Taher Touam, Dr Alireza Shooshtari and Dr Philippe Fournier and members of Photonics Research Group who always shared their experiences and knowledge in times of need.

My special thanks go to Kalai Saravanamutto and Shahram Alavian and Mandana Shadpour who kindly proof –read this thesis in a short period of time.

Finally, I gratefully acknowledge the support of my family in IRAN without which I would not have been able to study at Ecole Polytechnique de Montreal.

Résumé

Des guides d'onde amplificateurs optiques sont fabriqués sur des verres de phosphate, fortement co-dopés avec de l'erbium et l'ytterbium. Ceci est accompli à travers un processus d'échange ionique entre une matrice de verre et un sel de nitrate de potassium.

Dans la première partie, des guides d'onde plans sont fabriqués afin d' étudier la possibilité d'échange ionique dans le substrat. La profondeur de la diffusion relative au temps de l'échange ionique et le changement maximal de l'indice de réfraction sont calculés en utilisant le couplage par prisme

Dans la deuxième partie, la possibilité de fabriquer des guides d'ondes canaux droits est démontrée. La fabrication est faite par photolithographie en utilisant l'aluminium comme masque et l'échange ionique comme technique d'écriture. Un processus particulier a été développé pour minimiser la contamination due à l'humidité pendant la fabrication

L'excitation des ions dopant d'erbium à un niveau d'énergie plus élevé, métastable, mène à l'émission spontanée amplifiée (ESA) ainsi qu'à l'émission stimulée. La troisième partie de ce travail consiste en une caractérisation des guides d'onde en ce qui concerne leurs propriétés d'amplification d'un signal optique dans la gamme des longueurs d'onde de télécommunication autour de 1.55 μm. Les longueurs d'onde de pompage appropriées ont été choisies à partir des spectres d'absorption du verre dopé.

Plusieurs montages expérimentaux ont été conçus pour mesurer le profile de

mode de sortie et calculer les pertes, l'ESA ainsi que le gain du signal. Le pompage a été réalisé avec un laser ajustable qui émet à une longueur d'onde centrale de 980 nm. La source du signal à 1.55 μm était un amplificateur ajustable dopé avec de l'erbium (EDFA). Les pertes mesurées comprennent les pertes de couplage et les pertes de propagation. Le gain interne de l'amplificateur, défini comme étant le rapport de la puissance du sortie avec pompage sur la puissance du signal de sortie sans pompage, a été mesuré. Le gain a été déterminé pour les guides d'onde fabriqués sur des verres phosphatés, co-dopé à l'ytterbium, avec des concentrations d'Erbium de 1.65, 2.22 et 2.75% et une concentration d'ytterbium de 22% (en poids). La variation du gain avec la longueur d'onde du signal et la longueur d'onde du pompage, et la puissance de pompage ont été étudiées et des façons possibles pour améliorer l'amplification sont proposées.

Abstract

Optical waveguide amplifiers were fabricated on erbium and ytterbium co-doped phosphate glasses. This was achieved through ion-exchange processes between the glass matrix and potassium nitrate salt.

Initially a slab waveguide fabricated to determine the possibility of ion exchange in the substrate. The diffusion depth relative to the time of the ion exchange and the maximum refractive index change were also calculated using prism coupling.

As the first objective, possibility for the fabrication of straight channel waveguide was proven. The fabrication was done through photolithography using aluminum as mask and thermal ion exchange as the method. A process was developed to minimize moisture contamination during fabrication.

Excitation of the erbium dopants to a higher energy state, metastable, leads to amplified spontaneous emission (ASE) as well as stimulated emission. The second objective of this thesis was to characterize the waveguides with respect to their optical signal amplification properties at the telecommunications window of 1550 nm. Appropriate pump wavelengths were chosen by acquiring the absorption spectra of the doped glass.

Various experimental set-ups were designed to view the output mode profiles of the waveguides, calculate the loss, ASE as well signal gain. The pump was a tunable laser emitting at a central wavelength of 980nm. The 1550 nm signal source was also a tunable Erbium Doped Fiber Amplifier (EDFA). The measured losses took into account

contributions from coupling and propagation losses. The internal gain of the amplifier defined as the ratio of the output signal power with pump to the output signal power without pump was measured. The gain was determined for waveguides fabricated on erbium ytterbium co-doped, phosphate glasses with erbium concentrations of 1.65, 2.22 and 2.75 % and ytterbium concentration of 22 % (by weight). Gain variation with signal and pump wavelength and power was investigated and possible ways to improve amplification are proposed.

Condensé en français

L'optique intégrée (terme initialement proposé par S.E Miller en 1969) est basée fondamentalement sur le fait que la lumière peut être guidée par des couches minces de matériaux optiques. En utilisant de telle couches mince planaires, on peut fabriquer des dispositifs optiques capables de produire une large gamme d'opération un seul substrat.. Ces composantes étant compactes, leur intégration peut mener à une miniaturisation extrêmement efficace des circuits optiques avec des puissances de fonctionnement très faibles. Récemment, un de ces dispositifs photoniques, les guides d'onde amplificateurs en verre dopé avec du Er^{3+}, ont attiré considérablement l'attention des chercheurs car ils pourraient réduire le coût et la dimension des amplificateurs à 1.55μm et peuvent facilement être intégrés avec d'autres dispositifs photoniques.

Le verre est souvent le substrat de choix pour la fabrication de composantes optiques passives et actives, notamment les amplificateurs optiques dopés avec de l'erbium.

La transparence du verre dans les régions spectrales du visible et du proche infrarouge, et son indice de réfraction (1.48) permettent un couplage efficace avec les systèmes existants sur les fibres optiques. Le verre est aussi connu comme étant un milieu inerte proprio à l'accueil d'ions de terre rare ayant un seuil de résistance élevé au dommage optique.

Les ions de terre rare sont employés dans les applications optiques dû à leurs états métastables excités dans la gamme entière de fréquences optiques. Leur spectre

d'absorption révèle des longueurs d'onde possibles de pompage et donc la possibilité d'excitation à des niveaux d'énergie plus élevés. La relaxation subséquente au niveau non-excité peut survenir non-radiativement ou radiativement en impliquant l'émission de photon spontanée ou stimulée. L'émission stimulée est souhaitée pour l'amplification du signal.

L'échange ionique et l'implantation d'ions sont les deux techniques les plus utilisées pour fabriquer des structures à guide d'onde sur un substrat de verre dopé avec des éléments de terre rare. La déposition avec l'hydrolyse de flamme la pulvérisation radio-fréquentielle (RF), le procédé sol-gel et les guides d'onde composites comptant parmi les autres méthodes utilisées pour produire des couches dopées avec des éléments de terre rare.

Une alternative intéressante pour la fabrication de guides d'onde dopés avec des éléments de terre rare est l'échange ionique du potassium dans des verres de phosphate dopés à l'erbium. L'échange ionique donne lieu à un changement de la composition à la surface du verre dû à une diffusion massique induite par des gradients thermiques ou des gradients de champs électriques, ou une combinaison des deux. Ces changements de composition amènent une augmentation de l'indice de réfraction du matériau dans une région restreinte et donc à un guide d'onde à géométrie convenable. Cette géométrie peut être définie en utilisant un masque. Le processus d'échange ionique n'affecte pas la structure de base du verre et il ne peut modifier la concentration de dopant d'erbium ou ytterbium. Ce processus se fait à des températures moins élevées que le point de

transformation du verre.

La grande section efficace d'émission et les faibles interactions entre ions de terre rare permettent l'incorporation de concentrations élevées d'erbium d'être incorporées dans des verres de phosphate. L'efficacité du pompage peut être améliorée en introduisant des ions d'ytterbium (Yb^{3+}) dans le milieu hôte . L'énergie des ions excités d'yterbium est transférée aux ions Erbium adjacents. Une concentration très élevée d'Er et une haute densité de puissance de pompage sont nécessaires dans le cas de guides plans amplificateurs afin d'obtenir des gains suffisants d'amplification optique, car la distance d'interaction optique est plus courte. Cependant, pour des concentrations élevées d'erbium, la luminescence de l'erbium sera contrée par le processus de transfert d'énergie dû aux interactions entre ions. Avec une concentration élevée d'Er dans le guide d'onde, le transfert d'énergie d'un ion excité Er^{3+} à un ion adjacent au niveau fondamental est possible à travers une interaction entre les ions, ce processus qui peut se poursuivre jusqu'au transfert d'énergie à un ion d'Er^{3+} jumelé à un défaut ou un ion d'impureté, causant une perte d'énergie par évanescence non radiative.

En outre, un autre processus («cooperative upconversion») domine le processus d'amplification des dispositifs lorsqu'une puissance très élevée de pompage est appliquée. À des concentrations élevées d'Er^{3+}, et donc à de fortes inversions de population, un ion Er^{3+} excité peut transférer son énergie à un ion Er^{3+} excité adjacent. Par conséquent, l'ion donneur subit une transition vers son niveau fondamental non radiativement, tandis que l'ion accepteur est excité à un niveau plus élevé. par conséquent, la population de l'état

supérieur de «lasage» et l'efficacité d'amplification de la lumière à 1550 nm par l'émission stimulée sont réduites considérablement. Ce processus de répression («quenching») d'«upconversion» dépend fortement de l'hôte. Un choix approprié de la matrice hôte est crucial pour la fabrication des guides d'onde amplificateurs. Les deux mécanismes décrits de répression de luminescence influent sur l'efficacité d'amplification; donc une combinaison convenable de concentration des dopants de la longueur du guide d'onde et de le puissance de pompage est nécessaire afin d'optimiser la performance des guides d'onde amplificateurs dopés à l'erbium.

Dans cette étude, nous avons choisi le verre phosphaté fortement dopé à l'ytterbium et à l'erbium comme substrat pour la fabrication des guides d'onde canal amplificateurs par échange ionique.

Afin de fabriquer l'amplificateur optique, trois matrices différentes de verre ont été choisies comme substrat. Ces verres qui sont commercialement disponibles, possèdent la même structure de base et contiennent 22% (en poids) d'ytterbium et différentes concentrations d'erbium :1.65,2.22 et 2.75% (en poids). Un des avantages particulier du verre de base sélectionné est sa capacité à contenir de hautes concentrations de Yb_2O_3. La concentration d'ions d'Yb^{3+} dans ce verre de base était de $1.9 \times 10^{+21}$ ions/cc . Les mesures montrent bien qu'une augmentation de la concentration d'Yb^{3+} mène à une augmentation de l'absorption d'énergie de pompage et au transfert d'énergie non radiative d'Yb^{3+} à Er^{3+}, améliorant l'efficacité du laser d'Er^{3+}; mais les concentrations d'ion Yb^{3+} supérieures à $1.9 \times 10^{+21}$ ions/cc causent une baisse de l'efficacité due au transfert de retour d'Er^{3+} ($^4I_{11/2}$-

$^4I_{15/2}$) à Yb^{3+} ($^2F_{7/2}$-$^2F_{5/2}$) et au pompage non homogène. L'utilisation de différentes concentrations d'erbium nous pousse à choisir la meilleure longueur du guide d'onde ainsi que la meilleure puissance de pompage pour obtenir le gain le plus élevé .

Initialement, un guide d'onde planaire a été fabriqué pour étudier la possibilité d'échange ionique dans ce matériau et déterminer les paramètres fondamentaux du guide d'onde. La profondeur de diffusion dans guide d'onde était de 6μm et le changement maximal d'indice de réfraction était de 0.0065 après 5 heures d'échange ionique au contact de nitrate de potassium à 400°C. Ces paramètres ont été obtenus par la technique du couplage par prisme à 632.8nm. Ces mêmes paramètres sont utilisés pour concevoir un guide d'onde canal monomode à longueur d'onde de 1550 nm. Le design a été fait en utilisant le logiciel Optonex©.

Des anions d'hydroxyl sont présents dans le sel du nitrate de potassium même à des températures élevées (jusqu'à 400 °C). Le groupement OH non seulement contribue aux pertes à 1550 nm mais attaque aussi le verre phosphaté et endommage sa surface. Pour réduire la contamination due à l'humidité, le sel a été préchauffé à 280 °C pendant 24 heures dans un récipient en forme de bateau. Un vide modéré a été appliqué afin d'accélérer l'évaporation de l'humidité. La température a été augmentée à 400 °C pendant une heure pour faire fondre le sel. Finalement, les échantillons ont été placés dans le bain de sel fondu pendant 5 heures. Il est à noter que cette température est bien en dessous de la température de la transformation (450°C) du verre.

La fabrication de guides d'onde canal par échange ionique exige l'utilisation de la

photolithographie. Pour ce faire, une couche de 1000 A° d'aluminium a été déposée sur l'échantillon comme masque; ensuite, une couche mince de photorésine a été déposée avec une tournette sur le substrat. L'échantillon a été irradié avec de la lumière UV à travers un masque définissant les dimensions désirées du guide d'onde. Le développement de la photorésine a été suivi en gravant les régions exposées sur l'aluminium. Les canaux fabriqués avaient une longueur de 2.5 cm et des largeurs variant de 2 à 10 mm. L'acidité de la solution de gravure a été attentivement sélectionnée en considérant la réactivité du verre hôte envers avec les acides. Ensuite, les échantillons ont été placés dans un four pour l'étape d'échange ionique. La gravure de l'aluminium par les acides donne lieu à des réactions fortes et rapides avec le verre; par conséquent, le masque d'aluminium a été enlevé par polissage en utilisant une pâte de diamant avec des germes de 0.03 μm. Le canal de 6μm a été choisi pour la caractérisation optique à 1550 nm (voir le chapitre 3). Les pertes ont été mesurées en utilisant la technique de couplage avec une fibre optique. Les pertes de couplage mesurées pour les canaux étaient de 5 dB à chaque extrémité. Les pertes de propagation étaient faibles, de l'ordre de 0.1 dB. Les pertes par absorption, qui dépendent principalement de la concentration d'erbium, étaient respectivement de 0.4, 0.5 et 0.6 dB par mm pour les concentrations d'erbium de 1.65%, 2.22% et 2.75% (en poids). Le gain de l'amplificateur a été mesuré en considérant le gain interne défini comme le rapport de la puissance du signal avec et sans pompage

Le spectre d'absorption du verre (700nm-1600nm) a été obtenu à l'aide d'un spectromètre. Comme il est décrit dans le chapitre 4, la haute densité optique dans la

région de 800 -1000 nm peut être attribuée aux ions d'ytterbium, alors que la bande à 1550 nm est due à l'excitation électronique des ions d'erbium. La caractérisation des guides d'onde a été faite par couplage direct avec une fibre. Les échantillons ont été pompés en utilisant source laser émettant à 980nm et l'émission spontanée amplifiée (l'ESA) est mesurée avec un Analyseur Optique de Spectre (AOS). Les mesures du gain ont été faites en combinant la longueur d'onde de la source à 1550nm avec la longueur d'onde de pompage à 980nm en utilisant un multiplexeur et en dirigeant le faisceau à travers une fibre optique dans le guide onde. La longueur d'onde, la puissance du signal et du pompage ont été variées pour montrer leurs effets sur le gain. Les résultats présentés montrent la possibilité de fabriquer des guides d'onde de 6 mm de longueur avec une concentration de 1.65% (en poids) d'erbium donnant un gain interne de 4.5 dB en utilisant une puissance de pompage de 60mW. La caractérisation d'autres verres a aussi révélé la possibilité d'avoir des gains plus élevés en optimisant la puissance de pompage et la longueur du guide d'onde à partir des concentrations d'ytterbium et d'erbium. Les méthodes d'augmentation de gain de l'amplificateur comprennent un recouvrement plus efficace entre les profils de modes du signal et du pompage. Une couche sol-gel déposée sur la surface du dispositif permet un meilleur confinement des modes des guides, ce qui mène à l'excitation efficace des ions d'erbium et par conséquent à l'émission stimulée. «Pigtailing» du dispositif nous permet de réduire les pertes de couplage et d'avoir un gain plus élevé pour des longueurs plus grandes. La possibilité de fabriquer des lasers peut être étudiée en utilisant des réseaux de Bragg aux deux extrémités du guide.

Table of contents

PAGE

LIST OF FIGURES

PAGE

LIST OF TABLES

PAGE

Table 4.1 Loss measurement for different samples

LIST OF APPENDIXES

PAGE

Preview

The first chapter of this thesis gives an introduction to the concept of rare-earth-doped waveguide amplifiers, particularly doped with erbium. It also includes an overview of different fabrication process and advances on this topic. The second chapter is a theoretical reminder of the erbium-doped devices explaining energy transfers possible and interaction between ions including upconversion and cross relaxation. It also discusses the effect of ytterbium on the gain due to the above mentioned reactions. The third chapter explains the waveguide fabrication process which is based on the potassium ion exchange on highly erbium-ytterbium-doped phosphate glass. It covers the fabrication of slab waveguide and following that straight channel waveguide fabrication using photolithography to define opening and ion exchange to make the waveguides. In the fourth chapter the characterization is explained. It includes absorption measurement, viewing mode profile, loss measurement and finally gain measurements versus pump and signal power and wavelength. Finally the results and future work are discussed.

The original contribution of this thesis is the fabrication and characterization of the erbium-ytterbium co-doped waveguide amplifiers. A fabrication process was developed to make potassium ion-exchanged waveguides in erbium-ytterbium co-doped phosphate glasses. Integrated optics waveguide amplifiers with different erbium and ytterbium concentrations were successfully produced and characterized.

The author has also contributed to the simulation and theoretical study of erbium-ytterbium co-doped integrated optics amplifiers. This work which was carried out in

Photonics Research Group at Ecole Polytechnique investigated the effect of the ion-ion interactions and the prediction of gain for glass waveguide amplifiers and lasers.

This work has contributed to the following paper which was presented at the SPIE photonics west 97 symposium and published in Electronics Letters journal:

- P. Meshkinfam, P.Fournier, M.A. Fardad, M.P. Andrews and S.I. Najafi "Potassium ion-exchanged Er/Yb doped phosphate glass amplifier "Electronics Letters Vol. 33 No.4 pp. 293-295. 1997
- A. Shooshtari, P. Meshkinfam, T. Touam, M. P. Andrews and S. I. Najafi «Ion exchanged Er/Yb phosphate glass waveguide amplifiers and lasers,» J. Optical Eng. April 98 Vol. 37 No 4 pp. 1188-1192.

Author has also contributed to the following paper:

- M.A. Fardad, T. Touam, P.Meshkinfam, R.Sara,, X.M.Du, M.P. Andrews and S.I. Najafi «UV-light imprinted Bragg grating in sol-gel ridge glass waveguide with almost 100% reflectivity» Electronic Letters 5th June 1997 Vol. 33 No.12 pp.1069-1070.

Chapter 1

Introduction to Erbium doped wavegudie amplifiers

1-1 The evolution of optical amplifiers

The concept of Optical communication was introduced only 25 years ago when it became possible to reduce the attenuation in silica glass to a few decibels per kilometer. Since then Optoelectronics and silica fibers have been the subject of large-scale worldwide research and product development. As a result, optical communication has established itself as one of the most promising technologies in the area of short and long distance data transmission.

Ten years ago, most optical communication systems were based on multimode fibers in which the difference of propagation constants between the fiber modes caused considerable pulse broadening that were dispersion limited. An important turning point in the development of optical communication systems came when reliable semiconductor lasers with high intensity and spectral purity became commercially available. Multimode fibers were superseded by single-mode fibers, in which only a much weaker chromatic dispersion can result in pulse broadening at the specific signal wavelength of 1310 nm. Standard silica fibers have negligible chromatic dispersion at 1310 nm. This wavelength therefore became the most dominant, and the fibers were optimized for 1310 nm operation. Using these "standard fibers" systems was loss-limited. However, the intrinsic loss of silica fibers is at 1550 nm, where the chromatic dispersion is nonnegligible: 15 Ps/(km. nm).

The elimination of chromatic dispersion at 1550 nm became a major research effort in mid 1980s. Hence the compensation for chromatic dispersion was achieved with an opposite and equally large waveguide dispersion through a carefully controlled design and manufacturing process. However, such dispersion-shifted fibers introduce additional losses. Intensive international research and demands for coherent communication, which is based specifically on ultra narrow linewidth signal sources, indicated the necessity of installation of dispersion-shifted fibers and therefore compensating of their poor loss properties.

There were, however, practical problems that had to be overcome before a clean picture of future optical communication systems could be formed. Among the important subjects for clarifying this was the research on semiconductor amplifiers, which suffered from problems such as crosstalk and polarization sensitivity in addition to difficult fiber-to amplifier coupling.

At the same time, a parallel development took place, which has had a much larger impact on optical communication systems than that mentioned above. This was the development of the rare earth doped fiber amplifiers and lasers. With a point of reference in work on rare-earth-doped glass lasers initiated as early as 1963 [1-1], [2-1], the first fiber amplifiers (as possible useful devices for telecommunication applications [3-1]) were demonstrated in 1987. Progress since then has multiplied to the extent that amplifiers today offer far reaching new opportunities in telecommunication networks [4-1], [5-1], [6-1]. The Erbium-doped silica fiber amplifier for the 1550-nm telecommunication

window has now become a well-established research laboratory tool. The fiber amplifier has been used both in system demonstrations on land and under the sea, and operational systems are commercially available from a number of manufacturers.

The main reason for the very strong impact that the optical amplifiers have and will have on data communication systems is to be found in the fact that they are unique in two respects: they are useful for amplifying input signals of different bit rates or formats, and they can be used to achieve simultaneous amplification of multiwavelength optical signals over a wide spectral region. These multiwavelegth optical signals can carry different signal formats, including digital data, digital video, and analog video, allowing flexible upgrading in a broadband distribution network by adding extra wavelength division multiplexed (WDM) channels as needed. With optical amplifiers, therefore, the bottleneck of narrow and fixed bandwidths of electrical repeaters is avoided.

The outstanding properties offered by optical fiber amplifiers include:

- High gain
- High power conversion efficiency
- Low crosstalk
- High saturation power
- Polarization insensitivity
- Broad spectral bandwidth
- Very low coupling losses
- Low cost

- Low noise

1-2 Integrated optics and rare earth-doped amplifiers

The notion of "integrated optics" was introduced for the first time by S. E. Miller in 1969 [7-1]. The advantages, which are offered by optical circuits, can be explained as large bandwidth and insensitivity to interference by electromagnetic fields of low frequencies. Integrated optical components are compact and reliable, have high mechanical and thermal stability and low power consumption. Integrated optics offers the possibility for integration of several devices on a common substrate or chip. The optical function of an integrated optical component mainly depends on the physical properties of substrate material on which the component is made.

Glass is the most important substrate material suitable for fabrication of passive and active integrated optical components. The refractive index of a glass substrate is very close to that of the optical fibers (n=1.48), which minimizes the coupling losses between glass waveguides and optical fibers. Glass has excellent transparency in the visible and near infrared spectral regions and can easily be made in to different sizes and shapes with very high homogeneity. As an amorphous material distinct from crystals, it is easier to produce polarization insensitive integrated optical components in glass. In addition, glass has a high threshold to optical damage, it is mechanically very rigid and relatively inexpensive. Glass is also suitable host for rare-earth ions. This has allowed for the fabrication of optical amplifier and lasers.

Rare earth ions are employed in optical applications due to their metastable excited states over the entire range of optical frequencies [8-1], [9-1]. For many years, rare-earth-doped glasses have been used to make bulk laser and amplifier devices [10-1], [11-1]. Waveguiding structure provided by optical fiber allows high power densities for pump and signal wavelengths in rare-earth-doped devices fiber core, which results in lower threshold and higher operation efficiency compared to conventional bulk lasers. Also, the high surface area-to-volume ratio of the fiber geometry leads to efficient heat dissipation. The rapid development of rare-earth-doped silica fiber amplifiers and lasers has considerably increased the interest in rare-earth-doped planar waveguide devices. Furthermore, reliable high power CW (continuous wave) diode laser pumps provide the possibility of miniaturizing conventional solid state lasers and amplifiers [12-1], [13-1]. As laser diode pump are compatible with planar waveguide structure, higher pump densities and therefore higher gain compared to bulk devices can be achieved. Such glass based rare-earth-doped lasers and amplifiers are highly promising for producing small, compact, efficient and reliable communication, signal processing, sensing and medicine applications.

Rare-earth-doped glass waveguides offer the possibility of constructing active optical components from a material that has traditionally permitted only passive devices. They can be fabricated on rare-earth-doped and undoped substrates by similar techniques as used for making passive glass waveguides. Ion exchange and ion implantation are two major techniques to produce waveguiding structures on rare-earth-doped glass substrate.

Flame hydrolysis deposition, RF (radio frequency) sputtering, sol-gel methods are also used to create rare-earth-doped films on substrates. These methods will be described in details in the following chapters.

Compared to their optical fiber counterparts, rare-earth-doped glass waveguides have some distinct advantages such as higher dopant concentration. Usually rare-earth-doped fibers made by MCVD (modified chemical vapor deposition) or VAD (vapor phase axial deposition) allow rare earth dopant concentrations of only a few tens to several hundreds PPM (parts per million), where as rare earth doped glass waveguides can have dopant concentration from several to a few tens of thousands PPM.

During the past 5 years, the development and commercial availability of reliable erbium-doped fiber amplifiers allow to bridge considerable distances without converting optical signal back to electronics, and to compensate the losses due to large splitting ratios, thus making it possible to distribute optical signals to a large number of customers [14-1].

When an optical signal is transmitted through an optical fiber, attenuation will always occur to a certain extent, such that it is necessary to amplify the signal after a certain distance. Conventionally, for that purpose an electronic amplifier is used; the optical signal must be converted into an electrical signal, which is amplified in an electronic amplifier, and then the amplified electrical signal is converted back into an optical signal. This implies that the bandwidth and bit-rate of telecommunications networks are limited by their electronic components. In order to increase network

capacity and to improve overall system performance, erbium-doped fiber amplifiers (EDFA) were developed to directly amplify optical signal at 1550 nm wavelength, a principal optical communication window (5th windows of telecommunication wavelength) in which there are minimum of propagation losses. Today, thousands of EDFA's have been incorporated in long haul transmission links to achieve an all-optical high bit-rate fiber link. In 1993 KDD and AT&T Bell Laboratories proved this by selling 274 EDFA for a 10 Gbit/s in 9000 km system which shows a 120 times higher performance than competitors. In addition to the capability of amplification the wider bandwidth and lower losses attract the customers to buy EDFA. Due to their high gain and high efficiency, EDFA's are also attractive to WDM technology to compensate the losses introduced by WDM systems. WDM is a key technology to upgrade the transmission capacity of the present fiber links.

The rapid development and application of EDFAs in telecommunication systems are of great significance for the telecommunication industry. On the other hand, this fast growing industry provides also a great challenge for the field of integrated optics. While fiber amplifiers may provide the initial need for telecommunications networks, the rich and complex optical functionality, promised by integrated-optic devices and circuits, will be essential for the deployment and evolution of these systems.

New research on optical integrated circuits specially on glasses and fabrication of many devices such as splitters, combiners, couplers, grating, etc. using different methods of fabrication, requires an on-board amplification to have a smaller and compact chips.

This leads the researchers to produce the same capability of EDFA's but on glasses, to have a complete set of simple devices on a same chip, the Planar Waveguide Amplifiers. This also will reduce the coupling losses and the expenses resulting of coupling between fibers in EDFA's and optical integrated circuits.

Several research groups pursue erbium-doped planar optical waveguide amplifiers. While an EDFA usually has a length of more than 10 meters, a planar waveguide device has a small dimension of around a few centimeters. Due to their small size, Planar Optical Waveguide Amplifier devices are expected to be of low cost, and more importantly, they offer the promise of integrating passive and active functions on the same substrate.

Optical glass amplifiers have been demonstrated to be efficient with a low Er^{3+} doping [15-1]. For planar optical waveguide amplifiers, a high Erbium concentration and a high pump power density are needed to obtain sufficient optical amplification gains because the optical interaction path is shorter. At high Erbium concentration, however, the Erbium luminescence will be quenched by energy transfer process due to ion-ion interactions. Furthermore, another cooperative upconversion quenching process dominates the amplification process of the devices when a high pump power is applied. These two luminescence quenching processes strongly influence the amplifier efficiency of planar waveguide amplifier [16-1]. Nevertheless, Erbium-doped planar optical waveguide amplifiers have been demonstrated in the past few years and the amplification properties of the devices are being improved. More recently, the need for a cost effective

lossless splitter for CATV optical networks has led to the integration of waveguide amplifiers with a passive splitter [17-1] and combiner[18-1]. Demonstration projects have been carried out using the waveguide amplifier as an in-line repeater or a pre-amplifier in a fiber communication system at 10 Gb/s [19-1].

1-3 Fabrication Methods

As discussed earlier, because of relatively low cost, excellent transparency, high threshold to optical damage, and availability in substantially large sizes glass is an interesting material for integrated optics [20-1]. It is rigid and amorphous which makes it easier to produce polarization-insensitive components. It also has a refractive index close to that optical fiber and therefore coupling losses between the waveguides made in glass and optical fibers are smaller.

There are different numbers of processing methods [21-1], which have been employed to make glass waveguides amplifiers as follow:

1-3-1 Ion Implantation

Ion implantation was used to make rare-earth-doped and in particular Er-doped, glass waveguides [22-1]. In the case of Erbium implantation, implantation of MeV Erbium ions into micron-thick silica and phosphosilicate glass films is done. This process requires 3.5 MeV energy that is costly in the point of view of industry and also needs thermal annealing to remove the defects and increasing the photoluminescence lifetime. The temperature of the thermal annealing in order to reach the maximum photoluminescence intensity is around 900°C for silica-based waveguides and 1175 °C for

silicon nitride based waveguides. In another experiment [23-1] using $Si_3N_4/SiO_2/Si$ as a substrate the energy has reduced to kilo electron volt energy. In this process the lifetime of transition between the metastable state $^4I_{13/2}$ to ground state $^4I_{15/2}$ has measured 7ms. The above mentioned fabrication process needs lots of costly equipment and time and the main drawback is using high temperature annealing to repair the damage substrate. It seems it is unlikely that this method will be used for a large-scale fabrication of rare-earth-doped components.

1-3-2 Sputtering/PECVD/EBVD

Sputtering [24-1], [25-1] was also utilized to fabricate erbium-doped glass waveguides. In sputtering, the waveguides are fabricated on a thin film of rare-earth-doped glass results from the adhesion of atoms, ejected from a target by bombardment of ions created in discharge plasma or by an ion beam, to a substrate. The fabrication mechanism is a RF sputtering or magnetron assisted RF sputtering and the substrate is normally an SiO_2 layer.

An erbium-doped waveguide amplifier fabricated by plasma enhanced chemical vapor deposition is reported [26-1]. The Erbium doped waveguide has a core of Er-doped phosphosilicate glass formed by PECVD, which is clad with silica glass formed by flame hydrolysis deposition (FHD) on a Si substrate. The core layer was deposited on the FHD undercladding layer at a substrate temperature of 400°C with conventional PECVD equipment using SiH_4 and N_2O gases. The P and Erbium doping were controlled by carefully transporting the vapor of the heated source into the plasma region with N_2

carrier gas. The core layer was annealed at a higher temperature for densification after deposition. Channels were formed in the core layer by reactive ion etching and then embedded with an FHD overcladding layer.

There is also another report of erbium-doped glass ridge waveguide amplifiers fabricated with a collimated sputter deposition technique [27-1]

In another attempt [28-1] an erbium-doped silica glass waveguide was fabricated on a quartz glass substrate using EB vapor deposition, high temperature annealing, metal film formation, photolithography, reactive ion etching (RIE) and cladding glass formation By the FHD techniques.

In order to achieve low loss waveguides, the used substrate should be heated and/or annealed at high temperature after deposition. These techniques are also relatively time consuming and equipment intensive.

1-3-3 Flame hydrolysis

This method followed by reactive ion etching techniques has been used to fabricate [29-1], [30-1], [31-1] erbium and phosphorus codoped silica waveguides (8 μm wide, 7 μm thick and 23 cm long). The long S-shaped waveguide with an area of $7.9X3.5cm^2$ was deposited on a silicon substrate. This is a very high temperature routine for fabrication of a glass waveguide. The waveguides have low propagation losses. However the rare-earth concentration is usually low and waveguides are relatively long.

1-3-4 Composite Waveguides

An Erbium-doped laser glass is pressed against an ion-exchanged waveguide to form a composite erbium-doped waveguide[32-1],[33-1]. If the waveguide and the erbium-doped glass refractive indices are selected adequately, a significant amount of light is guided in the doped glass. This process is simple and low cost, but the device performance is sensitive to the pressure applied to hold the two components together. This problem can be resolved by depositing a rare-earth-doped glass, using for instance sol-gel process [34-1], on the ion exchanged waveguide.

1-3-5 Sol-gel

Sol-gel technology has tremendous potential for the fabrication of low-cost integrated optics and optoelectronic devices [35-1] ,[36-1] ,[37-1]. However rare-earth-doped sol-gel amplifier and laser fabrication is in its early stages. Erbium-doped sol-gel waveguides have been produced [38-1], [39-1], [40-1].

Sol-Gel processing allows for both high and low temperature fabrication. In high temperature fluorescence properties of Er^{3+}-doped sol-gel glasses are investigated [41-1]. The samples were prepared from tetraethoxysilane (TEOS), water and Ethanol, using $Er(NO_3)_3.5H_2O$ as the Er^{3+} precursor. Two different test matrices with precursors molar ratios of (TEOS: H2O: C2H5OH=1:4:4 and 1:16:0) for Er_2O_3 concentration ranging from 0.1 to 10.0 wt% were prepared. All of the samples fluorescenced at room temperature. Processing temperature of at least 800°C was required to obtain acceptable fluorescence intensities which is quite high. High percentage of Er_2O_3 and Al/Erbium ratio is also required to increase fluorescence intensity.

Recently a channel waveguide consisting of 4 layers of : Si as substrate, 2microns SiO_2 over the substrate, a layer of 2micron Sol-Gel :$Er^{3+}Al_2O_3$-SiO_2 and finally a waveguide with the dimensions of 1 micron by 0.6 of SiO_2 has been fabricated which resulted into a gain of 3dB with an injected power of 6 mW [42-1]. The time for the postbake of this sample is 900 °C and it needs multi deep coating for making the film.

Presently there are lots of efforts to fabricate the $Er^{3+}Yb^{3+}$ Sol-Gel waveguides at low temperature.

1-3-6 Ion-exchange

Ion exchange involves a local change in composition which is brought about by mass transport driven by thermal or electric field gradients or some combination of the two, using generally a mask which defines the region altered. The change in composition leads to a change in refractive index, and thus to waveguiding region of suitable geometry. In common glass substrate, there usually exist sodium ions which act as matrix modifiers of glass network. These sodium ions have high mobility and therefore exchange easily with other monovalent alkali ions such as K^+, Cs^+, Ag^+, Rb^+ and Ti^+. The substitution of sodium ions by ions having higher polarizabilities and larger ionic radii results in local increase of refractive index in glass substrate, thus waveguiding structures may be formed. Usually, the ion exchange process has no effect on the basic structure of network formers in glass if it is carried out at temperatures well below the softening point of the glass. The ion exchange can be purely a thermal diffusion process, or an electric field assisted diffusion process. Both a molten salt and a metallic film such as silver can be

used as ion sources. Ion Exchange is simple and flexible in choosing various pairs with different ion radii and polarizibilities, and in fabrication parameters. Ion exchange offers wide possibilities in choosing the numerical aperture and dimensions of waveguide. The index change can be controlled easily by proper choice of the exchanged ions and the glass compositions. The index profile can be tailored from shallow graded to a step like function with the assistance of electric field. Ion exchanged waveguides are reproducible, low cost and have low propagation loss.

Ion exchange assumes a host structure in which there is some form of network, rigid and covalently bonded, through which mobile ions can move. The technique is thus particularly appropriate for silicate and phosphate glasses, which have this structure. A similar process can be carried out on crystals such as lithium niobate and potassium titanyl phosphate (KTP). Ion exchange thus stands in contrast to fabrication techniques which "sculpt" the index distribution, generally through some kind of etching of a deposited film: it is more similar to ion-implantation, but involves processes which are much less energetic and thus less damaging to the host.

As a diffused process that does not damage the host network, ion exchange tends to produce smooth, well-graded structures, with fairly low propagation losses. Since ion exchanged waveguides are usually produced by alteration of the glass surface through contact with a molten salt bath or metal film, the propagation losses can be reduced further by burial of the waveguide, in which an electric field is applied to drag the altered zone into the glass host. The surface composition being reconstituted by simultaneous

immersion in a bath of the appropriate salt mixture. By moving the optical field away from the relatively rough surface and by allowing further smoothing of the profile, burial leads to waveguides with extremely low losses, claimed to be around 0.01 dB/cm. While not approaching the losses of optical fibers, these are the best values claimed in integrated optics. It should be noted that very similar values have been obtained for waveguides made by entirely different methods, involving FH deposition followed by etching to define the confined waveguides [43-1]. For all the techniques, propagation losses in rare-earth-doped glasses turn out to be substantially higher than in undoped glasses.

One of the advantages of ion exchange is that it appears suitable for a wide range of glasses. However, it is necessary that the ions in the raw glass and in its ion-exchanged composition be immobile at normal temperatures, so that devices will last up to 20 years demanded by the telecom industry, while becoming sufficiently mobile at elevated temperatures for acceptable processing times. In practice, only the monovalent ions, especially the alkaline cations, meet these criteria; bivalent and trivalent ions will not diffuse appreciably under concentration gradients at whatever temperature, and the electric fields required to move them can alter the glass network structure. Exceptionally, exchange of monovalent anions has been used in fabricating waveguides in fluoride glass substrates [44-1]. The limited choice of exchangeable mobile ion pairs leads to a similarly limited maximum of ion types. Thallium and silver ions lead to the largest index change when exchange with Na^+ or K^+. Thallium is highly toxic, and demands great care in handling; despite this, it has been the basis of a successful industrial process developed by

Corning Europe for the fabrication of passive splitters. Silver ions have a tendency to reduce to metallic silver, leading to high propagation losses. Nevertheless silver exchange also forms the basis of an industrial process, being used by IOT of Germany to make passive splitters. Thus a successful ion exchange process, which leads to a reproducible, stable, low-loss waveguides demands control of host glass composition and much effort to determine the ideal processing conditions of temperature and salt-bath composition, as well as the development of compatible masking procedures [45-1]. The mobility properties of the ions make localized post-annealing possible, because the ions will move appreciably only where the temperature is high enough. This has been experienced several times very successfully to make tapers, permitting good coupling to single-mode fibers at the waveguide input while retaining the desirable features of a high numerical aperture (NA) guide away from the input [46-1,48-1]. Such processing may have further possibilities, permitting perhaps the trimming of couplers and other structures under the influence of localized heating, for example using a CO_2 laser.

Despite reports to the contrary, [49-1] the trivalent rare-earth ions are effectively immobile, and it is not possible to use ion exchange to localize rare earth doping. In ion-exchanged rare-earth-doped glass waveguide devices, the host is almost invariably bulk-doped with the rare earth, the only exception being the use of ion-implantation of Erbium [50-1].

Ion exchange has been the most popular technique to make rare earth doped waveguides in glass. Some of the research activities have been concentrated on

neodymium-doped waveguides. Silver and potassium ion exchange processes in silicate and phosphate glasses have been employed to demonstrate amplifiers and lasers around 1.06 , 1.08 and 1.3 μm [51-1,56-1]. Molten salts are used to make waveguides in silicate glasses. The silver-film technique is more convenient for waveguide fabrication in phosphate glasses, but recent developments in phosphate glass fabrications have offered phosphate glasses resistant to heat and chemical attacks by salts. Highly resistant glasses and special fabrication process are necessary to make ion exchange waveguides in phosphate glasses by molten salt technique.

The first report of any planar waveguide in an active medium was published in 1985, [57-1] and described the behavior of Ag^{+}-k^{+} ion-exchanged multimode planner waveguides in Nd^{3+}-doped silicate glass. A small signal gain was measured in a single mode waveguide fabricated by silver ion exchange on a commercially available neodymium doped glass [58-1,59-1]. Following that, ion exchanged Nd^{3+} lasers were demonstrated in phosphate [60-1] borosilicate [61-1] and silicate [62-1] glass hosts. Work on Nd^{3+}-doped waveguide lasers has moved to the development of more highly functional integrated sources. There are as yet no commercial applications for simple Nd^{3+}-doped waveguide sources.

The first erbium-doped ion exchanged device was realized in 1992, using K^{+}-Na^{+} exchange in Schott BK-7 glass, a borosilicate [63-1]. As a consequence of the difficulties above, the device showed a poor slope efficiency (0.55%) and high threshold (150 mW of launched 980nm pump power). The laser operated single-transverse-mode at 1540nm.

The smooth spectrum of Er^{3+}-doped glass, and the low polarization-dependence, makes the ion-exchange technologies well suited for the fabrication of optical amplifiers.

Chapter 2

Theoretical study of erbium–ytterbium co-doped ion-exchanged waveguide amplifiers

2-1 Introduction

A theoretical treatment of phosphate glass waveguide amplifiers doped with Er^{3+}, and co-doped with Yb^{3+} will be presented in this chapter which helps us understand the experimental results in the following chapters. The theoretical gain calculated in this chapter will use the approach implemented in [2-33] and [2-34] by Shooshtari et al. to explain ytterbium sensitized erbium doped ion exchange waveguide amplifiers on phosphate glass.

A high concentration of Er^{3+} in erbium doped planar waveguide amplifiers comparing to low concentration in long fibers in erbium doped fiber amplifiers for comparable gain, increases the probability of ion-ion interaction mechanisms and hence upconversion, cross relaxation and quenching [2-1] [2-2], [2-3]. These mechanisms reduce the pump efficiency and subsequently the gain. A well-known technique to minimize these effects is doping waveguides with Yb^{3+} sensitizer [2-4-2-8]. Most of the pump power is absorbed by ytterbium ions, and subsequently the absorbed energy is transferred to adjacent erbium ions through cross relaxation mechanism. Large absorption and emission cross section bandwidth [2-9] of Yb^{3+} allows for a wider choice of pump wavelength (800-1100 nm) in erbium doped waveguide amplifiers (EDWA).

Hence we focus on the effects of host materials and device parameters on Er^{3+}-doped and Er^{3+}-Yb^{3+}-codoped waveguide amplifiers. The effects of waveguide dimensions, Er^{3+} and Yb^{3+} concentration and distribution, as well as upconversion and cross relaxation on amplifier gain will be investigated. The electronic properties of erbium and the effect of ytterbium in general will be described in section 2. In section 3, the fundamental relations for two arbitrary energy levels in atomic energy levels will be discussed briefly. A mathematical treatment of Er^{3+}-Yb^{3+} amplifiers will be presented next. Section 5 presents the results of numerical calculations based on 2 different host glasses. A set of curves that could be used to design waveguide amplifiers with the desired performance is also presented. Finally, conclusions are drawn.

2-2 Electronic and optical Properties of Rare Earth Ions

The rare earth atoms are divided into two groups of 14 elements from which only the lanthanides are worth consideration for our purpose. Unlike actinides, lanthanides have isotopes stable enough to be useful for lasers and amplifiers. Table 2.1 lists 15 elements ranging from Lanthanum (La) with an atomic number of 57 to Lutetium (Lu) with an atomic number of 71. All the rare earth atoms have the same outer electronic structure of $5s^2 5p^6 6s^2$ which are filled shells [2-10]. Optical characteristics of rare earth ions dictated by the number of electrons occupying its inner 4f shell as described in [2-11]. La has zero and Lu has fourteen 4f electrons, and since optical absorption and emission cause transitions within the 4f shells, these two materials will therefore have special properties compared with the rest.

Ionization of the rare earths usually takes place to form a trivalent state. Two of the 6s electrons and one of the 4f electrons are removed, but the outer 5s and 5p shells remain intact. The remaining 4f electrons are therefore partially shielded from perturbation by external fields. The fluorescence and absorption wavelengths are consequently less dependent on external electric fields than other ions of the transition elements, which do not experience similar electronic shielding [2-10].

Important parameters in establishing the use of rare-earth-doped ions in amplifier applications are the strength and energy of absorption and fluorescence. The reason is that the absorption spectrum holds accurate information about the location of possible pump wavelengths and the ability to excite the rare-earth ions to higher energy levels.

From this higher energy level electron relaxes, transferring its packet of energy to the ground state either radiatively or non-radiatively. The non-radiative relaxation involves the creation of phonons (i.e., a quantized vibration of the surrounding medium), whereas radiative decay takes one of two forms.

Table 2.1 The rare earth Material with indication of atom number and electron configuration.

Lanthanum	La [57]	[Xe] (6s2 5d)
Cerium	Ce [58]	[Xe] (6s2 4f 5d)
Praseodymium	Pr [59]	[Xe] (6s2 4f3)
Neodymium	Nd [60]	[Xe] (6s2 4f4)
Promethium	Pr [61]	[Xe] (6s2 4f5)
Samarium	Sm [62]	[Xe] (6s2 4f 5d)
Europium	Eu [63]	[Xe] (6s2 4f 5d)
Gadolinium	Gd [64]	[Xe] (6s2 4f7 5d)
Terbium	Tb [65]	[Xe] (6s2 4f9)
Dysprosium	Dy [66]	[Xe] (6s2 4f10)
Holmium	Ho [67]	[Xe] (6s2 4f11)
Erbium	**Er [68]**	**[Xe] (6s2 4f12)**
Thulium	Tm [69]	[Xe] (6s2 4f13)
Ytterbium	**Yb [70]**	**[Xe] (6s2 4f14)**
Lutetium	Lu [71]	[Xe] (6s2 4f14 5d)

[Xe] stands for the electronic configuration of Xenon.

These are known as spontaneous and stimulated emission, and in both cases photons are emitted. Spontaneous emission always takes place when the electrons of a collection of atoms are in an excited state, and spontaneously emitted light may therefore not be avoided in a waveguide amplifier. Stimulated emission is the process that allows

signal amplification to take place and is therefore the desired property of the waveguide amplifier. The process may be explained as follows [2-10]: a photon incident on the medium, with an energy equal to the difference in energy of the ground state and an excited state, promotes deexcitation, with the creation of a photon that is in phase with the incident photon. The light produced in stimulated emission therefore exhibits a degree of coherence. It is naturally very important to identify the possible wavelengths where amplification is possible, and here the fluorescence spectrum is the principal tool, since it together with the absorption determines these wavelengths.

The absorption and emission possibilities can be described through energy level diagrams. Such diagrams are shown in Figure 2.1 for Er^{3+}, Nd^{3}, and Pr^{3+}, and typical wavelength transition values are included. In Figure 2.1, the atomic and ionic energy levels are conventionally labeled according to the angular momentum properties of the atom or ion. An atom or ion at an energy level labeled as $^{2s+1}L_j$ would have a spin quantum number of S, a total angular momentum quantum number of J, and an orbital angular momentum quantum number of L defined by the letters s, p, d, f, g, h, i,... , which correspond to L=0, 1, 2, 3, 4, 5, 6, ..., respectively. In a glass host, the lanthanide ion is subjected to electric fields, known as crystal fields due to the surrounding atoms in the host lattice. This causes a Stark splitting of the rare-earth ion orbitals (J manifolds), and site to site variation of the field due to the amorphous nature of glass results in an inhomogeneous broadening of the transition [12-1].

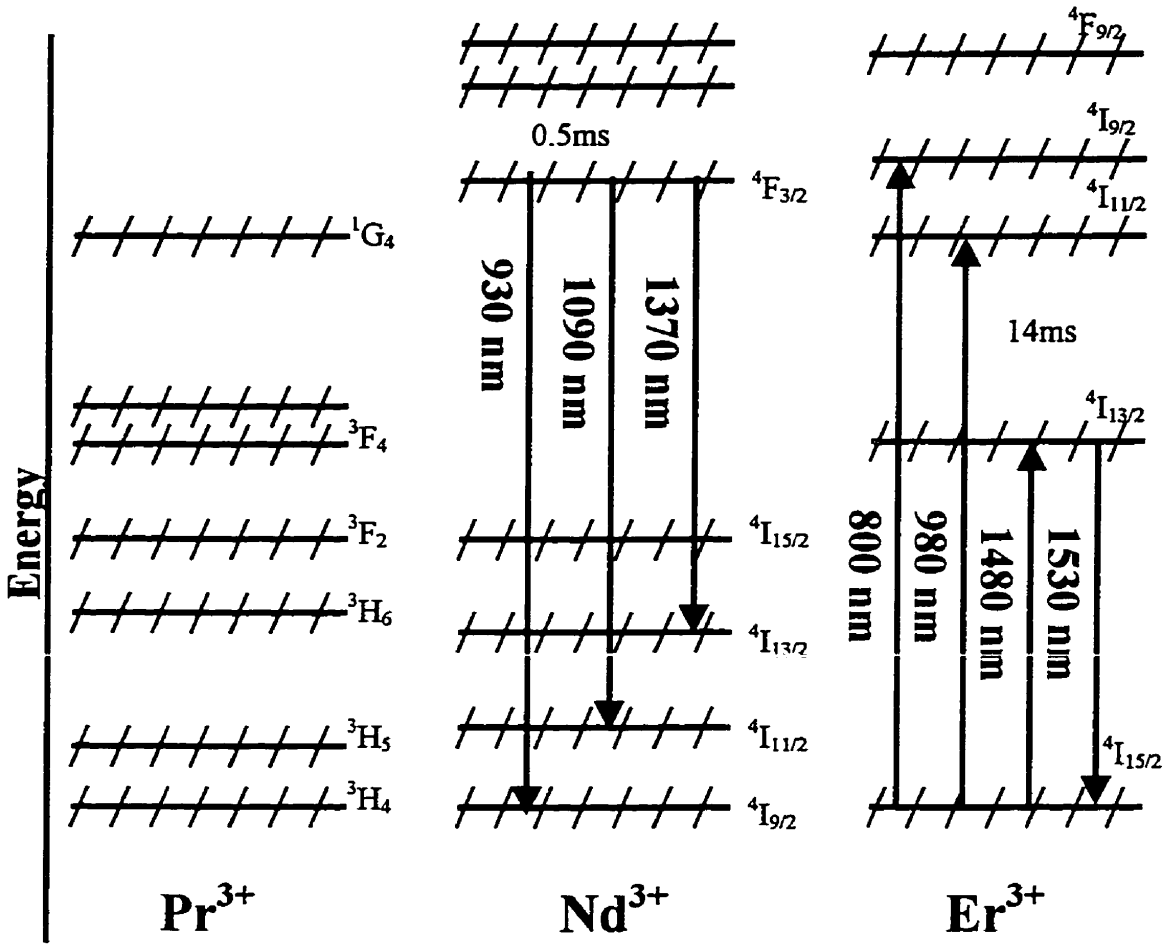

Figure 2.1. Energy level diagram for Er^{3+}, Nd^{3+}, and Pr^{3+}. The wavelengths of the optical transitions in SiO_2 glass are shown, together with the average lifetime in the upper laser levels.

Besides this broadening mechanism, phonon broadening (or homogeneous broadening) also takes place. This happens because energy exchange in the connection with a transition between two energy levels may include the creation or annihilation of a phonon.

When the ions are excited to levels above the upper laser level, the electrons

cascades down through intervening levels by nonradiative transitions and eventually populates the upper laser level. This level is normally described as metastable, since transition from this to lower manifolds only appears because the crystal field has broken the inversion symmetry of the ion's environment, permitting the electric dipole transitions to occur between Stark levels in different *LSJ* multiplets [2-13]. It is noteworthy that the lifetimes of the upper laser level are thus many orders of magnitude larger than the nonradiative lifetimes of the higher energy levels.

Another important property may be seen in Figure 2.1 by comparing the energy level diagrams of Er^{3+} and Nd^{3+}. The important difference is that the Er^{3+} doped system (for the lower pump level wavelengths) works as a three-level laser system, whereas Nd^{3+} may be described as a four level laser system (when considering the 1370 nm band). In a three-level system, the lower lasing level is either the ground state or a level so close to the ground state that it has a significant thermal population. In a four level laser, there is still a further transition from the lower laser level down to the ground state, which is usually nonradiative in nature. In a three level laser system, signal absorption from the ground state directly to the upper laser level takes place, causing competition with the stimulated emission of photons. This is also the case for the 1480-nm pumping of Er^{3+} fibers at which wavelength the Er^{3+} works as a two level system, meaning that the upper pump level and the upper laser level coincide. In a four-level laser system, the lower lasing level is depopulating rapidly, and pump power necessary to obtain population inversion becomes significantly smaller. This will result in the principal differences

between EDFAs and neodymium-doped fiber amplifiers (NDFA).

A schematic illustration of the amplification process for Er^{3+} three level systems is shown in Figure 2.2.

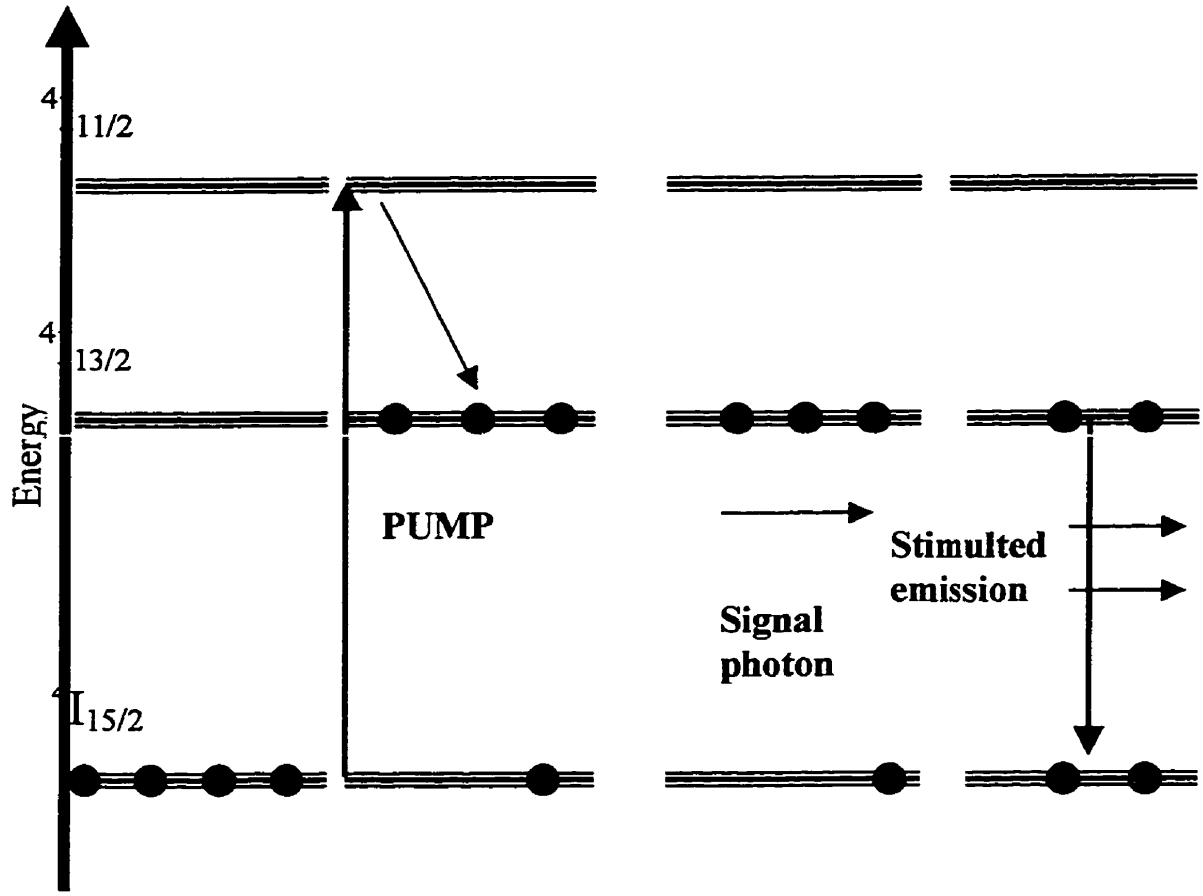

Figure 2.2 an illustration of the amplification process in an Er^{3+} three-level lasing system. Upon being excited to the $^4I_{11/2}$ state, Er^{3+} ions quickly relax to the upper lasing state $^4I_{13/2}$ by non-radiative decay. Through stimulated emission, signal light at 1.53μm can be amplified.

After being excited to a higher lying state above $^4I_{13/2}$ state, Er^{3+} ions quickly decay to the metastable $^4I_{13/2}$ state via non-radiative relaxation. Stimulated emission from

the $^4I_{13/2}$ state to the ground $^4I_{15/2}$ state can cause amplification of light at 1550 nm. Light amplification due to electronic transitions of Er^{3+} works as a three-level lasing scheme. Light amplification in a three level laser system can occur only when more than half of the population is excited to the upper lasing level ($^4I_{13/2}$ level for Er^{3+}).

2-3 Quenching process for Er-doped optical amplifiers

The principles of Er^{3+}-doped optical amplifiers, either in the form of fiber or planar waveguide, are the same. However, due to their short optical paths, Er-doped planar waveguide devices need a high concentration of dopant ions to obtain sufficient optical gains. Two quenching processes, both related to high Er doping levels, influence the efficiency of Er-doped waveguide amplifiers.

The first one is the concentration quenching. With a high Er concentration in the waveguide, one excited Er^{3+} ion has a probability to transfer its energy to a neighboring ion in the ground state through ion-ion interaction. This process may continue until the energy is transferred to an Er^{3+} ion which is correlated with a defect or an impurity ion, and the energy may be lost via non-radiative decay.

The second one, which is believed to be the dominant process causing the inefficiency of the Er-doped waveguide devices, is the co-operative upconversion process which is due to the ion-ion interactions of Er^{3+}. With a high Er^{3+} concentration and a high population inversion, one excited Er^{3+} ion may transfer its energy to another excited Er^{3+} ion, and one Er^{3+} ion non-radiatively decays to the ground state and the other Er^{3+} ion is excited to a higher lying state.

The net result of the upconversion process is that the population in the upper lasing state is strongly reduced and the efficiency of light amplification at 1550 nm by stimulated emission is strongly decreased. The upconversion quenching process is a material host related property, since it is caused by the ion-ion interactions of Er^{3+} ion in the host. Therefore, choice of an efficient Er host is a crucial issue for planar waveguide amplification devices.

2-4 Host materials for erbium

Erbium doped fiber amplifiers are predominantly silica based. Al is codoped in the fiber to increase the solubility of Er^{3+} ions. Furthermore, a wide choice can be made, in the balance between Er concentration in the fiber and the fiber length. It has been shown that an efficient Er-doped fiber amplifier can be achieved with an erbium concentration of ~ 10^{18} ions/cm^3 and a fiber length of a few tens of meters.

For planar waveguide devices, the optical length is limited to a few centimeters and so the Er concentration has to be ~100 times higher than that for the amplifiers. Fortunately there are more choices of fabrication techniques for planar waveguide devices. Until now, amorphous and crystalline materials have been explored for Er-doped planar waveguide amplifiers, including Al/P codoped silica [14-2], multi-codoped oxide glasses [2-15], [2-16], [2-17], [2-18], Al_2O_3 [2-19], $LiNbO_3$ [2-20], etc. Although fluoride glass is not a suitable for this application, but flourophosphate glass seems a suitable choice. Based on the study of the known Er-doped materials, we choose multicomponent glasses, more specifically phosphate glasses as Er hosts. The advantages

of phosphate glasses as Er host are as follows:

- good optical transparency
- refractive index compatibility with optical fibers
- high Er solubility
- high Er^{3+} emission cross sections
- wide luminescence spectrum for a broad amplification band
- easy to prepare due to its low glass melting temperature

2-5 Ytterbium Co-doping of erbium amplifiers

Previously we discussed how 2 ion processes such as cooperative up-conversion and quenching appear in erbium-doped glasses. It is therefore not surprising that process of energy transfer from neighboring but different rare earth ions can take place. A constructive application of such an effect is made in Er^{3+}-Yb^{3+}- doped fibers or planer waveguides. The purpose was at first to utilize the broader absorption spectrum of ytterbium at wavelengths above 800 nm. This is advantageous as the Yb^{3+} after absorption of the pump light undergoes a cross-relaxation process with adjacent ions of Er^{3+}, whereby the absorbed energy is transferred to the erbium system. This allows another route for pumping the erbium system, and the effective pump band of the fiber or planar waveguide is thus extended, as can be seen in Figure 2.3.

The effect of ytterbium co-doping is very significant, but it should be understood that it also implies some drawbacks. Namely, the successful energy transfer requires that ytterbium and erbium ions be located close to each other, and consequently a high

ytterbium concentration is necessary (a Yb^{3+}:Er^{3+} ratio of 20:1 is realistic). Besides the impact of this on fabrication techniques, it is therefore clear that a large number of ytterbium ions will be excited by the pump without being able to transfer this energy on to the erbium ions. Consequently, the pump efficiency must be expected to be very low for Yb-co-doped EDFA or EDPA, but this is the price that has to be paid to extend the pump wavelength band as illustrated.

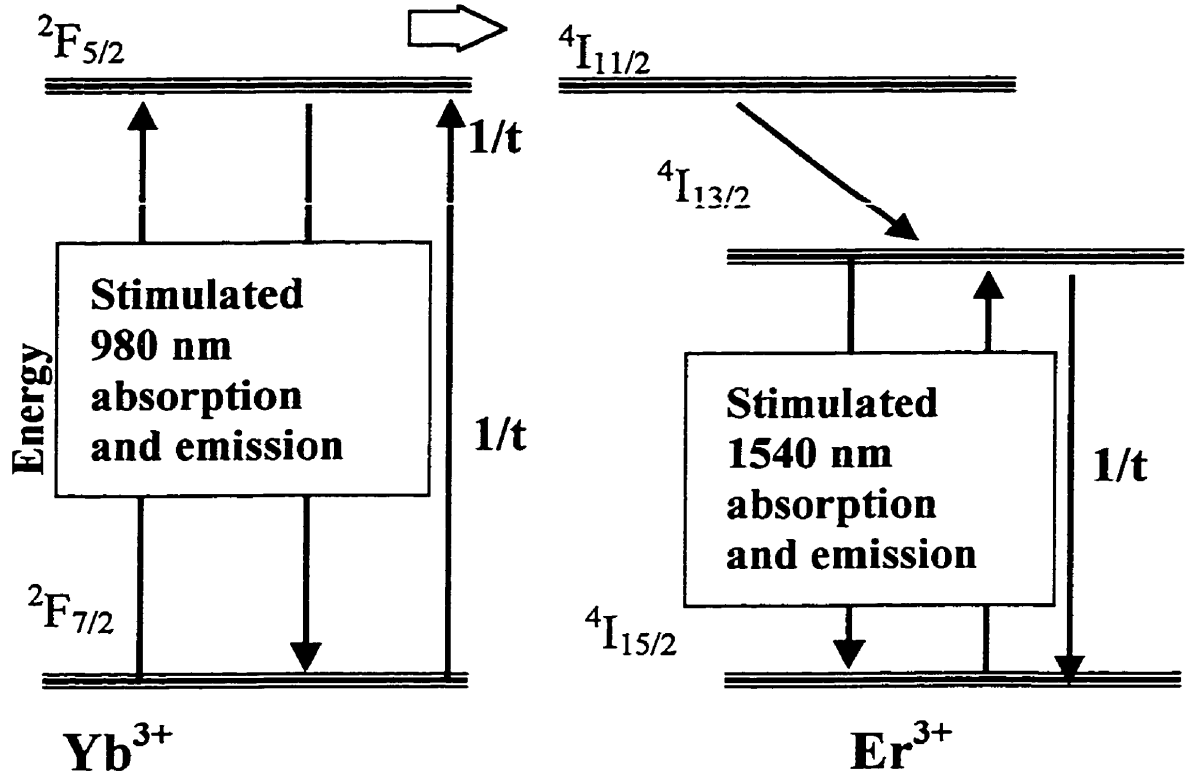

Figure 2.3 Erbium-ytterbium energy level diagram illustrating the 980-nm pumping possibility

It should, however, also be pointed out that even though high concentrations (several weight percentages) of ytterbium can be incorporated into a silica or phosphate

host, it can still give an efficient amplifier.

2-6 Fundamental equations

Figure 2.4 shows the energy levels of an arbitrary atom, such as erbium. In each two energy levels of this atom, several electronic transitions are possible. As we know spontaneous emission arises from by spontaneously radiative decay to lower energy level. The rate of this emission (electrons in m^{-3} s^{-1}) from higher energy level j to level i is given by, [2-24]

$$\left.\frac{\partial N_j}{\partial t}\right|_{spon.} = -A_{ji} N_j = -\frac{1}{\tau_{ji}} N_j \qquad (2\text{-}1)$$

Where $A_{ji}=1/\tau_{ji}$ represents the transition rate per electron and atom, and N_j is the electron concentration at level j. Generated photons by spontaneous emission have random phase and polarization which result in amplifier noise.

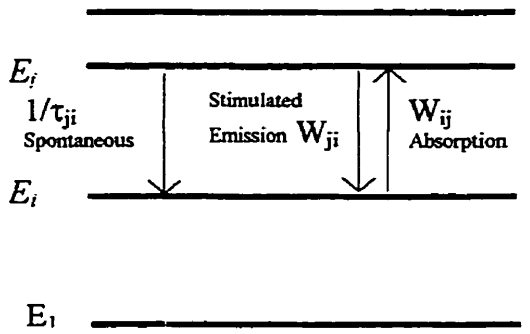

Figure. 2-4 Absorption, spontaneous and stimulated emission of two level E_i and E_j.

The rates of absorption and stimulated emissions are given by, [2-24] [App-1]

$$\left.\frac{\partial N_j}{\partial t}\right|_{stim.} = -\sigma_{e\,ji}(\nu)\frac{I_\nu}{h\nu} N_j = -W_{ji} N_j \qquad (2\text{-}2)$$

$$\left.\frac{\partial N_i}{\partial t}\right|_{absorp.} = -\sigma_{aij}(\nu)\frac{I_\nu}{h\nu} N_i = -W_{ij} N_i \qquad (2\text{-}3)$$

W_{ij} and W_{ji} in the above-mentioned formulas are absorption and emission rate per atom. N_i and N_j are electron concentration in levels i and j, h is the Planc constant, and σ_{aij} and σ_{eji} are the absorption and emission cross sections. A characteristic feature of a stimulated transition is that, as regards its phase and direction of its propagation, the emitted photon is coherent with the photon that has induced the transition.

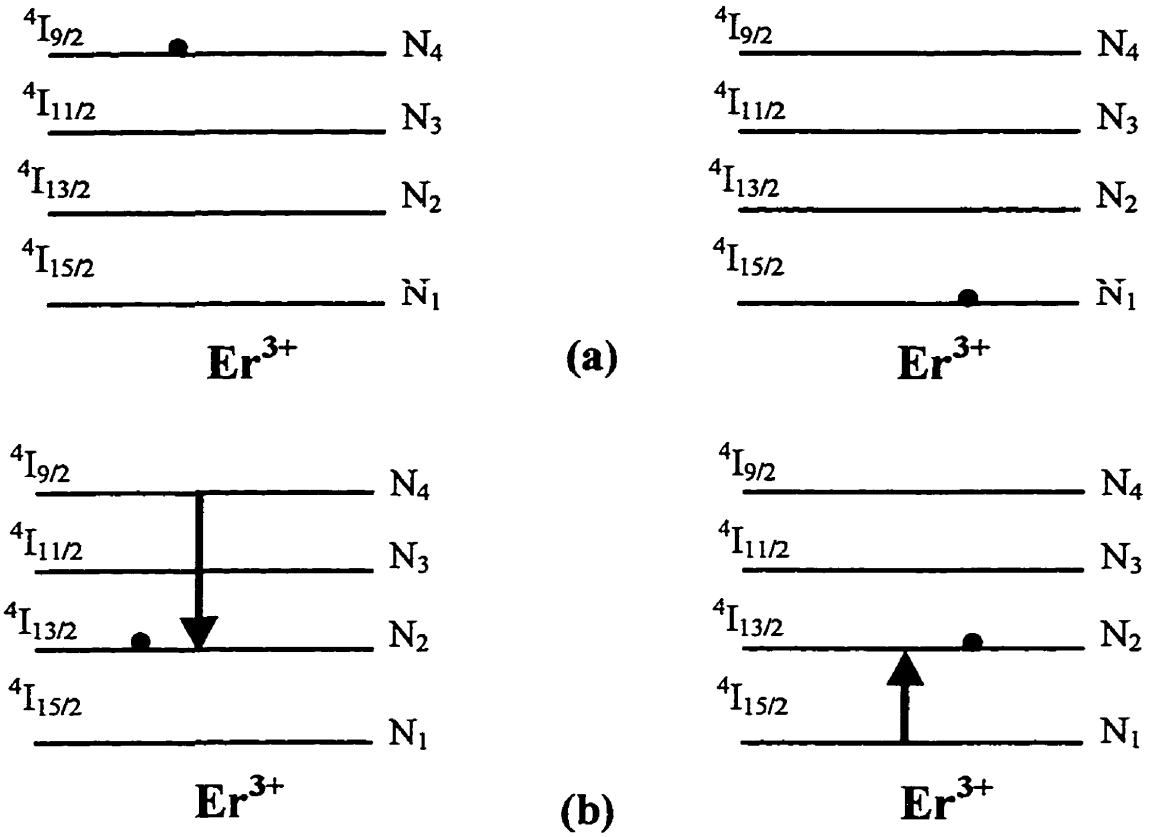

Figure 2.5 Cross relaxation process: erbium-erbium.

In non-radiative transitions between E_i and E_j, similar to the spontaneous emission, there is no photon involved and instead a phonon is released. This transition can be modeled using Eq (2-1) by changing the emission lifetime τ_{ji} to the non-radiative

lifetime $\tau^{NR}{}_{ji}$.

The transitions due to ion-ion interaction such as upconversion and cross relaxation are modeled by the second order equations of electron concentration in different levels [2-25] [2-26] and are described below.

Cross relaxation between erbium ions is one of the energy transfer mechanism due to ion-ion interactions in erbium doped glasses. This effect happens as illustrated in Figure 2.5, between two adjacent erbium ions in which one has already been excited to $I_{9/2}$ and the other one is in ground state. The donor ion transfers some of its energy to the acceptor ion and both electrons move to $I_{13/2}$ state. This interaction can be described as :

$$\left.\frac{\partial N_2}{\partial t}\right|_{cross} = 2 * C_{14} N_1 N_4 \qquad (2\text{-}4)$$

$$\left.\frac{\partial N_4}{\partial t}\right|_{cross} = \left.\frac{\partial N_1}{\partial t}\right|_{cross} = -C_{14} N_1 N_4 \qquad (2\text{-}5)$$

where C_{14} is a constant, based on the glass material and erbium concentration and is determined experimentally [2-27] [2-28].

Cross relaxation can also occur between erbium and ytterbium ions. Figure 2.6 explains this process. The excited Yb^{3+} ion transfers its energy to the adjacent ion and relaxes to its ground state and excites the erbium ion to $I_{11/2}$. This interaction is possible, as the energy differences between $F_{7/2}$ - $F_{5/2}$ in ytterbium and $I_{15/2}$ - $I_{11/2}$ in erbium is the same. The reverse interaction is also possible and the equations explaining are in the next page as:

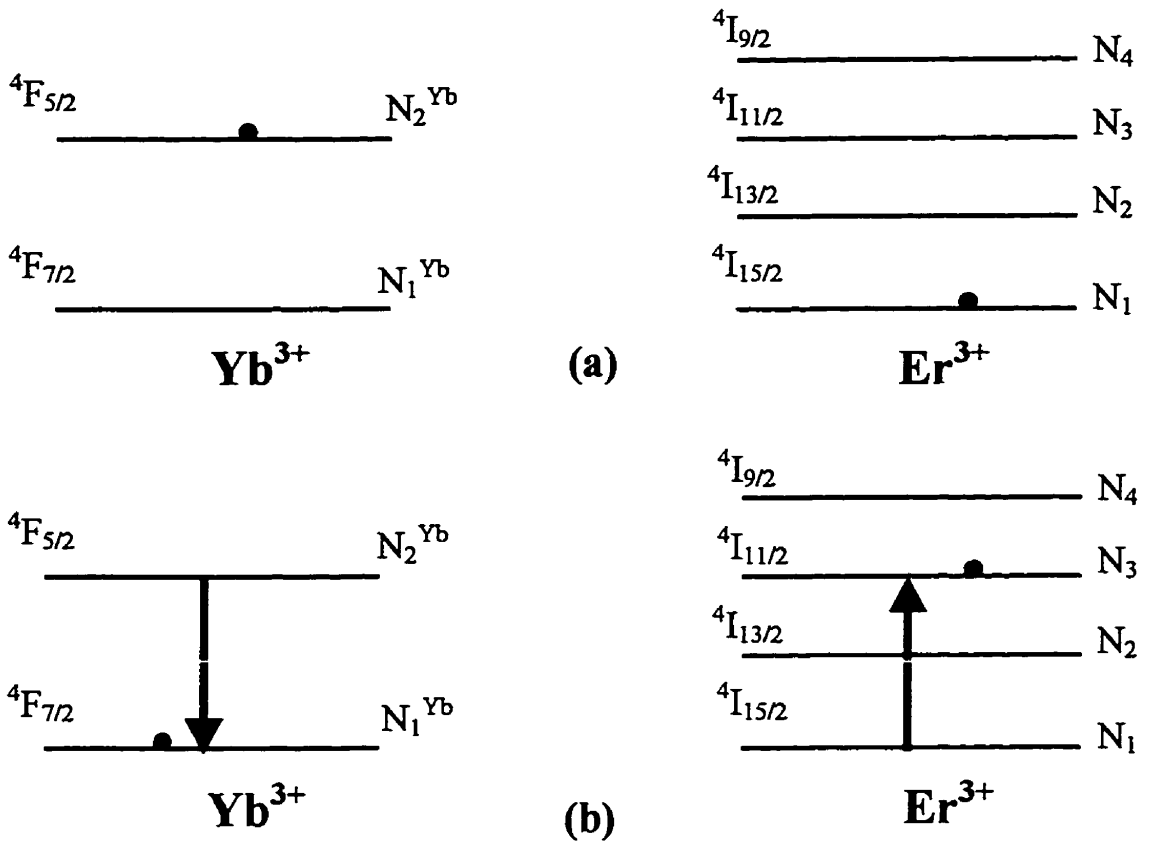

Figure 2.6. Cross relaxation process: erbium-ytterbium.

$$\left.\frac{\partial N^{Yb}{}_1}{\partial t}\right|_{cross} = K_{tr} N_2^{Yb} N_1 - K_{ba} N_1^{Yb} N_3 \tag{2-6}$$

$$\left.\frac{\partial N^{Yb}{}_2}{\partial t}\right|_{cross} = -K_{tr} N_2^{Yb} N_1 + K_{ba} N_1^{Yb} N_3 \tag{2-7}$$

$$\left.\frac{\partial N_1}{\partial t}\right|_{cross} = -K_{tr} N_2^{Yb} N_1 + K_{ba} N_1^{Yb} N_3 \tag{2-8}$$

$$\left.\frac{\partial N_2}{\partial t}\right|_{cross} = K_{tr} N_2^{Yb} N_1 - K_{ba} N_1^{Yb} N_3 \tag{2-9}$$

The above mentioned equations are based on experiments [2-29][2-30][2-31].

Upconversion is also considered here: This effect, on the contrary, is an interaction between two excited ions.

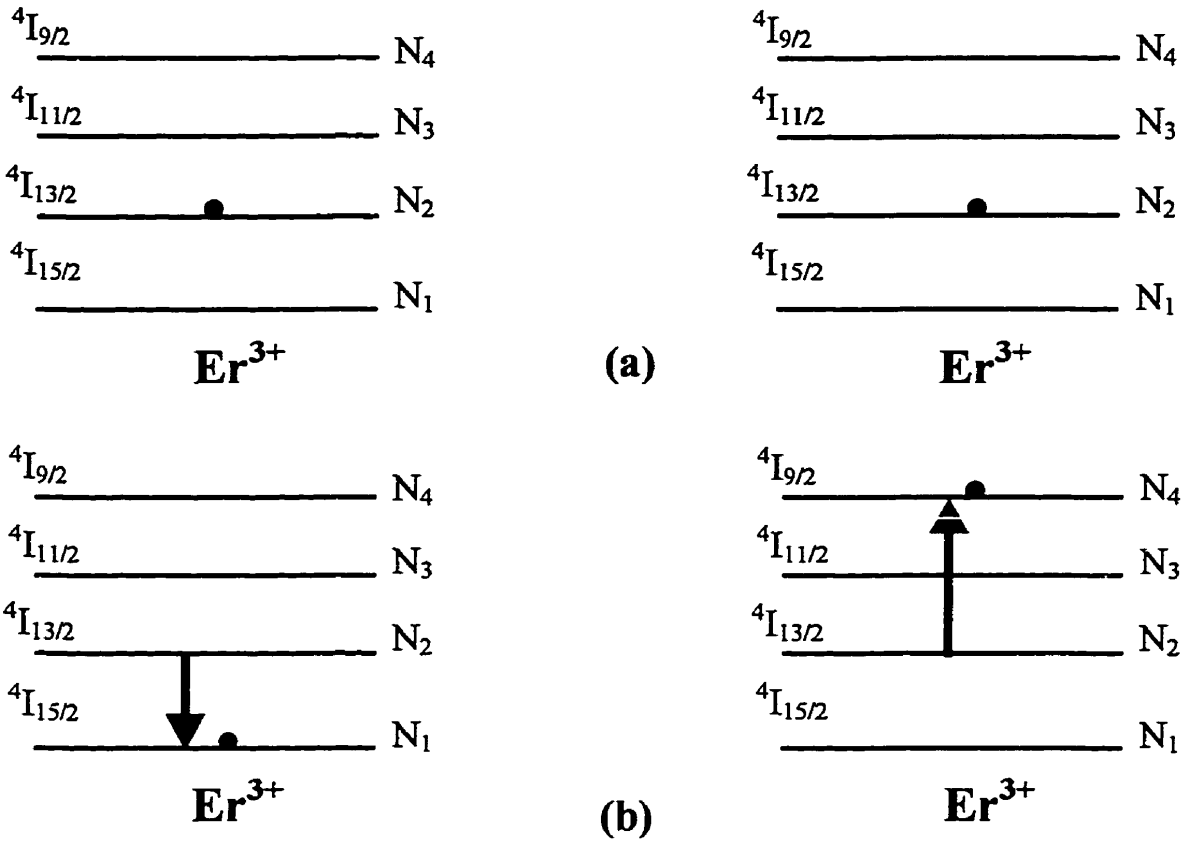

Figure 2.7 Upconversion process :Signal.

Equality in the differences of energy between $I_{15/2}$ - $I_{13/2}$ and $I_{13/2}$ – $I_{9/2}$ in erbium (as illustrated in Figure 2.7) provides the possibility of this interaction which has an importance at high erbium concentrations. The rate equation for this interaction can be summarized as:

$$\left.\frac{\partial N_1}{\partial t}\right|_{upconversion} = \left.\frac{\partial N_4}{\partial t}\right|_{upconversion} = C_{up} N_2^2 \qquad (2\text{-}10)$$

$$\left.\frac{\partial N_2}{\partial t}\right|_{upconversion} = -2 * C_{up} * N_2^2 \tag{2-11}$$

This effect for the pump wavelength will give result to the following equations:

$$\left.\frac{\partial N_1}{\partial t}\right|_{upconversion} = C_3 * N_3^2 \tag{2-12}$$

$$\left.\frac{\partial N_3}{\partial t}\right|_{upconversion} = -2 * C_3 * N_3^2 \tag{2-13}$$

$$\left.\frac{\partial N_4}{\partial t}\right|_{upconversion} = C_3 * N_3^2 \tag{2-14}$$

2-7 The rate equation in EDWA

Pump light is absorbed by the Yb^{3+} ion and excite it from ground state $^2F_{7/2}$, to the higher energy $^2F_{5/2}$ state (Figure 2.8). Then the excited Yb^{3+} (donor) transfers its energy to the nearby ground state Er^{3+} (acceptor). The next step is transition of the electrons of excited Er^{3+} acceptors to the pump level $^4I_{11/2}$. As explained before we consider two kinds of upconversion and cross relaxation's between erbium ions and erbium-ytterbium ions as shown in Figure 2.8. Therefore, the multilevel rate equations for the coupled Er^{3+}-Yb^{3+} system are as follows:

$$\frac{\partial N_1^{Yb}}{\partial t} = -R_{12}^{Yb} N_1^{Yb} + R_{21}^{Yb} N_2^{Yb} + \frac{N_2^{Yb}}{\tau_{21}^{Yb}} + K_{tr} N_2^{Yb} N_1 - K_{ba} N_1^{Yb} N_3 \tag{2-15}$$

$$\frac{\partial N_2^{Yb}}{\partial t} = R_{12}^{Yb} N_1^{Yb} - R_{21}^{Yb} N_2^{Yb} - \frac{N_2^{Yb}}{\tau_{21}^{Yb}} - K_{tr} N_2^{Yb} N_1 + K_{ba} N_1^{Yb} N_3 \tag{2-16}$$

$$N_1^{Yb} + N_2^{Yb} = N_{0Yb} \tag{2-17}$$

$$\frac{\partial N_1}{\partial t} = A_{21}N_2 + W_{21}N_2 - W_{12}N_1 - R_{13}N_1 + R_{31}N_3 + C_{up}N_2^{\,2} - C_{14}N_1N_4 + C_3N_3^{\,2} - K_{tr}N_2^{Yb}N_1 + K_{ba}N_1^{Yb}N_3 \tag{2-18}$$

$$\frac{\partial N_2}{\partial t} = A_{32}N_3 - A_{21}N_2 - W_{21}N_2 + W_{12}N_1 - 2C_{up}N_2^{\,2} + 2C_{14}N_1N_4 \tag{2-19}$$

$$\frac{\partial N_3}{\partial t} = -A_{32}N_3 + R_{13}N_1 - R_{31}N_3 + A_{43}N_4 - 2C_3N_3^{\,2} + C_3N_3^{\,2} + K_{tr}N_2^{Yb}N_1 - K_{ba}N_1^{Yb}N_3 \tag{2-20}$$

$$\frac{\partial N_4}{\partial t} = C_{up}N_2^{\,2} - C_{14}N_1N_4 - A_{43}N_4 + C_3N_3^{\,2} \tag{2-21}$$

$$N_1 + N_2 + N_3 + N_4 = N_{0Er} \tag{2-22}$$

In the above-mentioned equation $N_{0Yb}(x,y)$ and $N_{0Er}(x,y)$ are ytterbium and erbium ion concentrations (in m^{-3}), and $N_1^{Yb}(x,y,z,t)$ and $N_2^{Yb}(x,y,z,t)$ are the electron concentrations of Yb^{3+} in the ground and excited states, respectively . Similarly, N_1, N_2, N_3 and N_4 are electron concentrations of erbium energy levels, and R_{21}^{Yb}, R_{12}^{Yb} and τ_{21}^{Yb} are the pump emission rate, absorption rate, and stimulated emission lifetime of ytterbium, respectively. W_{12} and W_{21} are the signal absorption and emission rates. R_{13} and R_{31} are the pump absorption and emission rates of erbium (note that $R_{31} = 0$, since $\sigma_{e31} = 0$). $A_{21}=1/\tau_{21}$ represents the spontaneous transition rate, and $A_{32}=1/\tau_{32}$ and $A_{43}=1/\tau_{43}$ are the non-radiative relaxation rates. The upconversion coefficients C_{up} and C_3, and the cross-relaxation coefficient C_{14} are considered for modeling upconversion and cross-relaxation

effects [2-27]. Finally, K_{tr} and K_{ba} coefficients are for energy transfer from the Yb^{3+}-system to Er^{3+}-system and vice versa, respectively. In Figure 2.8 all transitions except cross relaxation pathways are shown.

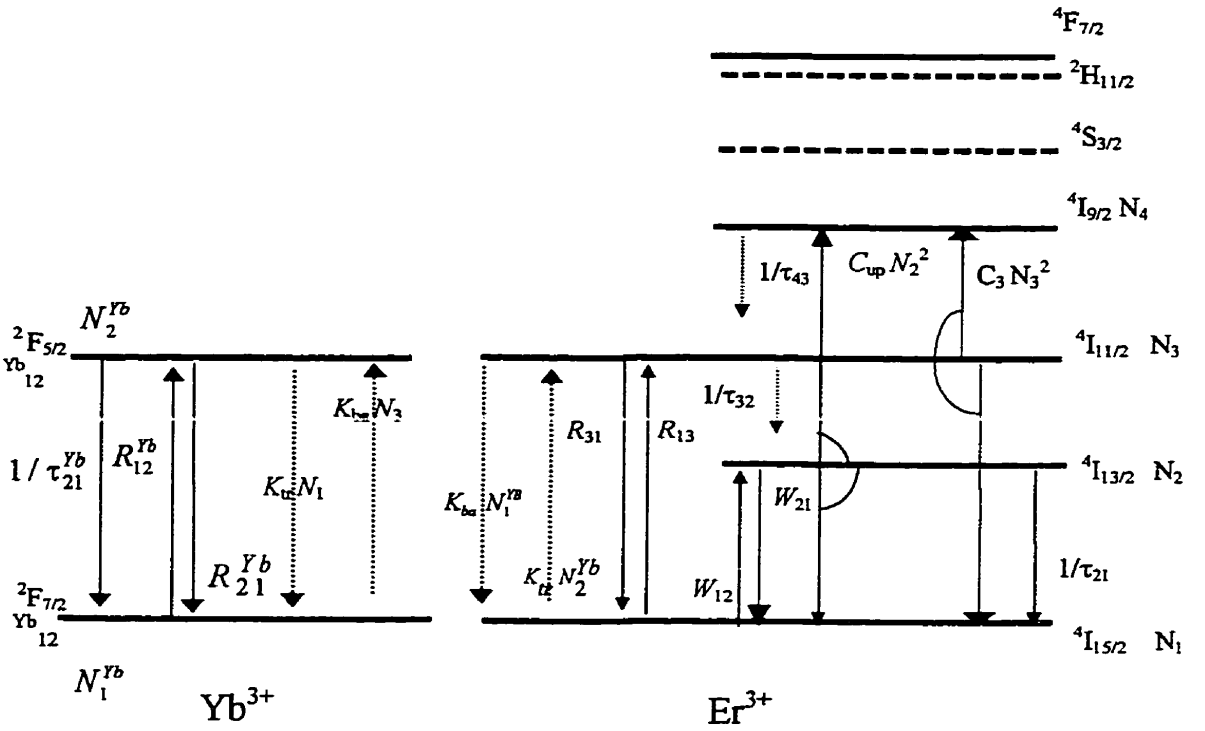

Figure 2.8 Energy level transitions for Er^{3+}/Yb^{3+} systems.

2-8 Gain definition and calculation

A numerical simulation was done by Shooshtari et all [2-33], using the parameters of the QX/Er glass. We explain the method briefly:

In a glass with N_i and N_j electron distributions, amplification of a plane wave propagating in the z-direction (in steady state regime) could be written as

$$\frac{dI_\nu(z)}{dz} = (\sigma_{eji} N_j - \sigma_{aij} N_i) I_\nu = g_{op} I_\nu(z) \qquad (2\text{-}23)$$

where g_{op} is the "optical gain" of i and j levels in a glass with N_i and N_j electron

distributions. A complete derivation of this formula is explained in appendix.2. This treatment assumes a single mode channel waveguide with propagation along the z-axis. In the steady state regime, having active ions with population densities of $N_i(x,y,z,t)$, $N_j(x,y,z,t)$ at energy levels of E_i and E_j, amplification of mode power can be calculated by imposing $\frac{\partial}{\partial t} \equiv 0$ in the rate equations.

Rate equations, ASE+, ASE- (Amplified Spontaneous Emission), signal and pump propagation will enable to analyze the erbium-ytterbium doped waveguides. The method and solution of these equations are detailed by Shoostari et al in (2-33) and briefly mentioned in appendix3.

2-9 Results

Figure 2.9 shows the variation of gain with pump power for several upconversion coefficients. There is good agreement between experimental and calculated curves for an upconversion coefficient of 1.4×10^{-23} m^3 s^{-1}. Hence it is assumed that the mode profiles, at pump and signal wavelengths, of the fabricated waveguide are identical to the theoretically calculated ones. In practice, this assumption may not be completely true and since gain is sensitive to the overlap between pump and signal mode profiles, some error may occur in the evaluation of upconversion coefficient.

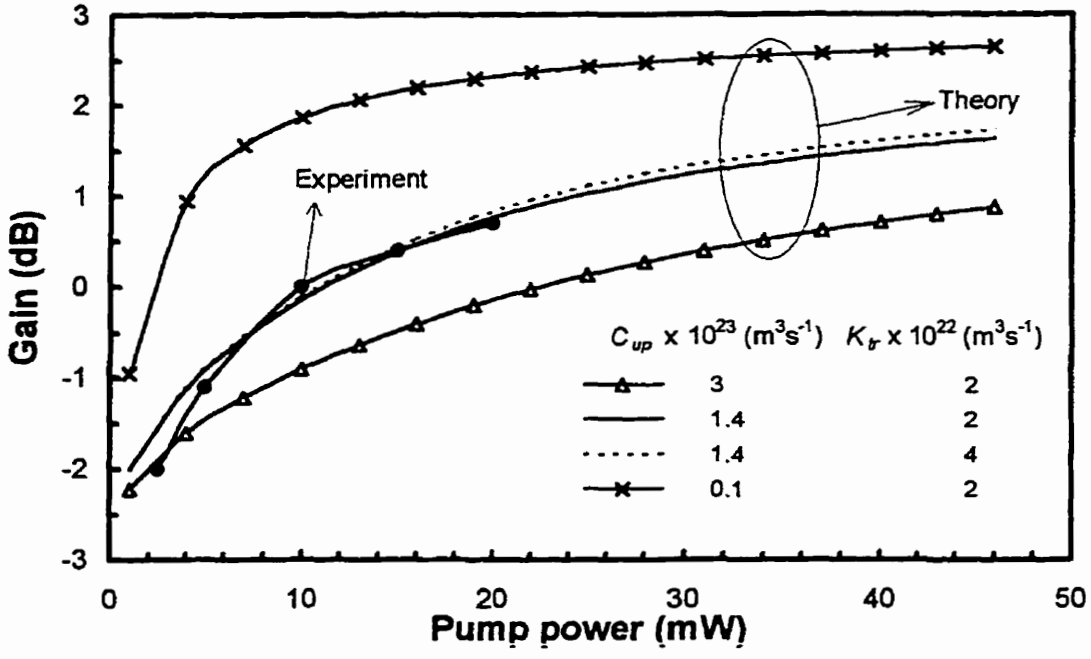

Figure 2.9 Experimental and theoretical gain versus pump power.

The amplifier length for the simulation is 6 mm. Input signal power is 10 μW at 1.530 μm, and pump wavelength is 1000 nm. Theoretical results are obtained with different upconversion coefficients and ytterbium to erbium cross relaxation's coefficients. Upconversion coefficient is also assumed to be a linear function of erbium concentration, as a consequence of the dipole-dipole interaction assumption [2-37].

For low Yb^{3+} concentrations, the coefficient of cross relaxation between erbium and ytterbium ions, K_{tr}, is largely independent of Er^{3+} concentration and is a linear function of Yb^{3+} concentration [2-38] [2-39]. In a silicate glass with 2 x10 $^{+27}$ m^{-3} of Yb^{3+} concentration, the reported K_{tr} is 5 x 10^{-22} m^3 s^{-1} [2-38]. In phosphate glasses, K_{tr} is smaller than in silicate glasses because of the larger separation between erbium and ytterbium ions. Figure 2.9 also shows that K_{tr} does not have a significant effect on

amplifier gain for this glass. From calculations, $K_{tr} = 2 \times 10^{-22}\ m^3\ s^{-1}$.

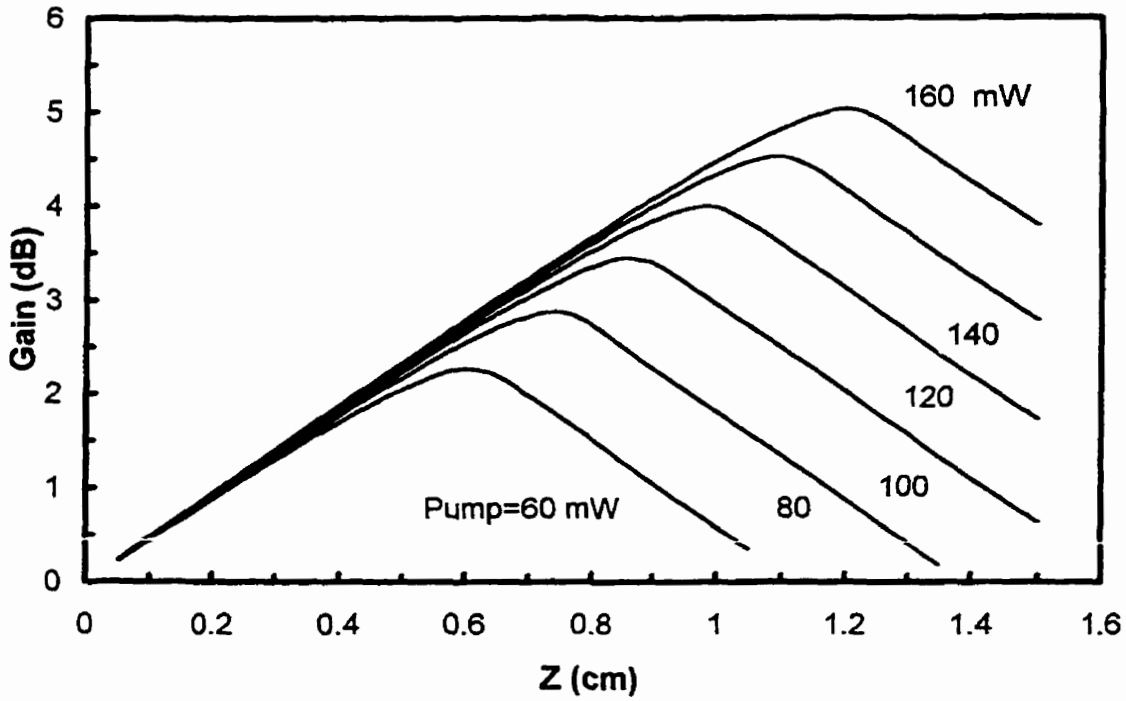

Figure 2.10 Small signal gain variation along waveguide amplifier, z, for several input pump powers.

The population densities N_3 and N_4 are much less than N_1 and N_2. Therefore, the values of the cross relaxation coefficient between erbium ions, C_{14}, and the upconversion coefficient of pump level, C_3, do not have a significant effect on amplifier gain for pump power employed in this study. The pump level upconversion rate, Er^{3+} ions cross relaxations and cross relaxation between Er^{3+} to Yb^{3+} rates have been neglected in the rate equations due to their small effect comparing to the other effects.

Figure 2.10 shows theoretical gain variations along the amplifier for several pump powers. The amplifier length is 1.5 cm, input signal power is 10 μW at 1.530 μm , and

pump wavelength is 974 nm.. At this pump wavelength, for large pump power, a maximum of amplifier gain was obtained.

Table 2-2. Parameters of QX/Er glass with 1.65 wt% Er_2O_3 and 22 wt% Yb_2O_3.

Er^{3+} concentration, N_{0Er}	$1.5 \times 10^{+26}$ m^{-3}
Yb^{3+} concentration, N_{0Yb}	$1.9 \times 10^{+27}$ m^{-3}
Er^{3+} emission cross section, σ_{e21} (1.530 μm)	9.0×10^{-25} m^2
Er^{3+} absorption cross section, σ_{a12} (1.530 μm)	6.5×10^{-25} m^2
Er^{3+} emission cross section, σ_{e31} (974 nm)	0
Er^{3+} absorption cross section, σ_{a13} (974 nm)	2.58×10^{-25} m^2
Er^{3+} emission life time, τ_{21}	7.9 ms
Er^{3+} emission life time, τ_{32}	1.0 ns
Yb^{3+} emission cross section, σ_{e21}^{Yb} (974 nm)	1.0×10^{-24} m^2
Yb^{3+} absorption cross section, σ_{a12}^{Yb} (974 nm)	1.0×10^{-24} m^2
Yb^{3+} emission cross section, σ_{e21}^{Yb} (1000 nm)	0.65×10^{-24} m^2
Yb^{3+} absorption cross section, σ_{a12}^{Yb} (1000 nm)	0.15×10^{-24} m^2
Yb^{3+} to Er^{3+} cross-relaxation coefficient*, K_{tr}	2.0×10^{-22} m^3 s^{-1}
Yb^{3+} emission life time, τ_{21}^{Yb}	2.0 ms
Er^{3+} emission life time, τ_{43}	1.0 ns
Upconversion coefficient, metastable level *, C_{up}	1.4×10^{-23} m^3 s^{-1}

* obtained by fitting .

Figure 10-2 shows that the small signal gain of a 1.0 cm long channel waveguide amplifier is ~ 4.2 dB at 120 mW pump power. The width of the beam is 6.7 μm and its height is 4.8 μm at signal wavelength, i.e. beam area is ~25 μm^2. Although the beam area is rather large, a high gain per unit length of 4.2 dB/cm can be attained due to the high ytterbium concentration. A 1.1 mm thick sample was used to measure the absorption cross section at signal wavelength. The fluorescence measurement results of the sample were also used to calculate its emission cross section at signal wavelength using McCumber theory [2-24]. This glass has similar characteristics at pump wavelength as the one used in [2-36]. Therefore, the reported values in [2-36] were used for absorption and emission cross sections and emission lifetime at pump wavelength.

In the next chapter we will discuss the characterization and measurement routines for mode profile, loss measurement and gain of EDWA.

CHAPTER 3

Erbium-doped waveguide fabrication process

3-1 Glass characteristics and parameters

Three different glasses were chosen to fabricate the optical amplifier. These glasses (commercially available from Kiger™ [3-1]) consisted of the same basic structure: QX/Er with varying concentration of the Erbium and Ytterbium dopants. The dopants concentrations of the glasses were as follows:

1- 22% wt Yb and 1.65% wt Er

2- 22% wt Yb and 2.22% wt Er

3- 22% wt Yb and 2.75% wt Er.

Note that in some of the references the concentration is given by ion/cc units instead of the weight percent (%wt), which can be calculated as

$$N_t = \frac{2 * D * Wt * N_A}{M}. \qquad [3\text{-}1]$$

In the above mentioned formula parameters are defined as:

D = Density of the glass, which is 2.90 g/cm^2 for all the QX/Er glasses.

Wt = Weight percent of Er_2O_3 and Yb_2O_3.

M = Molecular mass for Er_2O_3 = 382.52 g and Yb_2O_3 = 394.08.g

Thus we are able to calculate N_t (erbium concentration in ions/cc) for each.

Table 3-1 Erbium and Ytterbium concentrations in the QX/Er glass.

Glass # 1	Er = 1.65wt% Yb = 22wt%	Er = 1.50 X 10^{20} ions/cc Yb = 1.95 X 10^{21} ions/cc
Glass # 2	Er = 2.22wt% Yb = 22wt%	Er = 2.02 X 10^{20} ions/cc Yb = 1.95 X 10^{21} ions/cc
Glass # 3	Er = 2.75wt% Yb = 22wt%	Er = 2.51 X 10^{20} ions/cc Yb = 1.95 X 10^{21} ions/cc

A comprehensive study conducted by the Kiger™ Company determines the concentration of ytterbium that yield for optimal pump efficiency [3-2]. One of the distinct advantages of the selected base glass is its capability to accept high concentrations of Yb_2O_3. The Yb^{3+} ion concentration for this base glass could vary from 1.5×10^{21} to 2.25×10^{21} ions/cc and may even be increased to over 3.0×10^{21} ions/cc. Experiments show that Yb^{3+} ion concentrations of more than 1.9×10^{21} ions/cc cause a decrease in efficiency [3-2]. An increase of the Yb^{3+} concentration leads to increase in absorption of the pump energy and non-radiative energy transfer from Yb^{3+} to Er^{3+}, thus improving the Er^{3+} laser efficiency. On the other hand, excessive Yb^{3+} concentrations will cause an increase in the back-transfer rate from Er^{3+} ($^4I_{11/2}$-$^4I_{15/2}$) to Yb^{3+} ($^2F_{7/2}$-$^2F_{5/2}$). In addition, a high Yb3+ concentration leads to inhomogeneous pumping.

The specifications of the QX/Er Glass are collected in table 3-2.

Table 3-2. General Parameters of QX/Er glass

Laser wavelength peak (nm)	1535
Emission cross section ($X10^{-20}$ cm^2)	0.8
Fluorescence lifetime (μs)	7900
Fluorescence linewidth (nm) FWHM	55.0
Index of refraction at 589 (nm)	1.533
Index of refraction at 1535 (nm)	1.521
Transformation information (°C)	450
Deformation temperature (°C)	485
Density (g/cc)	2.90

The hydroxyl anion (OH^-) has a strong negative influence on fluorescence intensity for most infrared laser active ions. Non-radiative energy transfer between excited state of the active ion and the OH^- anion leads to a reduction in the fluorescence intensity. The OH^- concentration in QX/Er is below 0.1 wt % making it suitable enough for further experiments such as laser glasses.

In a phosphate glass, the PO_4^{3-} tetrahedron is the principal building unit. Due to the pentavalency of phosphorus, only three out of four corners of a tetrahedron network are connected resulting in a weak structure compared to silicate glasses. Glasses with such a structure typically exhibit low physical strength and poor chemical durability. The phosphate glass structure could be fortified by introducing glass network intermediates

such as B_2O_3 and Al_2O_3 [3-3]. The combination of a boron-oxygen tetrahedron or an aluminum-oxygen tetrahedron with a neighboring phosphorus-oxygen tetrahedron would increase the number of bridging oxygen resulting in a stronger structure. This helps the durability and strength of QX/Er glass types. The main components of the glass are PO_4, Al_2O_3, Na_2O and BaO.

One of the main objectives in laser applications is to have a glass with a high order of homogeneity that is required as laser materials. It means the glass should have no bubble or striae. The principle to achieve these requirements is simple, however it is usually difficult to be accomplished. The striae removal is the most difficult step of producing phosphate glasses due to their strong vaporization compared to silicate glasses. Thus the fine melt temperature selection is critical. This temperature must be high enough to maintain the glass at a low viscosity to remove bubbles. On the other hand the temperature has to be set as low as possible to minimize vaporization which would lead to striae. These factors were considered as mentioned by the producer, during the fabrication of the glass.

Another important factor especially during ion exchange is that it should be able to sustain good surface quality in the molten salt at elevated temperatures. This factor was investigated for $NaNO_3$ molten salt of the QX/Er family. The weight loss was measured as low as 0.15 mg/cm^2 for 20 hours at 350 °C [3-4], and the quality of the surface was evaluated suitable for ion exchange experiments.

To compare the surface quality of the glass and also possibility of the process for

other base glasses, we also checked two other Erbium-doped phosphate glasses, seemed suitable for ion exchange. Results from ion exchange in 400 °C for these series (QE-7) show corrosion and cracks indicating lower durability and resistance of these glasses to high temperature (Figure 3.1). The cracks on the samples after ion exchange show a low resistivity against the thermal shock. Therefore further ion-exchange experiments on these base glass are expected to be redundant.

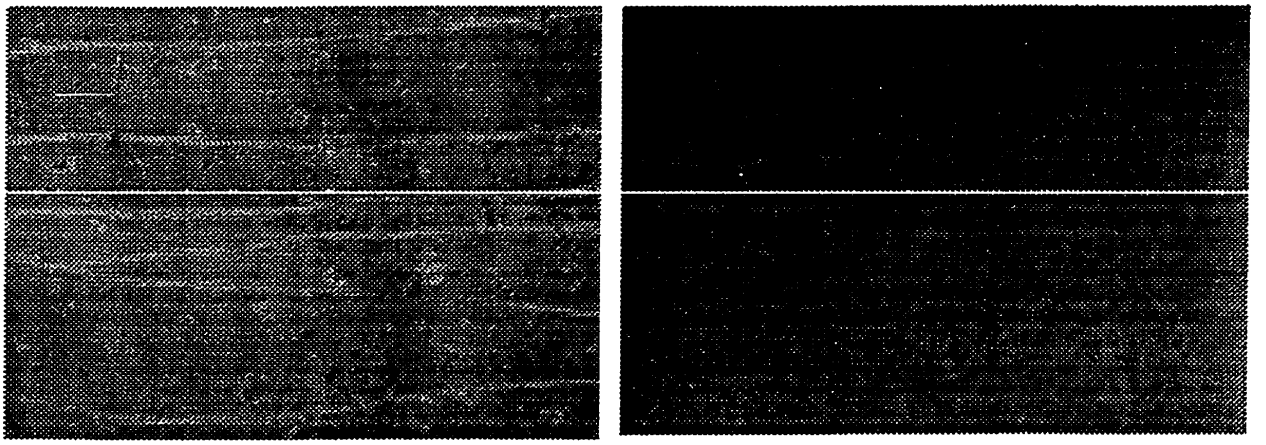

(a) (b)

Figure 3.1 (a) Cracks and damages in QE7 glass

(b) Qx/Er in ion exchange process

3-2 Ion-Exchange Process

Important parameters that need to be determined for the fabrication of the channel waveguides are:

- Diffusion depth
- Ion exchange time

- Effective refractive index
- Channel widths (to obtain a single mode channel waveguide at 1550 nm)

The first step to fabricate an ion exchange channel waveguide is to evaluate the diffusion depth, and the effective refractive index, Neff, using a slab. The following section details the method of fabrication and the calculations necessary for this process.

3-3 Slab waveguide fabrication on rare earth doped glasses by ion exchange

Samples dimensions were 1" × 1" × 1" transmission pink colored bulk size glass. To make the slab waveguide, glasses were cut to thickness of 1 mm and polished. Three different polishing powders were used in sequence. Smoothness of the samples was varified under the optical microscope and profilometer (Dektak 3030ST Surface texture analysis system) before ion exchange. Cleaning procedure included several steps: a regular detergent was used to remove residual organic material from the glass surface. The glass then was rinsed in diionized water. The samples were submerged in warm TCE (Tetrachloroethan) acetone and propanole in turn for the period of 15 minutes. Finally the glass was completely dried under a flow of nitrogen. The molten salt for the ion exchange was then prepared. One of the problems occurring during the ion exchange using phosphate glasses is the effect of OH^- present in the salt (which is in our case potassium nitrate KNO_3). The OH^- group are present in the salt even after the high temperature (up to 400 °C) reached during ion exchange process. The OH^- group not only contributes to the losses at 1550 nm wavelength but also attacks the phosphate glass

and damages its surface. Although the glass seems to be resistant against humidity, we tried to remove the OH^- groups from the salt before the melting point as it fixes its bonds after that. The salt was placed in the furnace in an aluminum boat. Aluminum was as our container (boat) due to its high melting point. The temperature could easily reach 400 °C (note that the melting point of the KNO_3 is 334°C) without having any chemical reaction between aluminum and salt or the glass. Also the low expansion coefficient of aluminum during cooling down (as compared to other materials like glass) enabled the recovery of the boat.

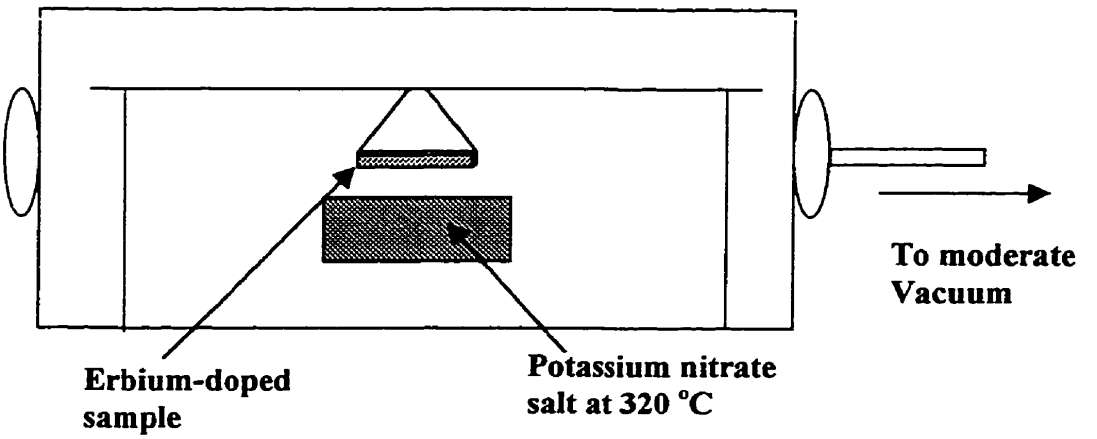

Figure 3.2. First step of preparation of ion exchange process.

The boat was filled up to $4/5^{th}$ of its volume with the white potassium nitrate powder and placed in the furnace together with the sample, which were mounted on an aluminum holder and kept out of the salt. The sample and the salt were heated up to 320 °C (around 15 degrees below the melting point of potassium nitrate) in moderate vacuum for 24 hours. The furnace had accurate thermostats in different places in order to stabilize

the variation of the temperature caused by the heat suction through vacuum. The air suction accompanying the heating of potassium nitrate in the boat shaped form container (designed for maximum surface contact for efficient moisture removal) removes residual hydroxyl anions from the salt. Figure 3.2 depicts this process. After 24 hours in vacuum, as the temperature of the furnace is increased to 400 °C the salt changed from the solid state to the melt as is shown in Figure 3.3

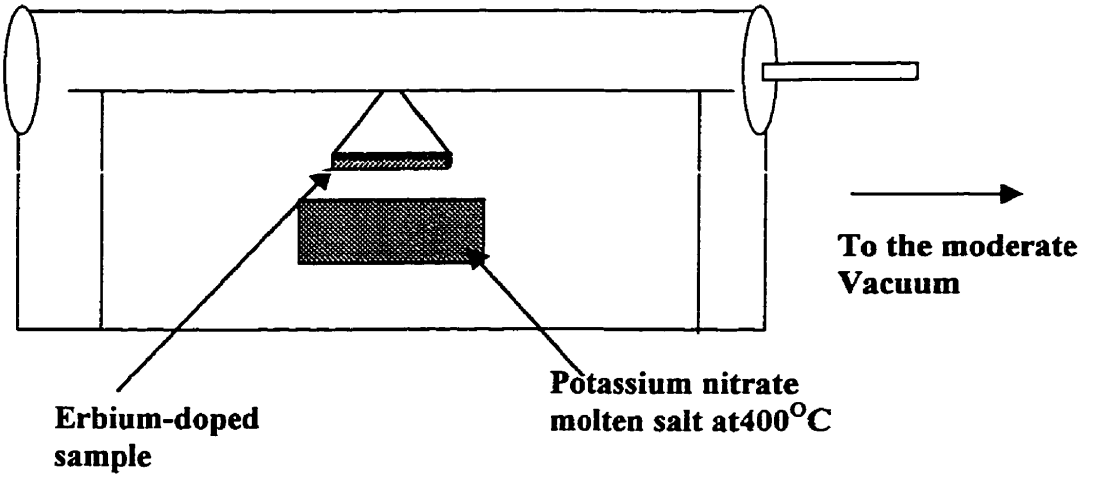

Figure 3.3 Second step of preparation of ion exchange process.

We also waited one hour for stabilization of the environment for the next step which would be the ion exchange. The temperature of the furnace was chosen to be 400 °C as at this temperature not only is the salt in a molten state (m.p 335 °C) but the mobility of the ions is enhanced, maximizing the chance of the ion exchange.

The transformation temperature of the glass is around 450 °C and the process was fairly far from this temperature. After an hour we injected argon flow to the furnace and

submerged the sample into the molten salt (Figure3.4) .

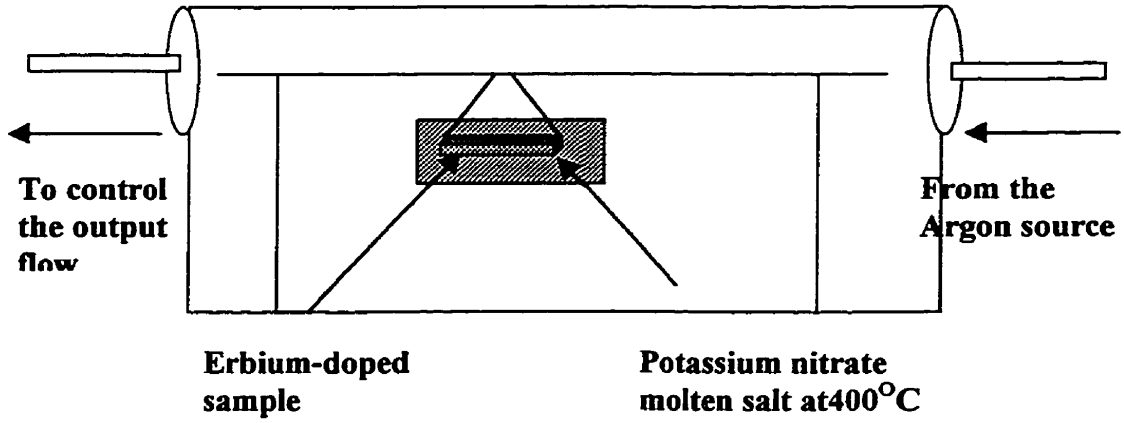

Figure 3.4 Ion exchange process.

All these steps should be done with a great deal of caution and very fast to minimize the contamination's introduce by impurity. From results obtained for glasses with similar molecular structure and same material to the QX/Er glass a 2-hour ion exchange period was chosen for slab waveguide fabrication. Prism coupling experiments revealed that in order to have at least 3 modes at 632.8 nm (which leads us to a single mode profile at 1.55 nm in 5μm channel) it is necessary to extend the time of ion exchange to 4 hours. After 4 hours, the waveguide was removed from the salt and gradually cooled down. This process should not be very fast because it would result very rapid expansion in the glass and hence cracking. However, slow cooling periods would cause continuation of the ion exchange process as well as expansion in the diffusion profile. After cooling down to the room temperature the samples were rinsed with de-ionized water to remove the solidified salt covering the glass. Sometimes this process requires heat but it should be noted that high temperature could cause continued ion

exchange. The waveguide was characterized in the following manner:

- Surface quality of the ion exchanged slab waveguide was examined under an optical microscope (Figure 3.1 (a)) which proved to be acceptable.
- Waveguiding at 632.8 nm He-Ne laser and the number of the modes were investigated by Prism Coupling setup as will be explained in the next section.

3-4 Prism coupling experimental results

The experimental set-up for the measurement of coupling angles θ_m is shown in Figure 3.5. The slab waveguide to be measured is mounted on a goniometer. The prism's base is pressed firmly on the waveguide surface with a spring-loaded clamp. A laser beam (He-Ne at 632.8nm) is coupled into the slab waveguide by the prism to excite guided modes. The guided light in each mode is coupled out of the polished end-face of the waveguide by an objective lens to a screen. By rotating the goniometer, the incident angle θ can be measured. When θ reaches the angle corresponding to the β_m or the effective refractive index (N_m) of one of the modes maximum intensities or the m line can be seen clearly on the screen. To measure the angle θ_m, a reference for which the beam normal to the plane of the incident is used as

$$\theta_m = \theta'_m - \theta_{normal} \qquad [3\text{-}2]$$

The angle θ'_m is read from the goniometer which is relative to its zero degree. To find θ_{normal}, the goniometer should be rotated to have the beam reflected off the prism back on the incoming beam. Then θ_{normal} is also read from goniometer relative to its zero degree.

Therefore, θ_m is the true angle illustrated in Figure 3.5. Once the two coupling angles for two different modes are measured, the thickness d and the refractive index n_f can readily be calculated.

By directing the output light corresponding to each guided mode and maximizing the output of the detector (or in our case the brightest position on the screen) while adjusting the incident angle θ we can determine the coupling angle θ_m for the m_{th} guided mode, and calculate the corresponding effective refractive index.

The dispersion equation governing the coupling modes of the film and the effective refractive index is given by [3-5]:

$$V\sqrt{(1-b_m)} = m*\pi + Tan^{-1}\sqrt{\frac{b_m}{1-b_m}} + Tan^{-1}\sqrt{\frac{b_m+a}{1-b_m}} \qquad \text{m=0,1,2...} \qquad \text{[3-3]}$$

With $V = \frac{2*\pi}{\lambda} * d * \sqrt{n^2_f - n^2_s}$, $b_m = \frac{N_m^2 - n_s^2}{n_f^2 - n_s^2}$ and $a = \frac{n_s^2 - n_c^2}{n_f^2 - n_s^2}$

where n_f, n_s n_c, are the refractive index for the film, substrate and the cover, respectively. Wavelength of the excitation source is λ and d is the thickness of the ion exchanged layer. The integer m assigns each equation to its corresponding modes. To obtain the refractive index and the thickness of the waveguide, we need two equations for two different m. Usually, the first two common modes, i.e. m=0 and 1, are used. Note that for every two modes one obtains a value for d and N_m. Therefore the measurement of more modes leads to more accuracy.

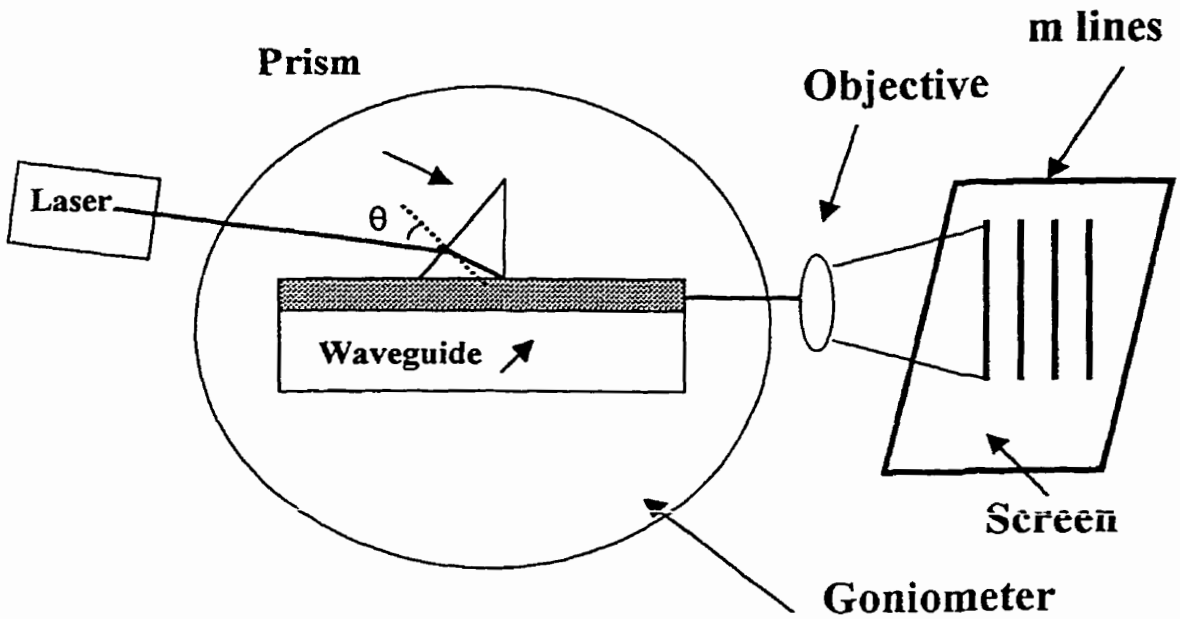

Figure 3.5 Prism Coupling Setup.

The solution for the dispersion equation was done numerically. The two equations obtained by the two modes can be solved simultaneously. However, an easier step is as follows. By calculating N_0 and N_1 in equation [app4-5] d can be found in equation [3-3] as a function of n_f.

$$V\sqrt{(1-b_1)} = \pi + Tan^{-1}\sqrt{\frac{b_1}{1-b_1}} + Tan^{-1}\sqrt{\frac{b_1+a}{1-b_1}} \qquad [3\text{-}4]$$

Then the function $d(n_f)$ is replaced in equation [3-4] and is then solved for n_f using a personal computer.

These measurements were done for the samples and results for the three different

concentrations did not show any noticeable difference in angles. After 4 hours of ion exchange using He-Ne at 632.8 nm in prism coupling method, the three different concentrations had 3 well guided modes. The measurements of prism coupling were carried out 3 times and the average was used to calculate the effective refractive index. Results are shown in table 3-3.

Table 3-3 Results from prism coupling method

$N_{effective}$ for different modes	
N_0	1.5369
N_1	1.5357
N_2	1.5343
Refractive index of the glass n_s at 632.8 nm	1.532
Maximum refractive index change Δn	0.0065
Diffusion depth d (μm)	6

Because of the same base structure on QX series, we developed the refractive index profile of the QX/Er series same as the QX/Nd and then according to the figure 3-6 by extrapolating we found the refractive index of the QX/Er glass at 632.8nm. The results are reflected in Figure 3.6 .

Optonex © (Integrated Optics Design Software developed by Optonex Ltd.) was used to model the mode profile channel waveguide.

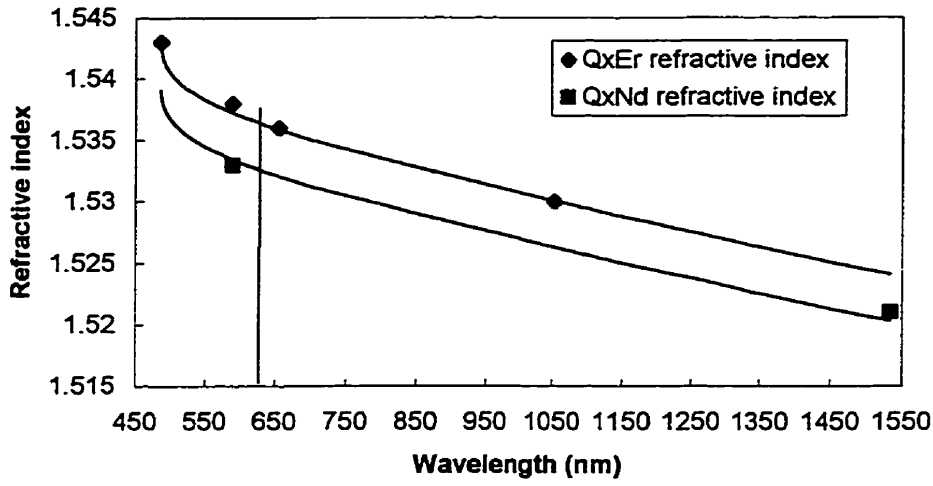

Figure 3.6 QX/Er and QX/Nd refractive index profile versus wavelength

There are three known parameters for the channel waveguide dimensions: diffusion *source width,* w, which could vary depending on the mask width, *Diffusion depth* d_x and *lateral diffusion distance* d_y which are the same as measured and calculated by the prism coupling method. The three different known parameters for the refractive index values are refractive index for *cover,* n_c ,which is air =1, *maximum index increase* Δn_{max}, calculated using prism coupling parameters as 0.0065 ,and *substrate* index n_s which is known from the data sheet provided by manufacturer . These parameters as well as the wavelength which will be used for the amplification experiment are in the table 3-4.

The refractive index distribution function from diffusion in the substrate is:

$$\Delta n(x,y) = \frac{\Delta n_0 * \exp(-y^2/d^2 y) * [erf(w/2 * d_x + x/d_x) + erf(w/2 * d_x - x/d_x)]}{2 * erf(w/2 * d_x)} \qquad y>0$$

which is used in Optonex © to develop the profile . The intensity of the mode profile is Figure 3.7 and Figure 3.8 .

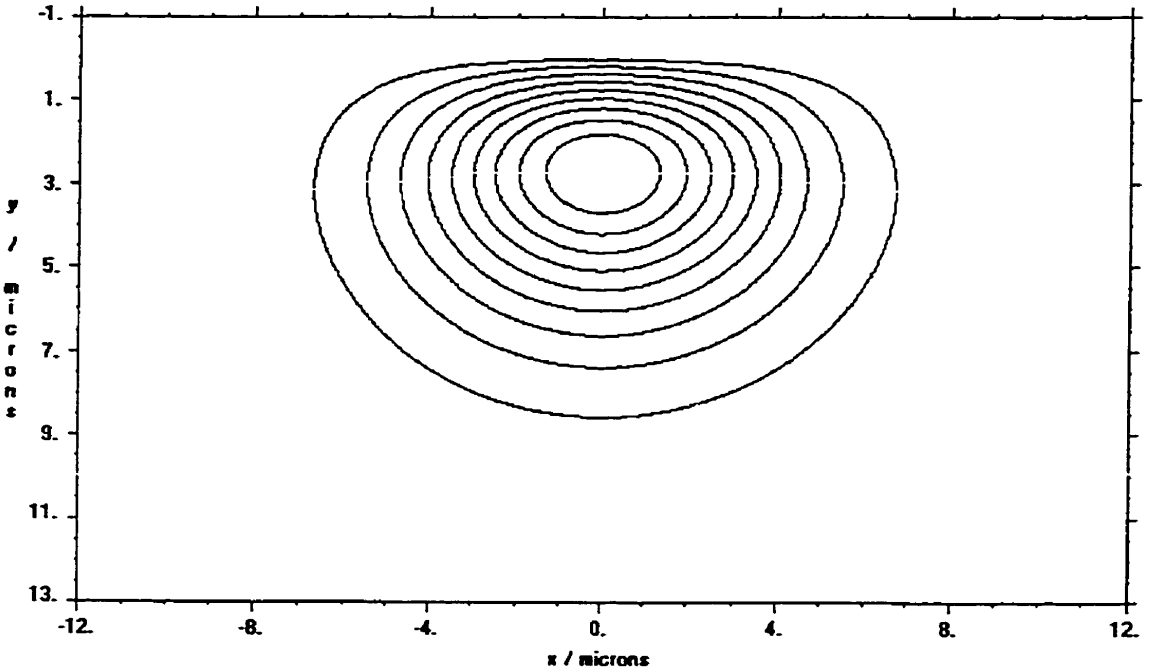

Figure 3.7 980 nm electric field profile from out to center 0.9 to 0.1 Neff=1.523749

Images of the ouput beam with an infrared camera (Plesae reffer to chapter 4) are in accordance with the simulation. Maximum mode intensities for signal wavelength 1.55μm and pump wavelength 980 nm are found at depth of 3.6 μm and 2.7 μm in the glass respectively. Using the Field Assist ion-exchange method could help in the confinement of the mode profile in the waveguide and also in matching both pump and signal as much as possible to improve the amplifications.

Table 3-4 Parameters for calculating the effective refractive index of the waveguide

Source width w (μm)	6
Diffusion depth d_x (μm)	6
Lateral diffusion distance d_y (μm)	6
Cover refractive index (Air)	1
Maximum refractive index increase Δn_{max}	0.0065
Substrate refractive index at1.55 nm	1.521

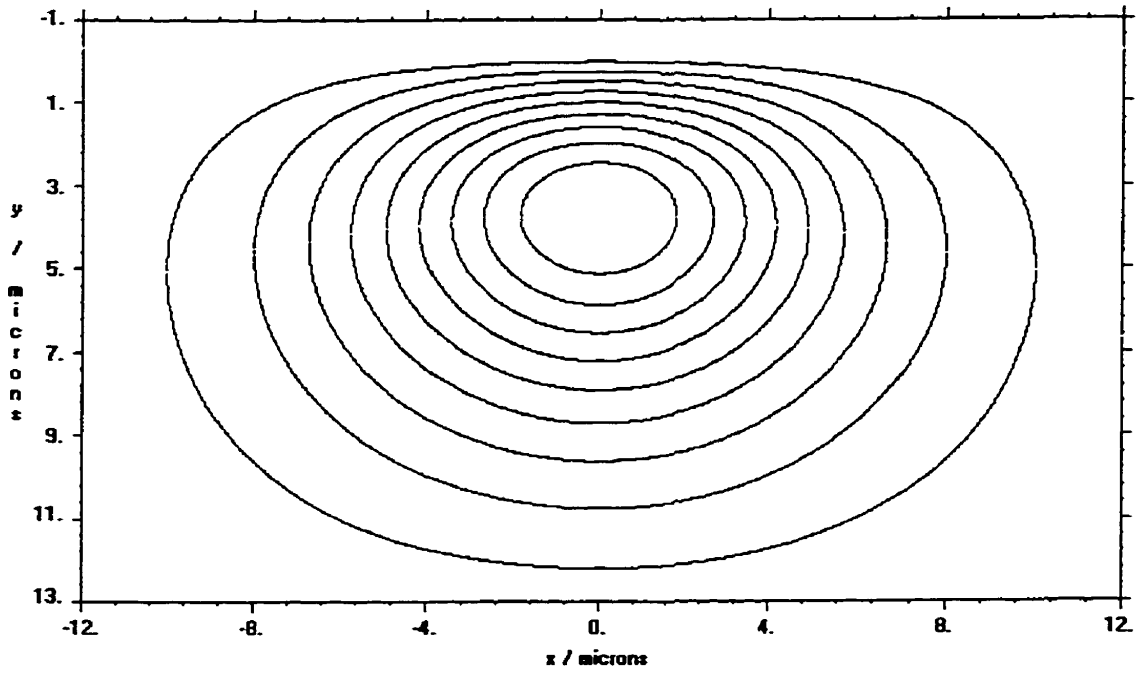

Figure 3.8 1550 nm electric field from out to center 0.1 to 0.9 Neff=1.522063

3-5 Erbium doped channel waveguide fabrication process

Fabrication of channel waveguide through ion exchange requires a photolithographic step. The channel fabrication process on QX/Er phosphate glass is summarized bellow:

Similar to slab waveguide fabrication, bulk glass was cut to be compatible with the size of the mask and polished. Uniform and smooth surface was ensured by a longer polishing time. Any bump or roughness in the glass would destroy attempts to fabricate waveguides with widths of 2 to 10 μm. The surface quality was checked under the microscope. The cleaning procedure was identical to the method previously described in slab waveguide fabrication section (chapter3,Å section3).

In the next step a mask is prepared for the ion exchange process . Aluminum was chosen due to its inertness toward the glass and salt. A layer of 1000 Å of aluminum was deposited on the sample as our mask, which was placed in an evaporator. Six pieces of aluminum wire with the length of 1 cm wrapped over the filament were evaporated in vacuum (10^{-6} mbar) when the current increased to 20 ampere to which is the start of the evaporation of aluminum.

The evaporation rate was controlled at 10 Å per second. An important factor is that the sample should be held in the same level of the detector and above the filament to have a uniform layer. This process continued until a layer of 1kÅ of aluminum covered the sample. A control sample was also put in evaporator as a witness to measure the layer

of the aluminum coated on the sample.

The sample was then spin-coated with a layer of photoresist. The speed was set to 3000 r.p.m. The spin coating of the HPR 504 photoresist from Shiply took 30 seconds. According to the data sheet of the Shiply and our results a uniform layer of 1 micron thickness was coated. This layer of the photoresist was suitable for the subsequent wet etching and UV exposure. The quality of the coated resist was also verified under the microscope to be a uniform film devoid of dust. The photoresist was filtered before to have a good film quality.

The sample was then placed inside the furnace and prebaked at 95 ^{0}C for 30 minutes. This process removed solvents and increased the viscosity of the film.

Next, using a chrome mask with 3 sets of 9 channels having 2-10 μm width and 2.54 cm length, the photoresist was exposed. The exposure time was 25 seconds and a mask aligner was used to ensure that the pattern and the edges of the glass was perpendicular to each other. This ascertains minimum coupling losses. It is also important to control the pressure of the mask on the film in order to prevent the underexposure film damages.

After exposure the photoresist was developed in HPRO 419 (from OCG.) For 2 to 5 minutes and the quality of the developed pattern was checked under the microscope. Due to the large differences in the waveguides widths, the broader waveguides developed faster than smaller ones. Longer development times resulted in over-developing and shorter time did not allow narrower ones to be developed completely. A compromise was

chosen. A positive photoresist was used, the exposed regions were removed during the developing, and the rest would work as a protection for etching. After developing step, the sample was completely rinsed by water to remove the traces of the developer.

To increase the strength of the bonds in the resist and help the resistance of the photoresist in the process of acid etching the samples were put inside the furnace for post-bake at 105 C^{o} for another 30 minutes.

In order to remove the aluminum in the opening, an acid solution consisting of 80% phosphoric acid, 5% nitric acid and 15% water was used. Selectivity of this mixture of acid was delicately in favor of the aluminum rather than the glass. It was important to

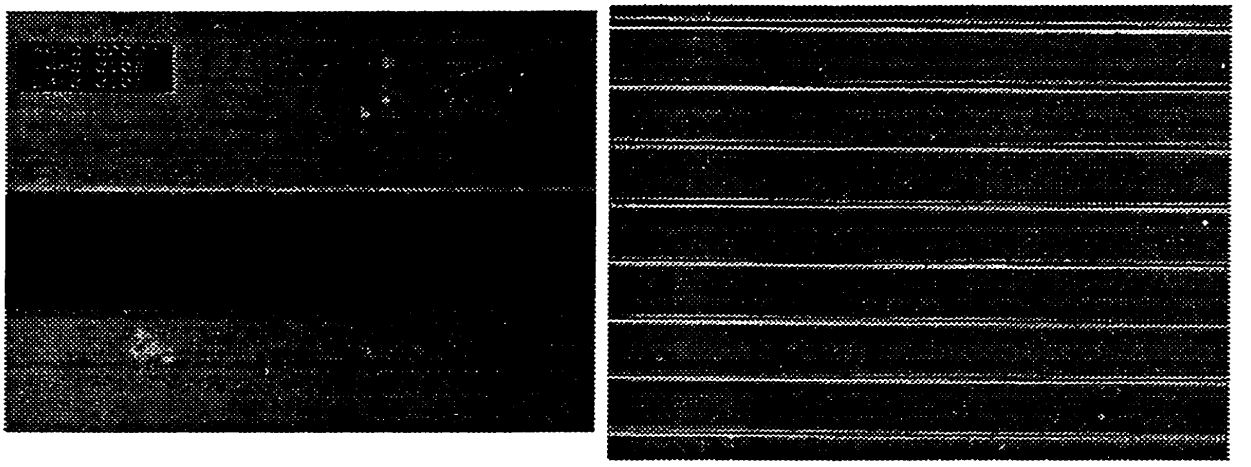

Figure 3.9 Different opening after photolithography

realize that the base, phosphate glass could be corroded by prolonged exposing to the acid. The sample was therefore placed in the acid for no more than 30-second periods to prevent etching of the base glass. Hence also, as the photoresist develops a compromise had to be reached in etching time due to the differences in channel widths.

Figure 3.9 shows the samples after the etching by acid. The photolithography is

uniform through the waveguide. It is worth noting that although we tried to control the etching rate and just etch the aluminum but a small amount of glass was etched by acid. Profilometry (DekTak) (Figure 3.10) showed that the etching depth was 1500 Å and comparing to the diffusion depths, and the small effect it has for the expanding of the ion exchange and changes of mode profile in ion exchange, it is negligible .

After each 30 second period of etching, the sample was rinsed completely with water to remove traces of acids, and inspected under the microscope.

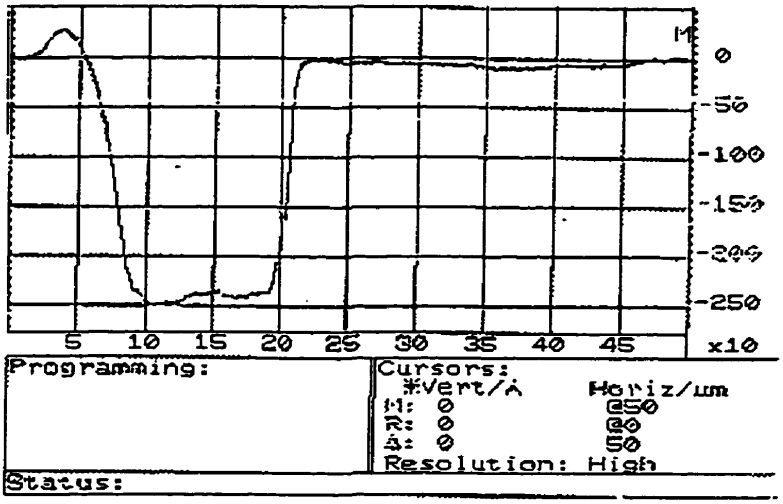

Figure 3.10 10μm channel after 30 second etching. Depth includes the 1000 Å of aluminum thickness

The ion exchange process then followed and was identical as slab waveguide fabrication especially with no changes in time and temperature.

After rinsing the sample with water, the remain of aluminum layer was removed. As further acid etching would damage the ion exchanged regions of the sample (we know that first few microns depth of ion exchange are the most important part in

refractive index change and therefore waveguiding) the aluminum was removed over the glass by carefully polishing using diamond paste up to 0.05 micron. The sample was secured onto a holder using wax and was polished manually with a special soft polishing cloth. Results (as seen under the microscope) proved no sign of aluminum (over the waveguides)(Figure 3.11).

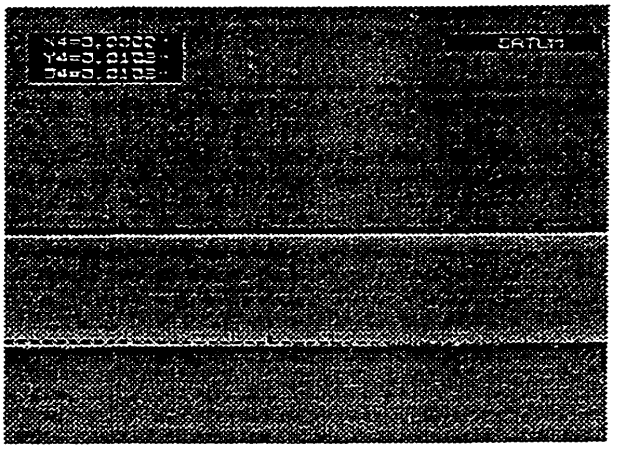

Figure 3.11 10μ channel after surface polishing.

Subsequently the sides of the sample were polished by 15 microns , 5 microns and 1 micron powder to maximize the coupling efficiency. Results show that the side which is polished should be as perpendicular as possible to the waveguide directions to minimize coupling losses .

Figure 3.12 shows the fabrication process, and the Figure 3.13 is the schematic of the waveguide. Characterization and relevant measurements made on the waveguide are described in the next chapter.

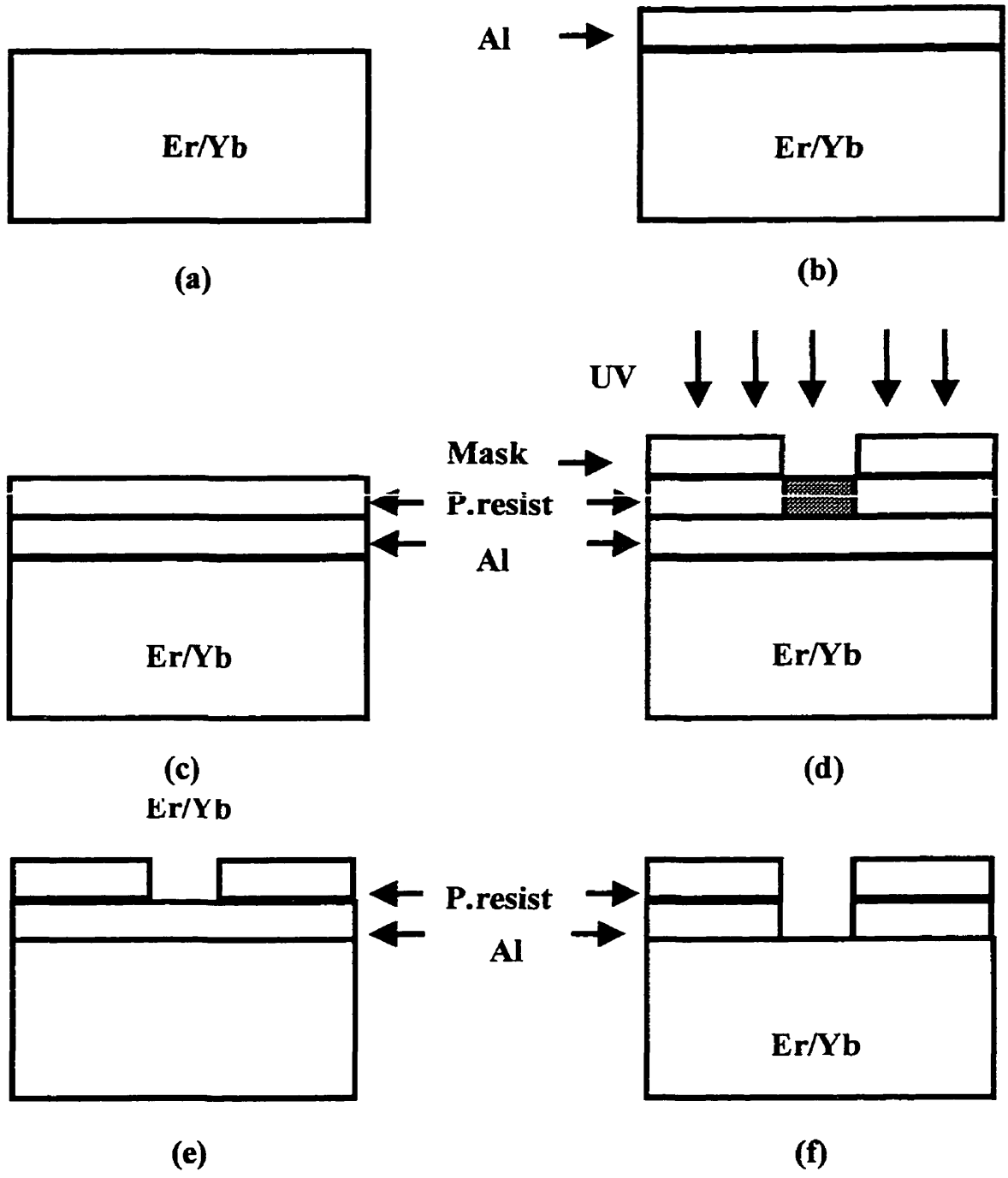

Figure 3.12 Photolithography process (a) through (f)

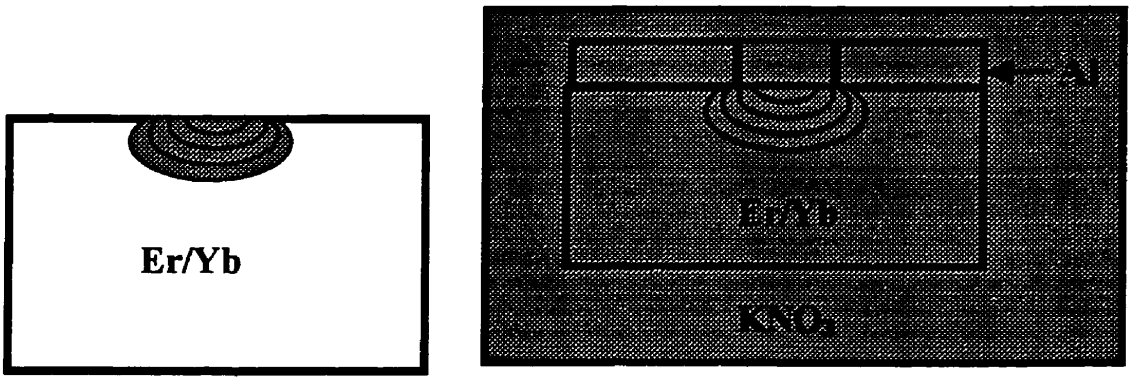

Ion exchange process

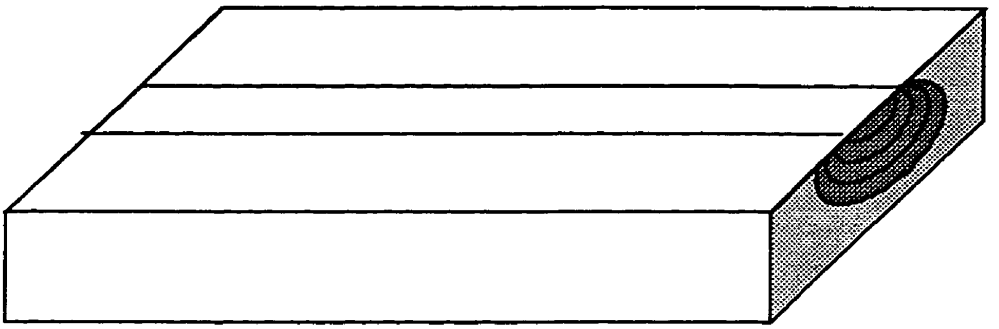

Figure 3.13 Schematic of the waveguide

Chapter 4

Erbium Ytterbium co-doped channel waveguide characterization

4-1 Introduction

This chapter describes characterization of Er/Yb co-doped channel waveguides fabricated by the ion exchange process. As well, optical signal amplification in the 1550 nm window will be discussed. This chapter is divided in three sections, the first of which describes the experimental setup for waveguiding at 632.8, 980, 1310 and 1550 nm. This is followed by coupling and propagation loss measurement at 1310 nm and 1550 nm, and finally gain measurement presented in different graphs with respect to pump and signal wavelength and power.

4-2 Guiding at 4 different wavelengths

Fabricated channel waveguides were tested using 4 different wavelengths. He-Ne laser emitting at 632.8 nm was used to align the setup. Figure 4-1 shows the schematic of this setup. The laser light was transmitted through a bare cleaved fiber which was placed as close as possible and perpendicular to the channel. The widths of the fabricated channels (as mentioned in chapter 3) were from 2 to 10 μm, all capable of guiding at this wavelength. A single mode fiber at1550 nm (SMF 28, 9 μm core diameter and 125 μm cladding) was chosen and placed on a micropositioner able to move in X-Y-Z directions to launch the light to the waveguide. In addition to that, two more degrees of freedom

was also added to the fiber setup by using a fiber holder capable of turning in two cylindrical coordinates of θ and ϕ angles to optimize the coupling efficiency. The sample itself was placed on an X-Y-Z micropositioner. The output light was collected with a 20X objective (lens) and passed through an attenuater before being captured by an infrared camera as shown in the figure 4-1. The results for 5 μm channel at 632.8 nm show that the output is multimode (3 modes) for this channel.

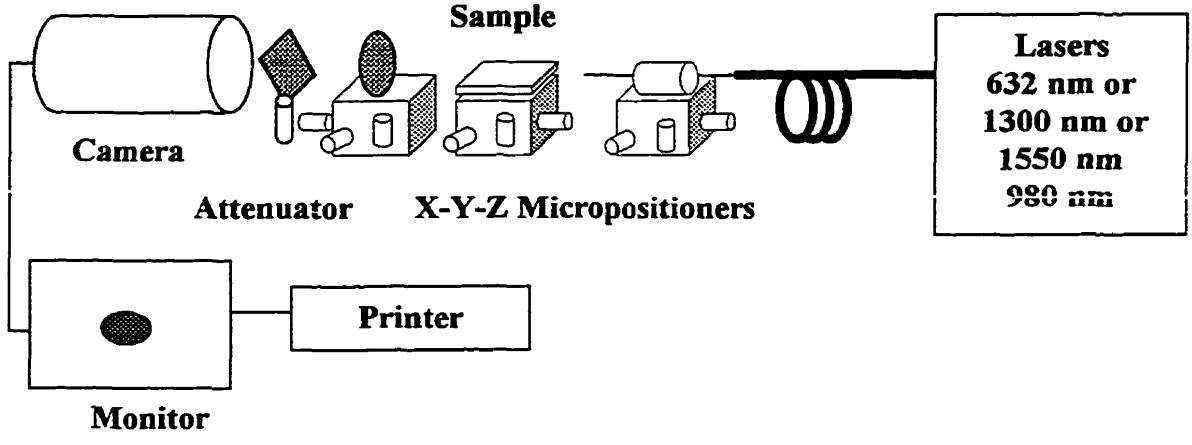

Figure 4.1 setup for viewing the mode profile

At 1310 nm , one well guided mode and one close to the cutoff were seen But using 1550 nm laser only a single but well guided mode were observed. Additional mode was not excited upon changing the angle of the fiber at 1550nm.

Next section will deal with loss measurement of the waveguides. The mode profiles of 5 μm and 6 μm wide channels at 1550 nm as captured by infrared camera and printed are shown in figure 4-2. As can be seen , mode profile is well circular and uniform.

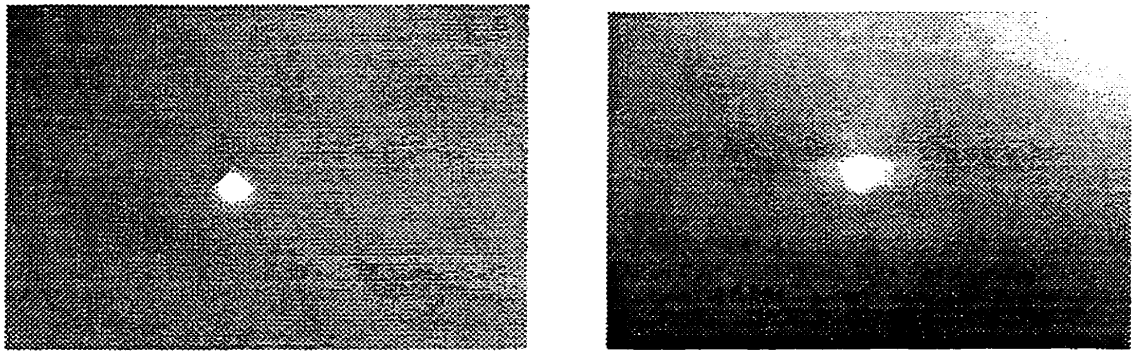

(a) (b)

Figure 4.2 Pictures of mode profile for (a) 5μm and (b) 6μm channel waveguide at 1.55 μm

4-3 Loss measurement

Loss measurements were performed using the techniques described in [4-1]. The loss measurement setup is shown schematically in figure 4.3 and the details of the measurement procedure are as follows: Laser light from the input fiber was coupled to the channel waveguide to be measured. Power from the output of the channel waveguide was collected by another fiber and directed to a germanium photodiode detector connected to a power meter. An optical microscope used to monitor the gap between the cleaved fiber end-faces and polished waveguide end-faces thus minimizing the misalignment errors. The input power and the output power from the fiber were measured. Next, instead of the fiber at the output, the light was collected by an objective (lens) through an iris and finally the light was directed from input fiber to the objective (lens) and then the detector. The net losses in each of the systems can be accounted for as:

- Fiber-Sample-Fiber-Lens-Detector

  The differences of power of input and output is due to these losses: $P_c + P_f + P_p + P_f + P_c + P_{obj}$, where P_c is coupling loss at the end-face which we assume the same for both faces due to the same polishing procedure at each side, P_f is Fresnel reflection loss which is negligible relative to the coupling loss and propagation loss, P_p is the propagation loss of the waveguide caused by fabrication and finally P_{obj} is the loss due to the lens.

- Fiber-Sample-Lens-Iris-Detector

  In the second setup the difference between input and output power is due to the following losses: $P_c + P_f + P_p + P_f + P_{obj}$. The losses are as defined before.

- Fiber-Lens-Detector

  Hence, the loss at this stage is due to the lens: P_{obj}.

Using the definition of loss as $dB = -10 * Log\left(\frac{P_{in}}{P_{out}}\right)$ and by measuring the input and output power at each step and assuming that Fresnel losses are negligible, the propagation loss and the coupling losses can be calculated. The measurements were done with a Germanium detector and an OSA (Optical Spectrum Analyzer). Fibers used were all SMF28 single mode at 1550 nm. The 1310 μm emission from a diode laser was used for loss measurement due to the fact that there is no material absorption at this wavelength. Propagation and coupling losses did not vary noticeably with channel waveguide dimensions. 5 μm channel was chosen due to its well guided single mode

profile on three type of glasses for loss, absorption and gain measurements. The results are collected in table 4-1.

Table 4-1 Loss measurement for different samples

	Er 1.65% Yb 22%	Er 2.22% Yb 22%	Er 2.75% Yb 22%
Length of the waveguide (mm)	6	12	12
Coupling loss (dB)	4.71	4.63	4.96
Propagation loss (dB)	0.1	0.05	0.05
Absorption loss (dB/mm)	0.4	0.5	0.6

The absorption losses were found by calculating the differences of total losses at 1310 nm and at 1550 nm. The setup is shown in figure 4-4. Assuming the same coupling loss for two wavelengths due to the fact that their wavelengths are very close, the difference will be due to absorption loss. The absorption losses were measured for total length of the waveguide and then divided by the length. Therefore the numbers in the table reflects the absorption per mm. The He-Ne was used to align the setup and all the fibers, sample objective were put on micropositioners for stability of setup. An important note is that in different steps the sample and input fiber were constant to keep the coupling and propagation losses unchanged. In order to verify the total loss we can use Fiber-Sample-Fiber-OSA.

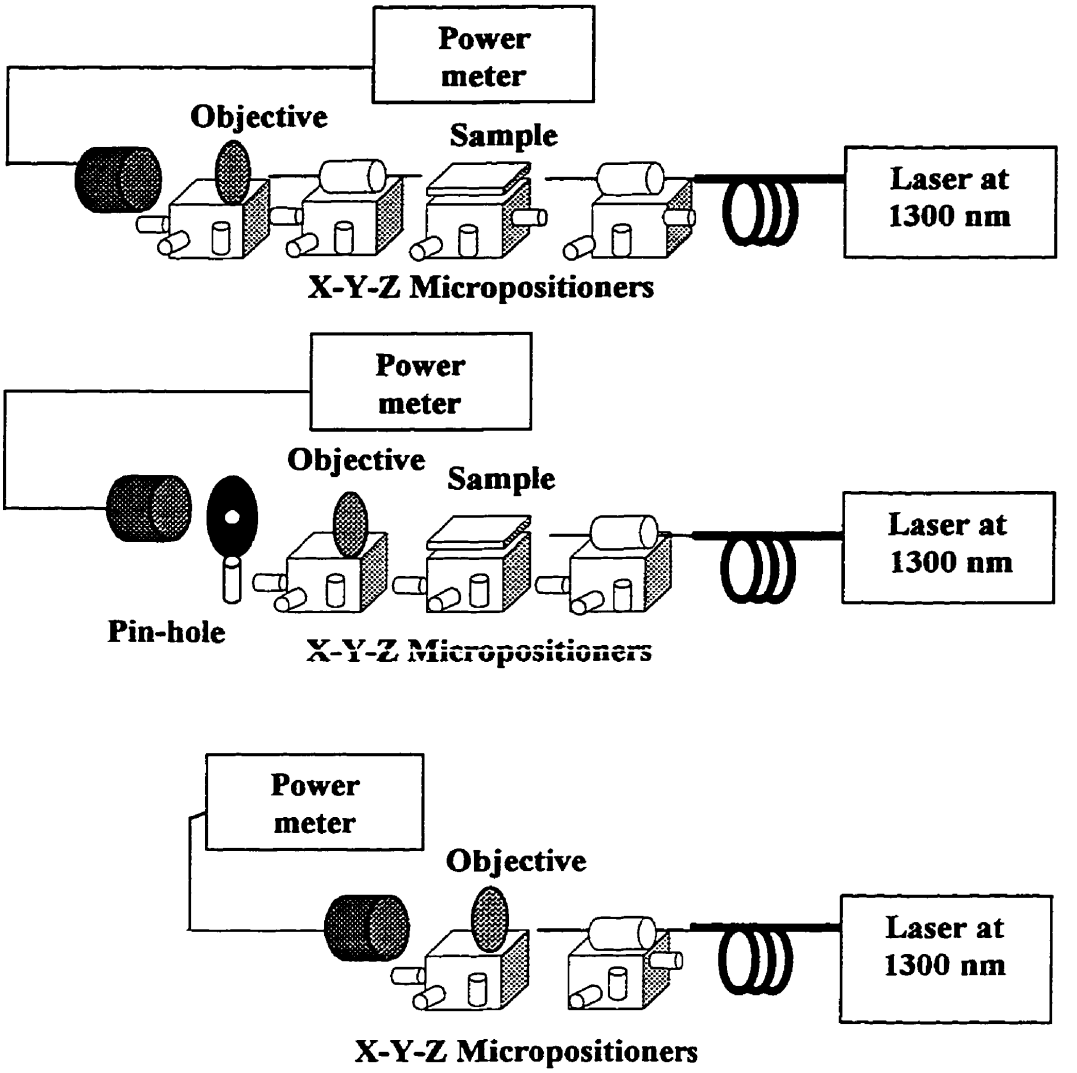

Figure 4.3 Loss measurement schematic setup

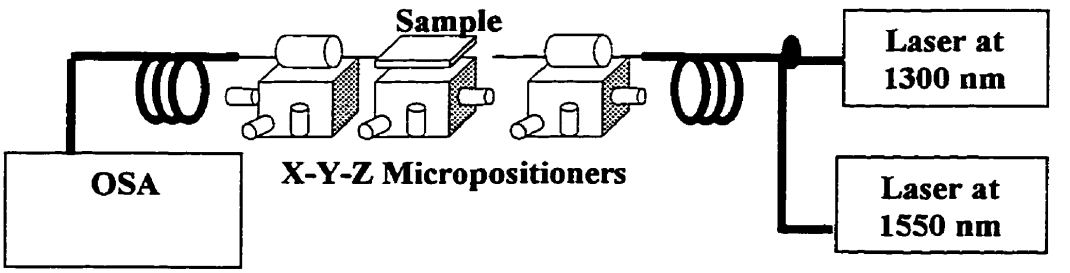

Figure 4-4 Absorption measurement schematic setup

4-4 Gain Measurement

In this section the ability of Erbium-Ytterbium co-doped channel waveguides fabricated by ion exchange techniques to amplify the optical signals at window of 1550 nm will be investigated. The first section describes the experimental setup used for measurements followed by the presentation of the results which has been done through different graphs.

4-4-1 Gain measurement setup

The optical setup which was used for amplification measurement is schematized in figure 4.6 The setup consisted of a laser pump emitting at 980 nm wavelength, a WDM to combine pump and signal, a 1550 nm source as signal, and finally an OSA to analyze the output. It consists of three different coupling setups: one to couple the 980 nm laser to a single mode fiber at 980nm, another to couple the pump and signal together to the sample and the last to couple the laser output from the waveguide to the fiber and finally to OSA. The pump laser used was a tunable CW laser with a maximum pump power of 500 mW output and tuning range of 963-1002 nm. Having a large raw beam diameter instead of a pigtailed laser led us use a coupling device which reduced the pump power from the 500 mW to 175 mW in the fibers. A coupling set up was prepared according to the specification of the pump (divergence, comma, astigmatism, etc..) to couple the beam to the single mode fiber at 980nm. To investigate the effect of the pump wavelength on the gain the laser was chosen to be tunable in the range of 963-1002nm. The tunability of the laser were provided by optical grating, but it was important to adjust the power

during the wavelength tuning due to the variation of the output power by adjusting the wavelength. The coupling device was set on a micropositioner capable of tilting in addition to the X-Y-Z translation. The coupling efficiency ratio was approximately 35% as can be seen in figure 4-5. This is the ratio of the output of the pump power measured by the pump detector to the output of the coupling system measured by OSA.

The measurements were done in constant power for the wavelength range (figure 4.5). Having 35% coupling efficiency the pump was coupled in a single mode fiber at

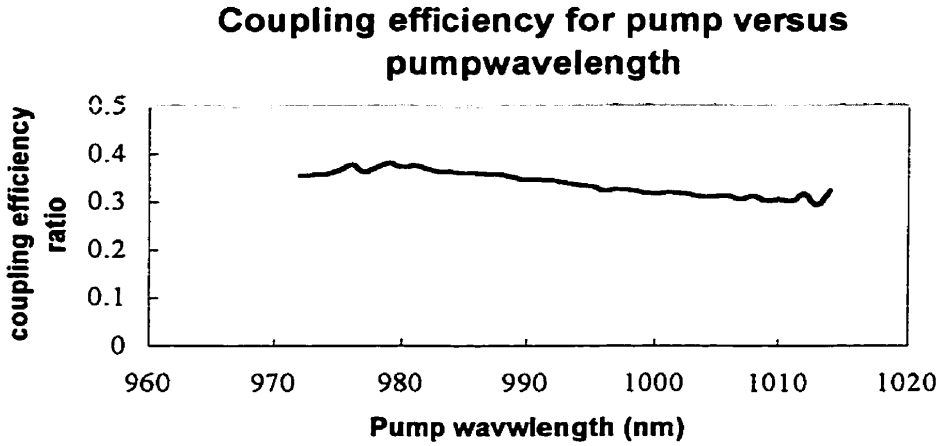

Figure 4.5 Coupling efficiency from the pump to fiber

980 nm and then connected (using Fc-Pc connectors) to a (WDM). This WDM acting as a combiner was used to combine pump at 980nm and signal at 1550 nm. The signal source was an erbium-doped fiber laser with a maximum power of 10 mW. This signal source is tunable from 1525 to 1565 nm and stable enough to use as a signal. The pump and signal were combined and directed to a separate fiber and subsequently launched to the sample. All fibers used (except single mode fibers at 980 nm for 980 nm coupling and

980 nm branch of the WDM) were SMF 28 single mode fiber at 1550 nm with a core diameter of 9 μm and cladding of 125μm.

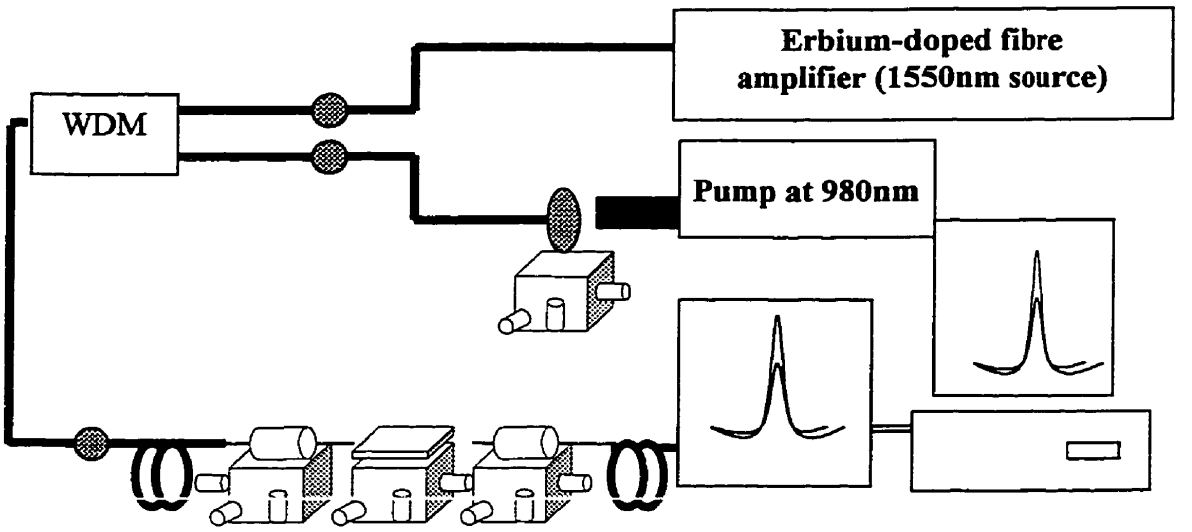

Figure 4.6 Amplification setup

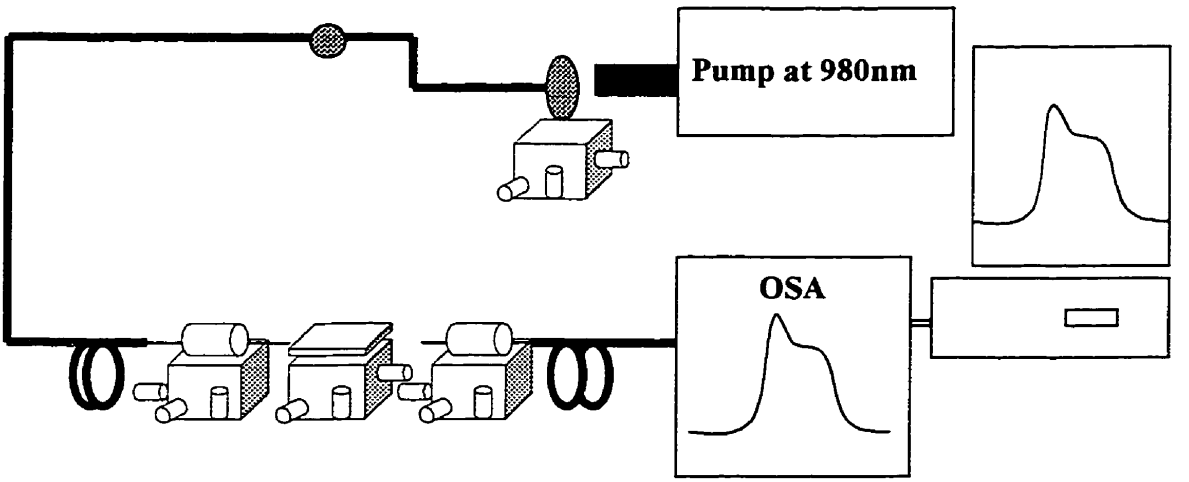

Figure 4.7 Photoluminescence setup

The output light from the waveguide was captured by another fiber that was connected to the OSA.

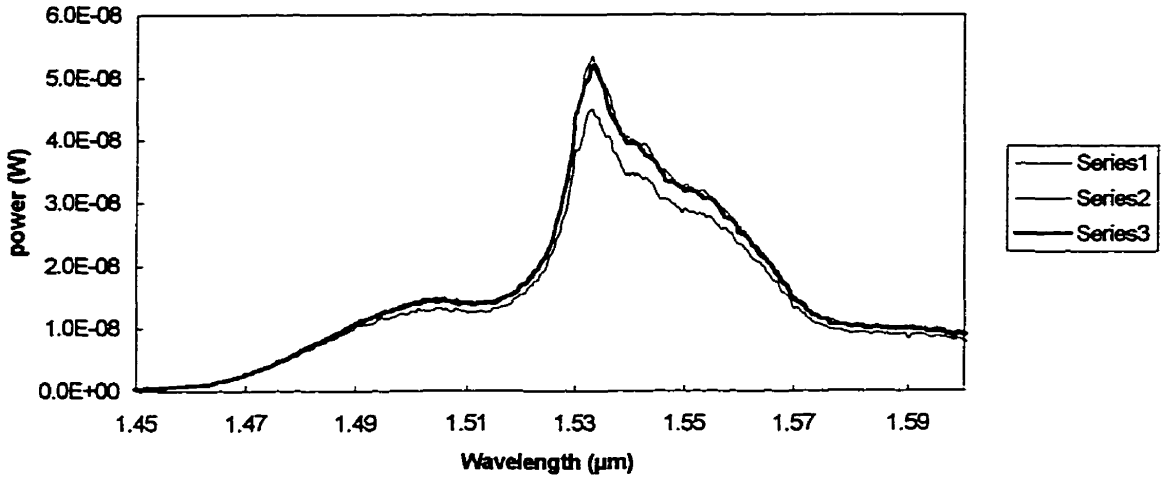

Figure 4-8 Amplified spontaneous emmision for QX/Er glass S1:1000,S2:990 and S3:980 nm

Prior to signal amplification measurement, an experiment was done to picture the amplified spontaneous emission caused by the excitation and dexcitation of the Erbium ions using pump at 980nm. The experimental setup is shown in figure 4-7 and the results captured by OSA were saved by computer and shown in figure 4.8. The absorption of the glass in the pump and signal range was also investigated using a spectrometer. The absorption measurement of a 2 mm thick sample is presented in figure 4.9. The absorption measurement shows the peak of absorption at 980nm and another absorption at 1.55 window which former justifies the pump wavelength. To determine the amplification ability of the glass the gain of the device was measured. The internal gain can be defined as the ratio of "the output signal power with pump measured by OSA to

output signal power without pump measured by OSA". Internal net gain can also be defined as: the ratio of "input power inside the wave guide at input (5dB less power than common port of WDM due to the coupling loss) to actual output signal power". This power is 5dB more than what we have at OSA due to the coupling loss .

Coupling loss measured at 1.3μm for all of the waveguides are approximately 5dB

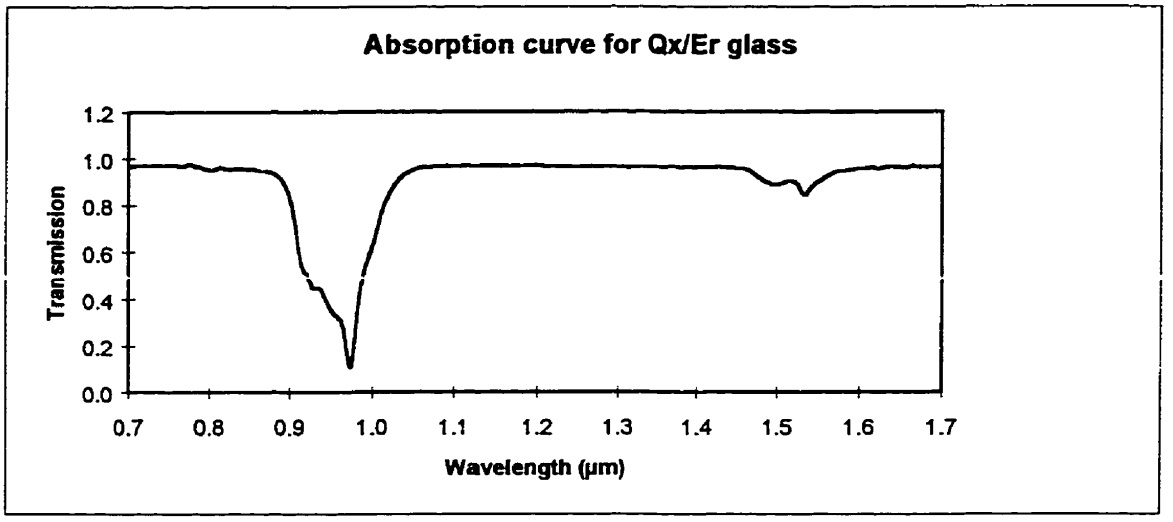

Figure 4-9 Absorption curve for QX/Er glass

per facet and losses due to absorption measured at 1.55μm are 0.38 dB/mm for 1.65% Er, 0.5 dB/mm for 2.22% Er and 0.6 dB/mm for 2.75% Er. The maximum power coupled to the fiber from 980 nm is175mW as measured by a thermal power-meter (The OSA is limited to measure no more than 50mW). Due to the importance of the pump wavelength, signal wavelength pump power and signal power in amplification measurement, the results of gain were measured with respect to these parameters. The measurements were done for 3 different concentrations of the Erbium with 22%

concentration of the Ytterbium. The length of the samples was 6mm for 1.65%Erbium and 12mm for the rest.

4-5 Discussion

Figures 4.10 to 4.13 show the gain variation with signal wavelength, pump power and signal power for sample # 1 (erbium concentration = 1.65 wt %, ytterbium concentration = 22 wt %). The length of the waveguide was selected 6mm because with our pump power the gain was maximum. The maximum gain is 4.5 dB at signal wavelength of 1532 nm (figure 4.10). The gain variation with pump power (figure 4.11) shows that saturation occurs at 150 mW pump power. This power corresponds to 45-mW pump power injected inside the waveguide. Figure 4.13 indicates that the gain is constant between 100 nW to 100 μW signal wavelength.

Figures 4.14 to 4.17 explain the same characteristics but for 2.22 wt% erbium concentration. At this concentration, with the same amount of pump, the maximum gain is 9.5 dB(figure 4.17). Figure 4.16 shows that with 600 mW pump power the amplifier has not reached gain saturation point, therefore the optimum power is more than 50 mW inside the waveguide. Figure 4.14 illustrates that the gain is almost constant for signal power between 100 nW to 100 μW. It is important to note that the length of the waveguide has not been optimized for this amplifier. Figures 4.18 to 4.21 are results for 2.75 wt % erbium and 22 wt % ytterbium concentration in the glass. Maximum gain for this glass was 5.5 dB. The reasons for lower gain are upconversion and other ion-ion interactions due to a high erbium concentration. As we can see from figure 4.20, 50 mW

injected power is below the pump required for the gain saturation. Finally, figure 4.19 illustrates the flatness of gain in the measured signal power range.

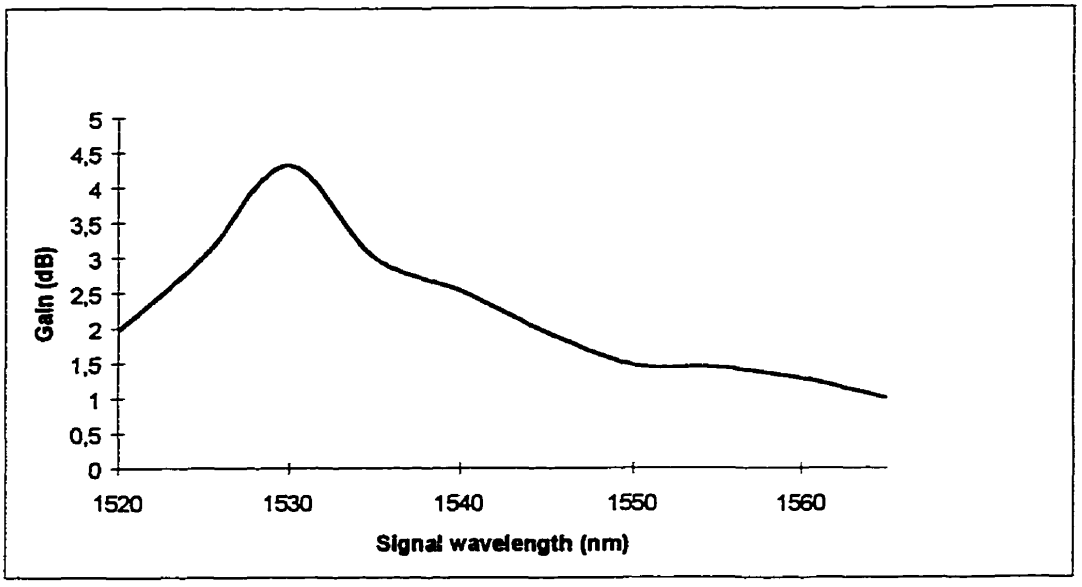

Figure 4-10 Gain versus signal wavelength : Er1.65% Yb 22%

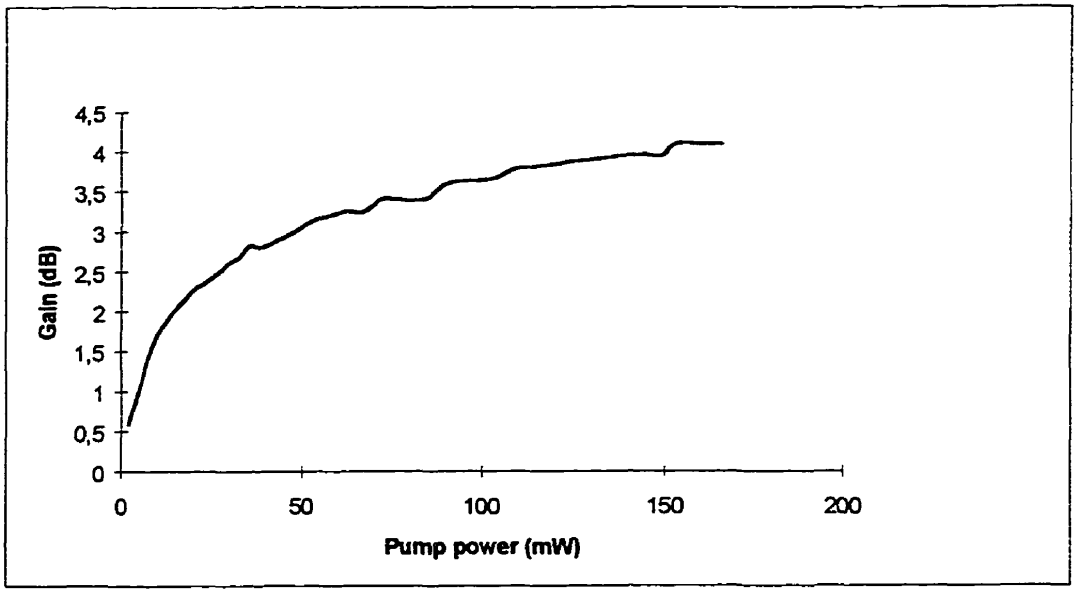

Figure 4-11 Gain versus pump power Er 1.65 Yb 22%

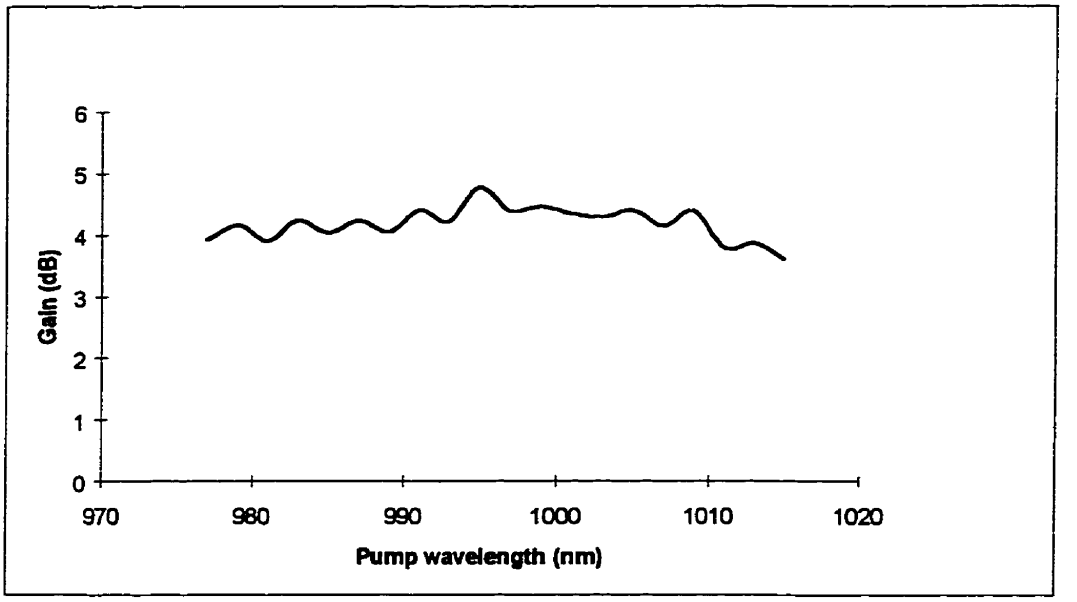

Figure 4-12 Gain versus pump wavelength Er 1.65% Yb 22%

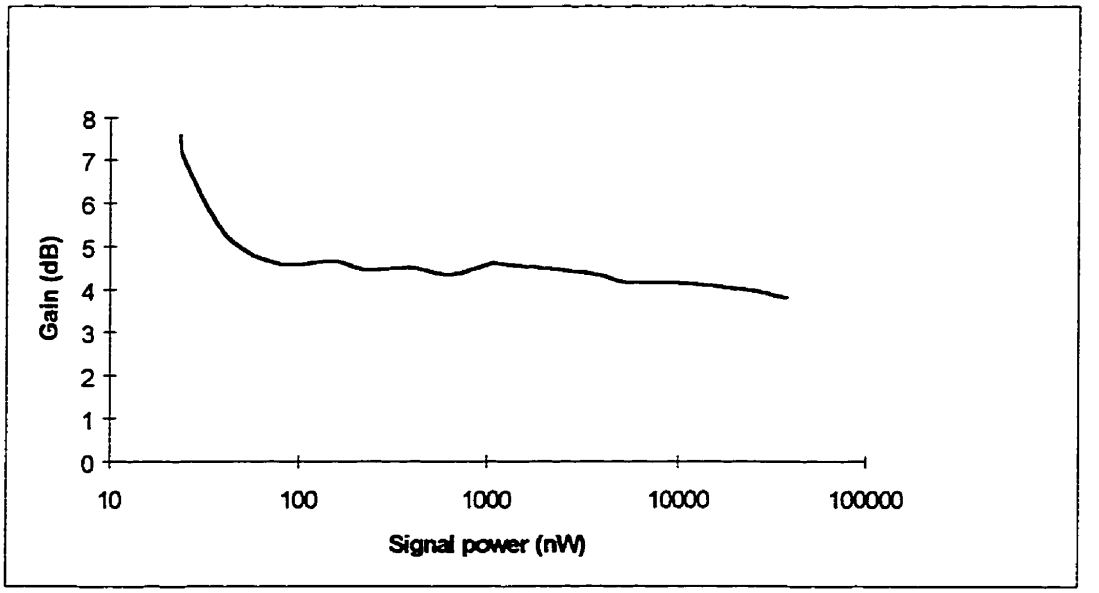

Figure 4-13 Gain versus signal power Er 1.65% Yb 22%

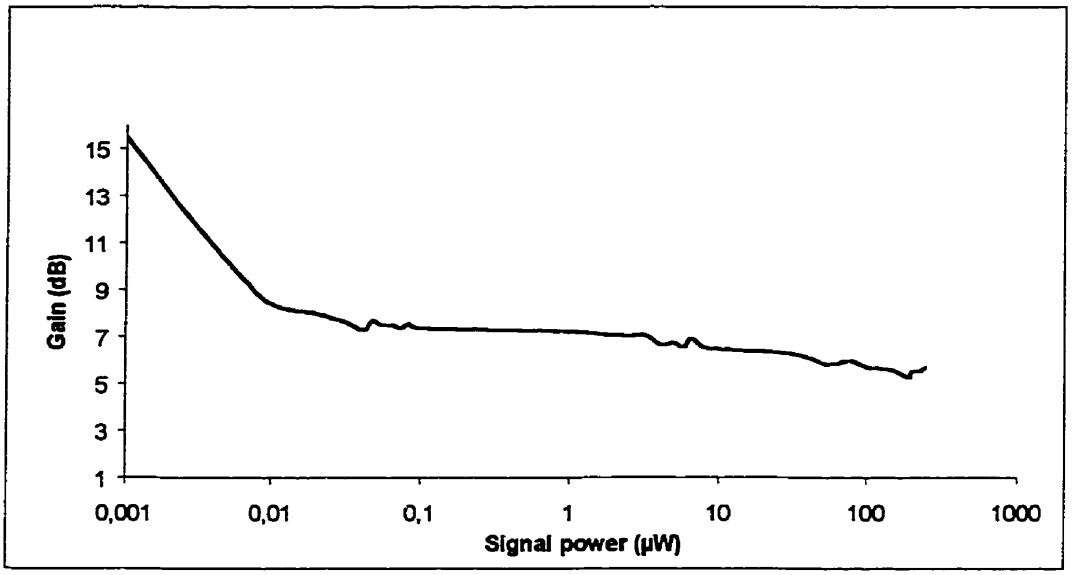

Figure 4-14 Gain versus signal power Er2.22% Yb 22%

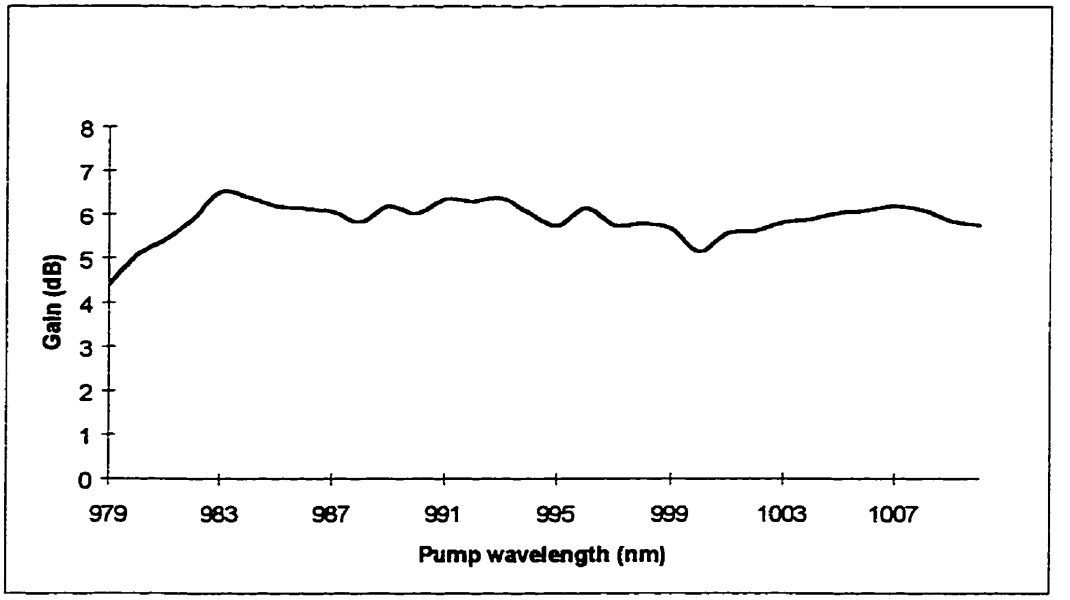

Figure 4-15 Gain versus pump wavelength Er 2.22% Yb 22%

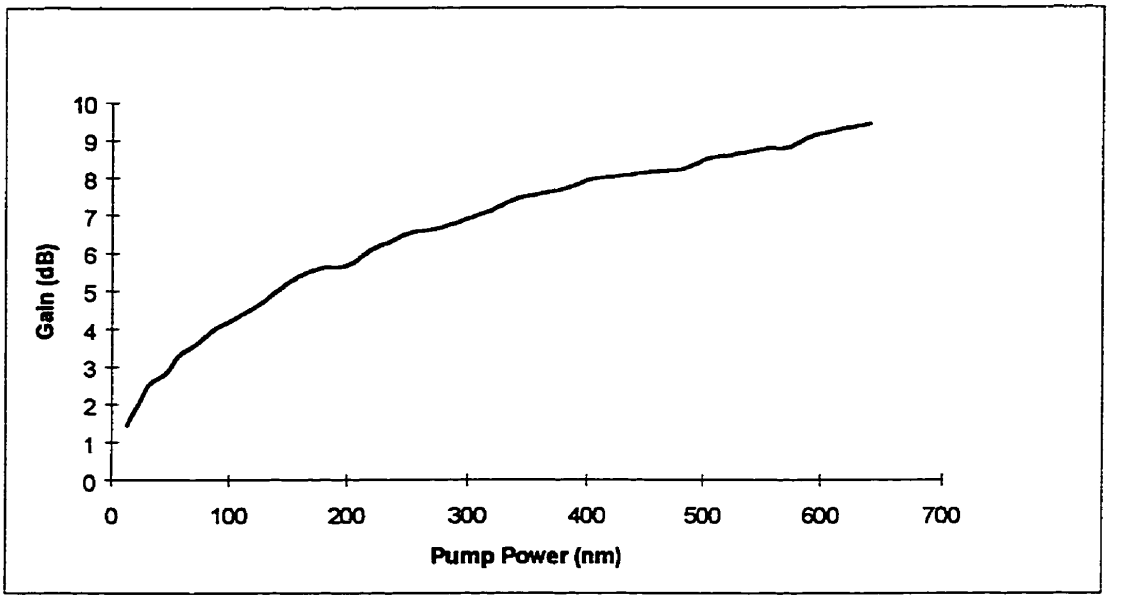

Figure 4-16 Gain versus pump power Er2.22% Yb 22%

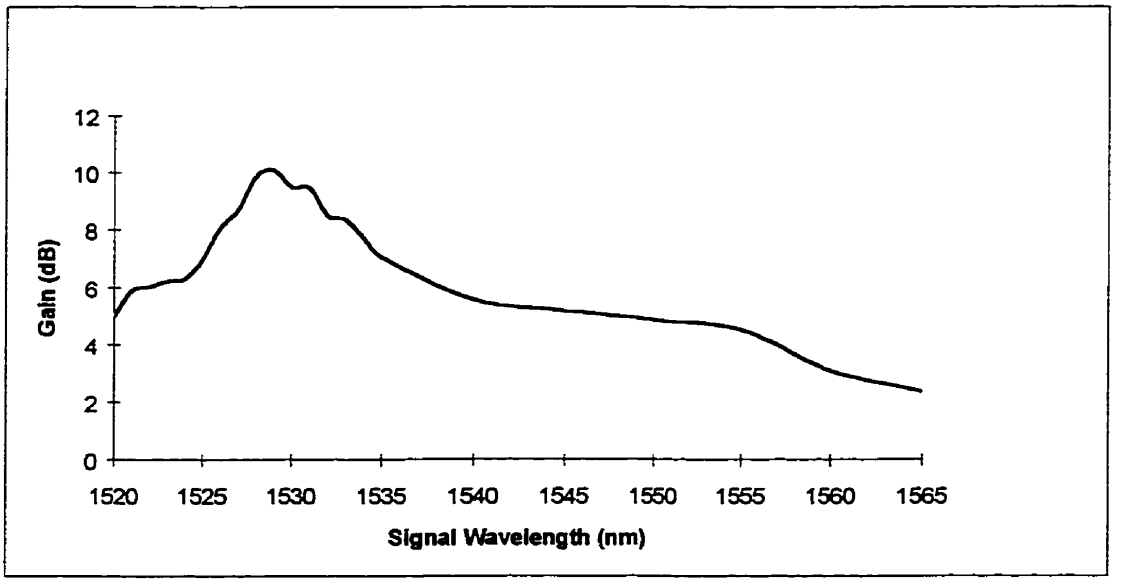

Figure 4-17 Gain versus signal wavelength Er2.22% Yb 22%

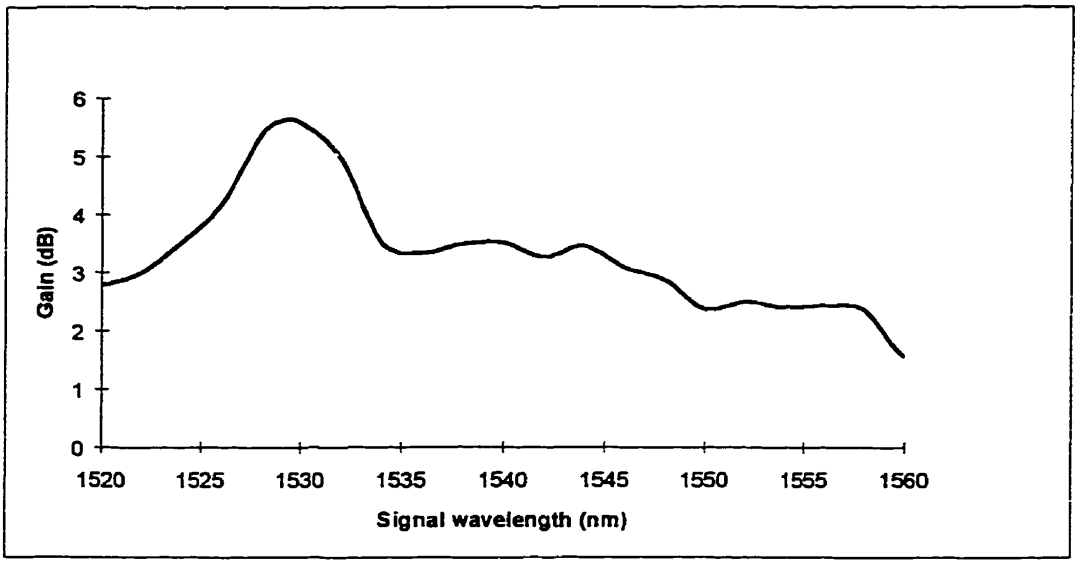

Figure 4-18 Gain versus signal wavelength Er2.75% Yb 22%

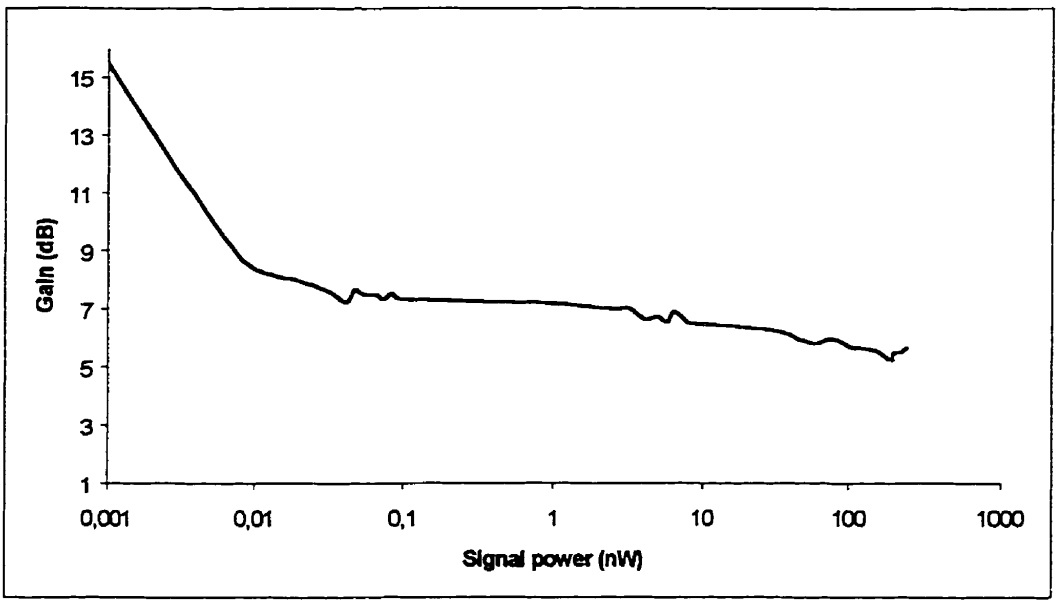

Figure 4-19 Gain versus signal power Er2.75% Yb 22%

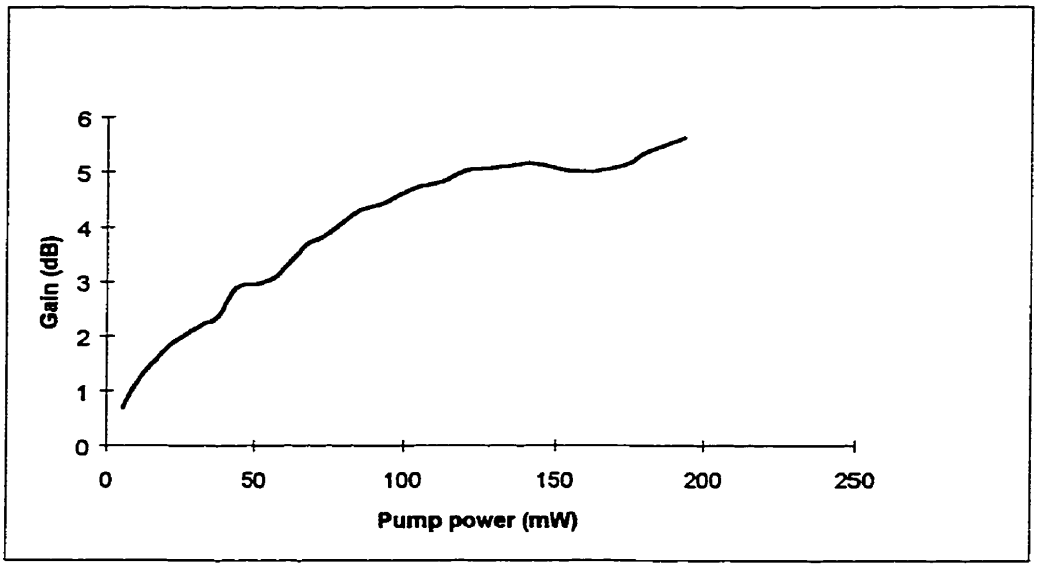

Figure 4-20 Gain versus pump power Er2.75% Yb 22%

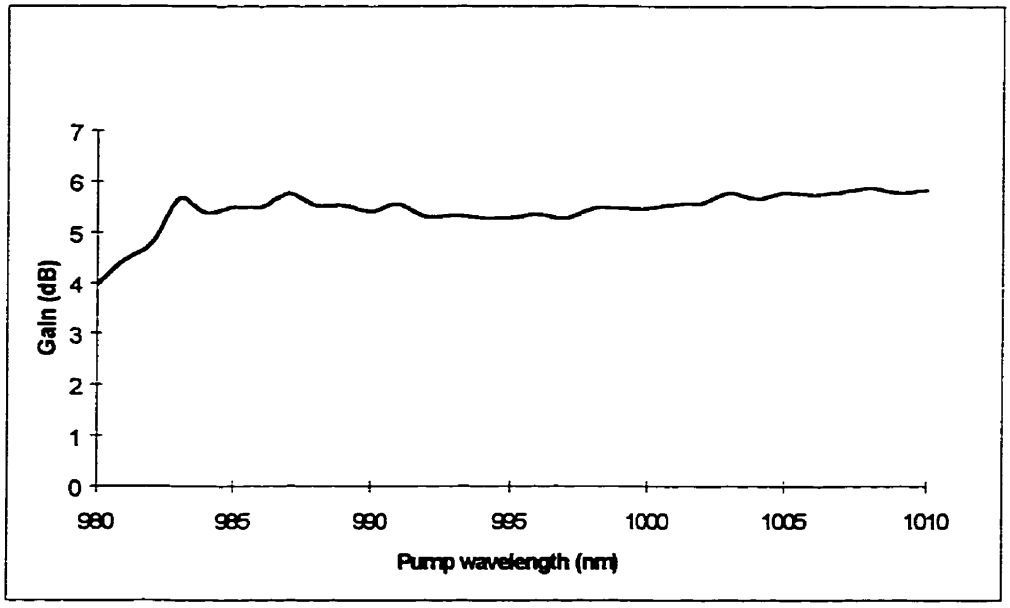

Figure 4-21 Gain versus pump wavelength Er2.75% Yb 22%

Chapter 5

Conclusion and future works

5-1 Conclusion

In the present work ion exchanged waveguide were fabricated on phosphate glasses co-doped with erbium and ytterbium. Potassium ion exchange for 4 hours at 400 °C formed the waveguides with 0.065 maximum refractive index changes. A method developed to remove moisture from the salt by preheating the salt in vacuum at 350 °C temperature for 24 hours. Diffusion depth and maximum refractive index changes resulting from prism coupling measurement helped us calculate the channel waveguide parameters. Channel waveguides, patterned by photolithography and fabricated using ion exchange, were able to guide 1.55 μm wavelength with low propagation losses (0.1 dB). A channel with 5μm width was chosen for characterization due to its single mode profile at the above-mentioned wavelength. Gain characterization proved the possibility of positive gain at 1.55μm in glasses. Gain measurements for three different glasses with 22 wt% ytterbium concentration and 1.65, 2.22 and 2.75 wt% erbium concentrations showed the effect of erbium concentration and the length of the waveguide on amplifier gain. Ytterbium concentration at 22 wt% improves the pump efficiency but very high erbium concentration could result in photoluminescence quenching and respectively gain due to upconversion and cross relaxation between erbium ions.

5-2 Future works

Higher pump power gives the opportunity of investigating the gain in longer waveguides, therefore using high power pigtailed pump lasers could result in more gain. Mismatch of the mode profile of the pump and the mode profile of the signal is one of the factors that reduces pump efficiency. In order to improve the efficiency of the erbium-doped waveguide amplifiers we should match them together. Using a thin film as the cladding layer over the ion exchange waveguide after fabrication can be a way to overcome this problem. This layer with a suitable refractive index can confine the mode and will help the mode profiles to match and improve the efficiency of the pump. One of the possible future works is investigating the noise figure for plannar waveguide amplifiers. The laser application can also be investigated using 2 mirrors at the end-faces of the waveguide.

REFERENCES

[1-1] SNITZER, E. (1963). Neodymium Glass Laser. Proceeding of 3rd International Conference on Quantum Electronics, 999-1019.

[2-1] KOESTER, C. J. and SNITZER. E. (1964). Amplification in a Fiber Laser. Applied Optics, 3, 1182-1186.

[3-1] MEARS, R. J., REEKIE, L.I., JAUNCY, M. and PAYNE, D. N., (1987) High-Gain Rare-Earth-Doped- Fiber Amplifier Operating at 1.54 μm. Optical Fiber Communications OFC '87, Washington, D.C., 3, 167.

[4-1] SIMPSON, J., Fiber-Based Amplifiers Progress in 1990. (1991). Optical Fiber Communications OFC '91, 2, 191-193.

[5-1] MILLAR, C. A., Future Prospects for Active Fiber Devices. (1990) European Conference on Optical Communications ECOC '90, II, 717-724.

[6-1] AINSLIE, B. J., (1991) Recent Advances in Discrete and distributed Fiber Amplifiers. European Conference on Optical Communications ECOC '91, 2, 47-50.

[7-1] MILLER, S. E., (1969) Integrated Optics: An Introduction. Bell Syst. Tech.J., 48, 2059-2068

[8-1] SIMPSON, J. (1992) Single-mode glass channel waveguides by ion exchange with ion masking. Opt Commm. 2, 234-240.

[9-1] WANG, W.J, (1992). Passive and Active Ion-Exchanged Glass Waveguides and Devices. PHD thesis Ecole Polytechnique de Montreal Canada.

[10-1] LUMHOLT, O., BERNS H., CHABLI (1992). A. Integrated Optical Devices in Glass by Ionic Masking. SPIE Proceedings, 1, 127-130.

[11-1] POLMAN, A. (1991) Potassium and silver ion-exchanged dual-core glass waveguides, with gratings. Appl. Phys. Lett., 58, 2607-2609.

[12-1] KANE, C.F. (1991). Optical Damage Threshold of ion-exchanged glass waveguide at 1.06 μm. SPIE Proceedings, 1 1538.

[13-1] KITAGAWA, T., OHMORI, Y. (1991). Glass waveguides by ion-exchange with ionic masking. SPIE Proceedings, 2, 434-440.

[14-1] ERMAN, M., (1995). Prospects for integrated optics in telecom applications. Proc. ECIO'95, 1, 27.

[15-1] KAGI, N. OYOBE, A., and K. NAKANURA, (1990) IEEE. Photon. Technol. Lett, 2, 559.

[16-1] MINISCALCO, W.J., (1991). Erbium-doped glasses for fiber amplifiers at 1550 nm. J.O. Lightwave Technol,. 9, 234.

[17-1] CAMY, P., ROMAN, J.E., WILLEMS, F.W., HEMPSTEAD (1996). Ion-exchanged planar lossless splitter at 1.5micrometer. Electron. Lett., 320-321.

[18-1] P.DELAVAUX, J., GRANLUND, S., MIZUHARA, O., TZENG, L. D., BARBIER, D., RATTAY, M., ANDRE, F.S. and KEVORKIAN, A., (1996). Integrated optics erbium ytterbium amplifier system in 10Gb/s fiber transmission experiment. Proc. ECOC'96, 37, 123.

[19-1] DELAVAUX, J. P., PARK, Y., MURPHY, K.E., GRUNLAND, S.,

MIZUHARA, O., BARBIER, D., RATTAY, M., CLAUSS, G. and KEVORKIAN. (1996). A. High performance Er-Yb planar waveguide amplifiers as in-line and pre-amplifier in 10 Gb/s fiber system. Proc. ECOC'96, 37, 127.

[20-1] NAJAFI. S.I, (1992). Introduction to glass integrated optics, Aretech House, 7

[21-1] NAJAFI. S.I, (1990). Overview of Nd-and Er-doped Glass integrated Optics Amplifier and lasers. Proc of SPIE , 2996, 54.

[22-1] POLMAN, A., JACOBSON, D. C., EAGLESHMAN, D. J., KISTLER, R. C., AND POATE, J. M., (1991). Optical doping of waveguide materials by Mev Er implantation. J.Appl.phys, 70, 3778.

[23-1] LUMHOLT, O., BERNS, H., CHABLI, A., CHAUMONT, J., GRAND, G., AND VALETTE, S., (1992). Low-Energy Erbium implanted $Si_3N_4/SiO_2/Si$ Waveguides. Elec. Lett. 28, no 24, 2242-2243.

[24-1] SHMULOVICH, J., WONG, A., WONG, Y. H., BECKER, P. C., BRUCE A. J., AND ADAR, R., (1992) Er^{3+} glass waveguide amplifier at 1.5μm on silicon", Electron. Lett, 28, 1181.

[25-1] GHOSH, R. N., SHMULOVICH, J., KANE, C. F., BARROS, M. R., X., NYKOLAK, G., BRUCE A. J., and BECKER, P. C., (1996). 8mW thereshold Er^{3+}-doped planar waveguide amplifier. IEEE photon. Tech. Lett, 8, 518.

[26-1] SHUTO, K., HATTORI, K., KITAGAWA, T., OHMORI Y., AND HORIGUCHI, M., (1993) Erbium-doped phosphosilicate glass waveguide amplifier fabricated by (PECVD). Electron. Lett, 29, 139.

[27-1] LI, C. C, KIM, H. K., MIGLIUOLO, G., (1997). Er-doped glass ridge-waveguide amplifiers fabricated with a collimated sputter deposition technique. IEEE photonics Tech Lett, 9, 1223.

[28-1] NAKAZAWA, M., KIMURAA, Y., (1992). Electron-beam Vapour-deposited Erbium-doped glass waveguide laser at 1.5 μm. Electronics Letters, 28, No.22, 2054.

[29-1] TUMMINELLI, R., HAKIM, F., AND HAAVISTO, J., (1991). Integrated optics Nd-glass laser fabricated by flame hydrolysis deposition. Optics Lett, 16, 1098.

[30-1] KITAGAWA, T., HATTORI, K., SHUTO, K., YASU M., KOBAYASHI M. AND HORIGUCHI, M., (1992). Amplification in Erbium doped silica based planar waveguide circuits. Electron. Lett, 28, 1818.

[31-1] HATTORI, K., KITAGAWA, T., OGUMA, M., WADA, M., TEMMYO J. AND HORIGUCHI, M., (1993). Erbium-doped silica-based planar waveguide amplifier pumped by 0.98 μm laser diods. Electron. Lett, 29, 357.

[32-1] HONKANEN, S., NAJAFI, S. I., AND WANG, W. J., (1992). Composite rare-earth-doped glass waveguides. Electron. Lett, 28, 746.

[33-1] WANG, W. J., NAJAFI, S. I., HONKANEN, S., HE, Q., WU, C. AND GLINSKI, J. (1992). Erbium-doped composite glass waveguide amplifier. Electron Lett, 28.

[34-1] SARUWATARI, N., and IZAWA, T., (1974). Nd-glass laser with three-dimensional optical waveguide. Appl. phys. Lett. 24, 603.

[35-1] NAJAFI, S. I., ANDREWS, M. P., FARDAD, M. A., MILOVA, G., TOUAM,

T., AND COUDRAY, P., (1996) UV-light imprinted surface, ridge and buried sol-gel glass waveguide and devices on silicon. Conference on Integrated Optics for Signal Processing, Berlin, 10-15.

[36-1] MCENTEE, J., (1996). Sol-gel devuces will meet cost targets of fiber to the home. Opto and laser Europe, 5.

[37-1] NAJAFI, S. I., and ANDREWS, M. P., (1997). Sol-gel integrated optics and optoelectronics. European Space Agency Workshop.

[38-1] LI, C. I., INGENHOFF, J., NAJAFI, S. I., CHISHAM, J., MACLACHLAN, M., ANDREWS, M. P., YU-HUA KAO, MACKENZIE, J. D., OHTSUKI, T., AND PEYGHAMBARIAN, N., (1995). Er-doped sol-gel glasses for integrated optics. Conf. on Optoelectronic Integrated Circuit Materials, Phsics, and devices, 2397, 430.

[39-1] SPANHEL, L., POPALL, M., AND MULLER, G., (1995). Spectroscopic properties of sol-gel derived nanoscaled hybrid materials. Proc. indian Acad. Sci. (Chem.Sci), 107, 637.

[40-1] MILOVA, G., NAJAFI, S. I., SKIRTACH, A., SIMKIN D., AND ANDREWS, M. P., (1997). Erbium in photosensitive hybrid organoaluminosilicate sol-gel glasses". Conference on Integrated Optics Devices: Potential for Commercialization, San Jose, 2997.

[41-1] STONE, B. T., BRAY, K. L., (1996) Florescence Properties of Er^{3+}-doped sol-gel glasses J. Non Crystalline Solids, 197, 136-144.

[42-1]MILOVA G., (1990). Florescence Properties of Er^{3+}-doped sol-gel glasses. PHD

thesis Ecole Polytechnique de Montreal Canada.

[43-1] SARUWATARI, N., AND IZAWA, T., (1974) Nd-Glass Laser with Three Dimensional Optical Waveguide. Appl. Phys. Lett., 24, 603-605.

[44-1] LI, M.J., AND NAJAFI, S., I., (1990) Rare-Earth-Doped Glass Waveguides and amplifiers. SPIE PROC., 1338, 82-87.

[45-1] STANFORD, N.A., MALON K. J. AND LARSON, D. R., (1990). Integrated Optic Laser by Field Assisted Ion-Wxchange in Neodymium Doped Soda Lime Silicate Glass. Tech. Dig. Integrated Photonics Research, 114.

[46-1] MWARANIA, E.K., (1990). Low Threshold Monomode Ion-Exchanged Waveguide Laser in Neodymium Doped BK-7 Glass. Electron Lett., 26, 1217-1218.

[47-1] AOKI, H., MARAYAMA, O., AND ASAHARA, Y., (1990) Glass waveguide Laser. IEEE phot. Tech. Lett., 2, 459-460 .

[48-1] AOKI, H., MARAYAMA, O., AND ASAHARA, Y., (1990). Glass waveguide Laser Operated Around 1.3 micrometer. Electron . Lett., .26, 1910-1911 .

[49-1] TAKADA, K., YAMADA, H., HIDA, Y., OHMORI, Y., AND MITACHI, S., (1996) Rayleigh backscattering measurement of 10m long silica-based waveguides. Electron. Lett, 32, (18) 1665-166,.

[50-1] KO, S.H., DOREMUS, R.H., GUO, X.S., and LANDFORD, W., "Refractive index gradient in the surface of a zirconimu fluoride glass by exchange with chlorine",J. Mater. Res. 5(1), pp. 202-205, 1990.

[51-1] RAMASWAMY, R. V., AND SRIVASTAVA, R., Ion-exchanged glass

waveguidees.

[52-1] MAHAPATRA, M., AND CONNORS, J. M., (1998). Thermal tapering of ion-exchanged channel waveguides in glass. Optics Lett. 13, (2) 169-171.

[53-1] ZHENGUANG, H., SRIVASTAVA, R., AND RAMASWAMY, V., (1989) Low-loss small-mode passive waveguides and near-adiabatic tapers in BK-7 glass. J.Lightwave technology. 7 (10) 1590-1596.

[54-1] CAMY, P., (1996). Realisation d'un amplificateur optique dans la bande 1.5 micron des telecommunications, PhD Thesis, Universite Pierre et Marie Curie, Departement de Physique, Paris, 160-164.

[55-1] ZHENG, X. H., MEARS, R. J., (1993). Planar optical waveguide formed by Erbium ion exchange in glass. Appl. Phys. Lett. 62 (8), 793-795.

[56-1] SNOEKS, E., VAN DEN HOVEN, G. N., POLMAN, A., HENDRIKSEN, B., AND DIEMEER, M. B. J., (1993). Doping fibre-compatible ion-exchanged channel waveguides with erbium y ion implantation. Proc. European Conference on integrated Optics, p.3-38.

[57-1] BABUKOVA, M. V., BERENBERG, V. A., GLEBOV, L. B., NIKONOROV, N. V., PETROVSKII, G. T., AND TERPUGOV, V. S., (1985). Investigationof neodymium silicate glass diffused waveguides. Sov. J. Quantum Electron. 15, (9) 1304-1305.

[58-1] FRANCOIS, V., OHTSUKI, T., PEYGHAMBARIAN, N., AND NAJAFI S. I., (1995). Length Optimization of single-mode Rare-Earth Doped Waveguides Using Saturated Absorption. IEEE Photonics Tech. Lett. 7, (8).

[59-1] FRANCOIS, V., OHTSUKI, T., PEYGHAMBARIAN, N., AND NAJAFI, S. I., (1995). Thermally silver ion exchanged integrated-optic lasers in Neodymium- doped silicate glass. Optics Communications, 119, 104-108.

[60-1] AOKI, H., MARUYAMA, O., AND ASAHARA, Y., (1990). Glass waveguide laser. IEEE Photonics Tech. Lett, 2, (7) 459-460.

[61-1] MWARANIA, E. K., REEKIE, L., WANG J., AND WILKINSON, J. S., (1990). Low threshold monomode ion-exchanged waveguide lasers in neodymium-doped BK-7 glass. Electron. Lett, 26, 1317-1318.

[62-1] SANFORD, N. A., MALONE, K. J., AND LARSON, D. R., (1990). Integrated optic laser fabricated by field-assisted ion exchange in neodymium-doped soda-lime-silicate glass. Optics Lett., 15, (7) 366-368.

[63-1] FEUCHTER, T., MWARNIA, E. K., WANG, J., REEKIE, L., WILKINSON, J. S., (1992). Erbium-doped ion-exchanged waveguide lasers in BK-7 glass. IEEE Photonics Technol. Lett, 4, (6) 542-544.

[2-1] LUMHOLT, O., RAMUSSEN, T., AND BJARKLEV, A., (1993). Modeling of extremely high concentration erbium-doped silica waveguides. Electron. Lett., 29, (5), 495-496.

[2-2] FEDERIGHI, M., MASSAREK, I., AND TRWOGA, P. F., (1993). Optical amplification in thin film waveguide with high Er concentration. IEEE Photon. Technol. Lett, 227-229.

[2-3] MINISCALCO W.J., (1991) Erbium-doped glasses for fiber amplifiers at 1500nm. J. Lightwave Technol, 9, (2) 234-250.

[2-4] MAURICE, E., MONNOM, G.,DUSSSARDIER, B., AND OSTROWSKY, D. B., (1996). Clustering effects on double energy transfer in heavily ytterbium-erbium codoped silica fibers. Journal of optical Society of America B, 13, (4) 693-701.

[2-5] NILSSON, J., SCHEER, P., AND JASKORZYNSKA, B., (1994). Modeling and optimization of short Yb^{3+} -sensitized Er^{3+} -doped fiber amplifier. IEEE photonic Technology letters, 6, (3), 383 385.

[2-6] ARTEMEV, E. F., MURZIN, A. G., FEDROV, K., AND FROMZEL, V. A., (1981). Some characteristics of population inversion of the $^4I_{13/2}$ level of erbium ions in ytterbium-erbium glasses. Sov. J. Quantum Electron., 11, 1266-1268.

[2-7] VEASEY, D. L., GARY, J. M., AND AMIN, J., (1997). Rigorous scalar modeling of Er and Er/Yb waveguide lasers. Rare-Earth-Doped Devices, 2996, 109-120.

[2-8] WINICK, K., VOSSLER, G. L., (1997). Erbium: ytterbium planar waveguide laser in ion-exchanged glass. Rare-Earth-Doped Devices, 2996, 121-134.

[2-9] LESTER, C., BJARKLEV, A., RASMUSSEN, T., DINENESEN, P. G., (1996) Modeling of Yb^{3+} sensitized Er^{3+}-doped silica waveguide amplifiers. Journal of lightwave Technology, 13, (5), 740-743.

[2-10] URQUHART, P., (1988). Review of rare earth doped fiber lasers and amplifiers. IEEE proceeding, pt.j, 135, (6) 385-407.

[2-11] FRANCE, P.W., (1987). Optical loss mechanisms in Fluorozirconate Glasses and

Inferared Fibers. Ph.D. thesis,University of Sheffield, U.K.,

[2-12] SASAKI, I., PAYANE, D. N., AND ADAMS, M. J., (1980). Measurement of Refractive -Index Profile in an Optical Fiber Perform. Electronics Letters, 16, (6) 219-221.

[2-13] FRANCE, P. W., DREXHAGE, M. J., PARKER, J. M., MOORE, M. W., CARTER, S. F., AND WRIGHT, J. V., (1990). Fuoride Glass Optical Fibers. Blackie and Son, Ltd..

[2-14] KITAGAWA, T., K.HATTORI, M., SHIMIZU, Y., OHMORI O., AND KOBAYASHI, M., (1991) Guided wave laser based on erbium-doped silica planar lightwave circuit. Electron. Lett, 27, 334.

[2-15] CAMY, P., ROMAN, J. E., WILLEMS, F. W., HEMPSTEAD, M., VAN DER PLAATS, J. C., PREL, C., BEGUIN, A., KOONEN, M. J., WILKINSON J. C., AND LERMINIAUX, C., (1996). Ion-exchanged planar lossless splitter at 1.5 μm. Electron. Lett., 32, 321.

[2-16] GATES, J. V., BRUCE, A. J., SHMULOVICH, J., WONG, Y. H., NYKOLAK, G., BARROS M. R. X., AND GOSH, R., (1995). Fabrication of Er-doped glass films as used in planar optical waveguides. Mat. Res. Soc. Symp. Proc., 392, 209.

[2-17] SNOEKS, E., VAN DER HOVEN G. N., AND POLMAN, A.,(1993). Optical Doping of Soda-Lime-Silicate Glass with Erbium by Ion Implantation. J. Appl. Phys., 73, 8179.

[2-18] BARBIER, D., GASTALDO, P., HYDE, B., JOUANNO J., AND

KEVORKIAN, A., (1995). Amplification in Erbium-Doped Microguides Realised on Phosphate Glass. Proc. ECIO'95, TuC4, 241.

[2-19] VAN DER HOVEN, G. N., SNOEKS, E., POLMAN, A., VAN DAM, C., VAN UFFELEN J. W. M., AND SMIT, (1996). Net Optical Gain At 1.53 μm in Er-doped Al_2O_3 Waveguides on Silicon. Appl. Phys. Lett. 68, 1886.

[2-20] VAN WEERDEN, H. J., HOEKSTRA, T. H., LAMBECK P. V., AND POMPA, J. A., (1996). Low Threshold amplification at 1.5 μm in Er:Yb_2O_3 IO-amplifiers. Proc. Symposium of the IEEE/LEOS'96 59, .

[2-24] DESSURVIRE, E., (1994). Erbium Doped Fiber Amplifier, J. Wiley & Sons Inc.

[2-25] LUMHOLT, O., RAMUSSEN, T., AND BJARKLEV, A., (1993). Modeling of erbium-doped silica waveguides. Electron. Lett., 29, (5) 495-496.

[2-26] FEDERIGHI, M., MASSAREK, I. AND TRWOGA, P.F., (1993). Optical amplification in thin film waveguide with high Er concentration. IEEE Photon. Technol. Lett, 227-229.

[2-27] PASQUALE, F. D., ZOBOLI, M., FEDERIGHI, M., MASSAREK I., (1994) Finite element modeling of silica waveguide amplifiers. IEEE J. Q Elec, 30, 1277-1282.

[2-28] PASQUALE, F. D.,FEDERIGHI, M., MASSAREK, I.,(1995). Modeling of uniform and pair induced upconversion mechanism in high concentration erbium-doped silica waveguides. IEEE J. lightwave technology, 13, (9).

[2-29] ARTEMEV E.F., MURZIN, A. G., FEDROV, K., AND FROMZEL, V. A., (1981). Some Characteristics of population inversion of the $^4I_{13/2}$ level of erbium ions in

ytterbium-erbium. Sov.J.Quantum Electron., 11, 1266-1268.

[2-30] NILSON, J., DCHEER, P., AND JASKORZYNASKA, B., (1994). Modeling and optimization of short Yb^{3+}-sensitized Er^{3+} doped fiber amplifier. IEEE photonics Technology Letters, 6, (3), 383-385.

[2-31] PASQUALE, F. D., FEDERIGHI, M., (1994). Improved gain characteristic in high concentration Er^{3+} Yb^{3+} codoped glass waveguide amplifiers. IEEE J. Quantum Elecron, 30, (9) 2127-2131.

[2-32] PASQUALE, F. D., AND ZOBOLI, M., (1993). Analysis of Erbium-doped waveguide amplifiers by a full-vectorial finite element method. J. Lightwave Technol, 11, (10) 1565 -1574.

[2-33] SHOOSHTARI A., TOUAM, T., SAFAVI-NAEINI, S., HATAMI-HANZA, H., AND NAJAFI, S. I., (1998). Yb^{3+} sensitized Er^{3+} doped waveguide amplifiers :a theoretical approach. Optical and quantum electronics, 30.

[2-34] SHOOSHTARI A., MESHKINFAM, P., TOUAM, T., ANDREWS, M. P., AND NAJAFI, S. I., (1998). Ion exchanged Er/Yb Phosphate glass waveguide amplifiers and lasers. SPIE journal of optical Engineering, 37, (4) 1188-1192.

[2-35] NAJAFI, S. I., (1992). Introduction to glass integrated optics, Artech House.

[2-36] JIANG, S., MYERS, M.J., RHONEHOUSE, D. L., HAMILTON, S. J., AND MYERS, J. D., (1997). Ytterbium doped phosphate laser glasses. SPIE Proceeding Solid State Laser VI, 2986.

[2-37] FREDERIGHI. M., AND PASQUALE, F. D., (1995). The effect of pair-induced

energy transfer on the performance of silica waveguide amplifiers with high Er^{3+}/Yb^{3+} concentrations. IEEE Photon. Technol. Lett, 7 (3) 303-305.

[2-38] LESTER, C., BJARKLEV, A., RASMUSSEN T., AND DINENESEN, P. G., (1996) Modeling of Yb^{3+} sensitized Er^{3+}-doped silica waveguide amplifiers. Journal of Lightwave Technology, 13, (5) 740-743.

[2-39] NILSSON, J., SCHEER, P., AND JASKORZYNSKA, B., (1994). Modeling and optimization of short Yb^{3+} -sensitized Er^{3+}-doped fiber amplifier. IEEE photonic Technology Letters, 6, (3) 383 385.

[3-1] KIGER INC. 100 Marshland Road, Hilton Head, Sc 29926 .Tel:803-681-5800

[3-2] JIANG, SH., MYRES, J., RHONEHOUSE, D., MAYRES, M., BELFORD, R., HAMLIN, S., (1995). Report on Laser and thermal performance of a new erbium doped phosphate laser glass .

[3-3] VOGEL, W., (1985). Chemistry of glass, The American Ceramic Society.

[3-4] JIANG, Sh., MYRES, J. D.,(1995). Development of a new rare earth doped phosphate glass for ion exchanged waveguide glass amplifiers report.

[3-5] ULRICH. R., AND TORGE. R., Measure of Thin Film Parameters with a Prism Coupling. Appl. Opt. 12, 2901.

[4-1] WANG, W.J., HONKANEN, S., AND NAJAFI, S. I., TERVONEN, A., (1993) Loss characteristics of potassium and silver double-ion-exchanged glass waveguides. J. appl. Phys., 74, (3) 1529-1533.

Appendix-1

Derivation of absorption and stimulated emission equation

The probability density of spontaneous emission into a single prescribed mode is given by $P_{sp} = \frac{C}{V}\sigma(\nu)$. in which C is the speed of the light and V is the volume of the cavity. The function $\sigma(\nu)$ is a narrow function of ν which is known as "transition cross section" with a dimension of area. In order to generate the stimulated emission we need an external optical field. Therefore in the presence of an external plane wave optical field, with a light intensity I_ν (in W m^{-2}) and optical frequency $\nu \approx (E_j - E_i)/h$, both absorption and stimulated emissions may take place.

The next step is to drive the rates of absorption and stimulated emissions : mean photon flux density (photons/cm^2-s) is given by $\phi = \frac{I_\nu}{h\nu}$ and we wish to determine the probability densities for stimulated emission and absorption $W_i = P_{abs} = P_{st}$. The number of photons N involved in the interaction process is determined by constructing a volume in the form of a cylinder of area A and height C whose axis is parallel to the direction of propagation of the light (its k vector). The cylinder has a volume V=CA. The photon flux across the cylinder base is ϕA (photons per second). Because photons travel at the speed of the light C, within one second all of the photons within the cylinder cross the cylinder base. It follows that at any time the cylinder contains $N = \phi A$, or $N = \phi \frac{V}{C}$

photons so that $\phi = (\frac{C}{V})N$. To determine W_i we know that P_{ab} and P_{st} can be calculated as $P_{ab} = N\frac{C}{V}\sigma_{ab}(\nu)$ and $P_{st} = N\frac{C}{V}\sigma_{st}(\nu)$ then $W = P = N\frac{C}{V}\sigma(\nu) = \sigma(\nu)\phi = \sigma(\nu)\frac{I_\nu}{h\nu}$.

Therefore we can conclude that the rates of absorption and stimulated emissions is given by, [2-24]

$$\left.\frac{\partial N_j}{\partial t}\right|_{stim.} = -\sigma_{eji}(\nu)\frac{I_\nu}{h\nu}N_j = -W_{ji}\,N_j$$

$$\left.\frac{\partial N_i}{\partial t}\right|_{absorp.} = -\sigma_{aij}(\nu)\frac{I_\nu}{h\nu}N_i = -W_{ij}\,N_i$$

Appendix-2

Derivation of the optical gain formula

Assuming a thin slab of thickness Δz and the transverse area A, containing densities of N_1 and N_2 atoms in the lower and upper energy levels of some atomic transition we can say that each lower-level atom has an effective area or cross section σ_{12} for power absorption from the wave, and similarly each upper-level atom has an effective cross section σ_{21} for emission back to the wave .The total number of lower-level atoms in the slab will then be $N_1 A\Delta Z$, and the total absorbing area that results from all the lower-level atoms will be the total number of atoms times the cross section per atom, or $N_1\sigma_{12} A\Delta Z$. Similarly, the total effective "emitting area " that results from all the upper level atoms will be $N_2\sigma_{21} A\Delta Z$. The net power absorbed by the atoms in the slab from an incident wave carrying a total power P distributed over area A will then be $\Delta P_{abs} = (N_1\sigma_{12} - N_2\sigma_{21})P\Delta Z$ .Note that the area factors in the slab volume $A\Delta Z$ and in the power density $I = \frac{P}{A}$ just cancel. The net growth or decay with distance caused by an atomic transition for a wave carrying power P or intensity I through an atomic medium can then be written as $\frac{dP}{dZ} = -\lim_{\Delta z \to 0}(\frac{\Delta P_{abs}}{\Delta Z}) = (N_1\sigma_{12} - N_2\sigma_{21})P$ .If converted into units of intensity I(z) ,in a glass with N_i and N_j electron distributions, the amplification of a plane wave propagating in z-direction (in steady state regime) could be written as

$$\frac{dI_\nu(z)}{dz} = (\sigma_{eji}\, N_j - \sigma_{aij} N_i)\, I_\nu = g_{op} I_\nu(z)$$

where g_{op} is called "optical gain" of i and j levels in a glass with N_i and N_j electron distributions.

Appendix-3

Solution for Rate and gain equation

Light power can be calculated using two quantities: $P_s(z)$ and $\psi_s(x,y)$ which are, respectively, mode power and normalized mode intensity [2-24][2-33][2-34]:

$$I_v = P_s(z)\psi_s(x,y) \qquad \text{(App3-1)}$$

$$\int_{-\infty}^{+\infty}\int_{-\infty}^{+\infty}\psi_s\,dxdy = 1 \qquad \text{(App3-2)}$$

and the following equation governs the propagation of the mode profile through the waveguide at steady state [2-32]:

$$\frac{dP_s(z)}{dz} = \gamma_s P_s \qquad \text{(App3-3)}$$

$$\text{with } \gamma_s = \int_{-\infty}^{+\infty}\int_{-\infty}^{+\infty}\psi_s g_{op}\,dxdy \qquad \text{(App3-4)}$$

$$\text{and } g_{op} = \sigma_{eji}N_j - \sigma_{aji}N_i \qquad \text{(App3-5)}$$

in which g_{op} is optical gain.

Noise which is produced by spontaneous emission can be amplified with stimulated emission and the equation .Equation (App3-3) not only governs the field at frequency also governs noise but we should note that noise is a wide band signal .In order to model the noise we can divide the band (l=1,2,3,…,M) .Noise is propagating in two directions ,one is through the positive direction of z and the negative direction of z. These two waves ,ASE+ ,ASE- (Amplified Spontaneous Emission),are being amplified through the waveguide. The equation governing ASE are as follow:[2-24]

$$\frac{dP_{ASE\pm}(z,\nu_l)}{dz} = \pm[\gamma_e(z,\nu_l) - \gamma_a(z,\nu_l)]P_{ASE\pm}(z,\nu_l) \pm mh\Delta\nu_l\gamma_e(z,\nu_j) \qquad \text{(App3-6)}$$

The first sentence declares the amplification of the noise and the second one is the noise production in z . The coefficient are as :

$$\gamma_e = \iint_A \psi_s(x,y)\sigma_{eji}N_j dxdy \qquad \text{(App3-7)}$$

$$\gamma_a = \iint_A \psi_s(x,y)\sigma_{aij}N_i dxdy \qquad \text{(App3-8)}$$

The stimulated emission and absorption transition rates of signal and pump are given by,

$$W_{12} = \frac{\sigma_{a12}(\nu_s)}{h\nu_s}I_s + \sum_{m=1}^{M}\frac{\sigma_{a12}(\nu_m)}{h\nu_m}\left[I_{ASE+}(x,y,z,t,\nu_m) + I_{ASE-}(x,y,z,t,\nu_m)\right] \qquad \text{(App3-9)}$$

$$W_{21} = \frac{\sigma_{e21}(\nu_s)}{h\nu_s}I_s + \sum_{m=1}^{M}\frac{\sigma_{e21}(\nu_m)}{h\nu_m}\left[I_{ASE+}(x,y,z,t,\nu_m) + I_{ASE-}(x,y,z,t,\nu_m)\right] \qquad \text{(App3-10)}$$

$$R_{13} = \frac{\sigma_{a13}(\nu_p)}{h\nu_p}I_p \qquad \text{(App3-11)}$$

$$R_{31} = \frac{\sigma_{e31}(\nu_p)}{h\nu_p}I_p \qquad \text{(App3-12)}$$

$$R_{12}^{Yb} = \frac{\sigma_{a12}^{Yb}(\nu_p)}{h\nu_p}I_p \qquad \text{(App3-13)}$$

$$R_{21}^{Yb} = \frac{\sigma_{e21}^{Yb}(\nu_p)}{h\nu_p}I_p \qquad \text{(App3-14)}$$

where h is Plank constant. M is the number of slot frequencies of width $\Delta\nu_j$, centered at frequencies ν_j, required for modeling of (Amplified Spontaneous Emission)

$ASE\pm$ noise [2-32]. $I_s(x,y,z,t)$, $I_p(x,y,z,t)$ and $I_{ASE\pm}(x,y,z,t,\nu_j)$ represent in order the signal, pump (co-propagate) and $ASE\pm$ intensities, at frequencies ν_s , ν_p and ν_j. The steady-state variation of pump, signal and $ASE\pm$ powers along the waveguide are given by [2-32],

$$\frac{dP_p}{dz} = -\gamma_p(z)P_p(z) \qquad \text{(App3-15)}$$

$$\frac{dP_s(z,\nu_s)}{dz} = [\gamma_{21}(z) - \gamma_{12}(z)]\ P_s(z,\nu_s) \qquad \text{(App3-16)}$$

$$\frac{dP_{ASE\pm}(z,\nu_j)}{dz} = \pm[\gamma_{21}(z,\nu_j) - \gamma_{12}(z,\nu_j)]P_{ASE\pm}(z,\nu_j) \pm 2h\Delta\nu_j\gamma_{21}(z,\nu_j)$$

$$j=1, 2, \ldots M \qquad \text{(App3-17)}$$

with the boundary conditions:

$$P_p(0) = P_{p0}, P_s(0,\nu_s) = P_{s0}\ ,\ P_{ASE+}(0,\nu_j) = P_{ASE-}(L,\nu_j) = 0 \qquad \text{(App3-18)}$$

in which L is the waveguide length and m is number of guided modes at signal wavelength, by taking into account two different polarizations (for single mode, this factor will be equal to 2). P_{p0} and P_{s0} are input pump power and input signal power, respectively. The pump and signal absorption and emission coefficients $\gamma_p(z)$,$\gamma_{12}(z,\nu_j)$ and $\gamma_{21}(z,\nu_j)$ appear in the propagation equations are given by,

$$\gamma_p = \gamma_{pEr} + \gamma_{PYb} \qquad \text{(App3-19)}$$

$$\gamma_{pEr} = \iint_A \psi_p(\sigma_{a13}N_1 - \sigma_{e31}N_3)dxdy \qquad \text{(App3-20)}$$

$$\gamma_{pYb} = \iint_A \psi_p(\sigma_{a12}^{Yb}N_1^{Yb} - \sigma_{e21}^{Yb}N_2^{Yb})dxdy \qquad \text{(App3-21)}$$

$$\gamma_{12} = \iint_A \psi_s \sigma_{a12}(\nu_j) N_1 dxdy \qquad \text{(App3-22)}$$

$$\gamma_{21} = \iint_A \psi_s \sigma_{e21}(\nu_j) N_2 dxdy \qquad \text{(App3-22)}$$

where A is the area of the active region, and $\psi_p(x,y), \psi_s(x,y)$ are the normalized pump and signal intensities. The background is neglected loss. These normalized intensities can be obtained by Maxwell equations using, for example, effective index, finite difference or finite element methods [2-35].

Appendix-4

Prism coupling method

To measure the refractive index and the thickness of the thin transparent dielectric films we commonly use prism coupling technique. In this technique laser light couples into a planner waveguide through the interface between the prism and the film .It can also be applied to the small layer produced by ion exchange which has a different refractive index. The prism coupler applies the principal of distributed coupling through evanescent fields to the guided modes of the slab waveguides. A prism, Whose refractive index is n_p, is placed above a slab waveguide and is separated from it by a small air-gap, which has refractive index n_a. When a plane wave with an incident angle θ enters the prism, the refracted plane wave propagates at an angle ϕ with respect to the normal of the prism base. Total internal reflection occurs at the prism base if

$$\phi > \phi_c = Sin^{-1}(n_a / n_p) \quad \text{[App4-1]}$$

where is the critical angle of total internal reflection. Under the above mentioned condition, the superposition of the incident wave and the reflected wave in the prism yields a standing wave in the vertical direction of the prism base. But in the air-gap, an evanescent field decaying exponentially is generated. The waves in the prism and in the slab waveguide are coupled through their evanescent field in the air-gap. The field amplitudes are as indicated in figure [App4-1]. The coupler permits excitation for each of guided modes by proper orientation of the direction of the incident beam. The energy

interchanged through the evanescent field coupling is complete only if the components of the wave vectors parallel to the air-gap are equal for the waves in the prism and the wave in the slab waveguide. That is

$$k_p Sin\phi_m = \beta_m \qquad \text{[App4-2]}$$

where $k_p = k * n_p$, and k is propagation constant in vacuum, $\beta_m = k * N_m$ is propagation constant for the mth guided mode (m = 0, 1, 2,....), and N_m is the effective refractive index for the mth mode. Condition [App4-1] is also called a phase-matched condition. It determines a set of discrete angles ϕ_m (m = 0, 1, 2, ...) corresponding to the guided modes.

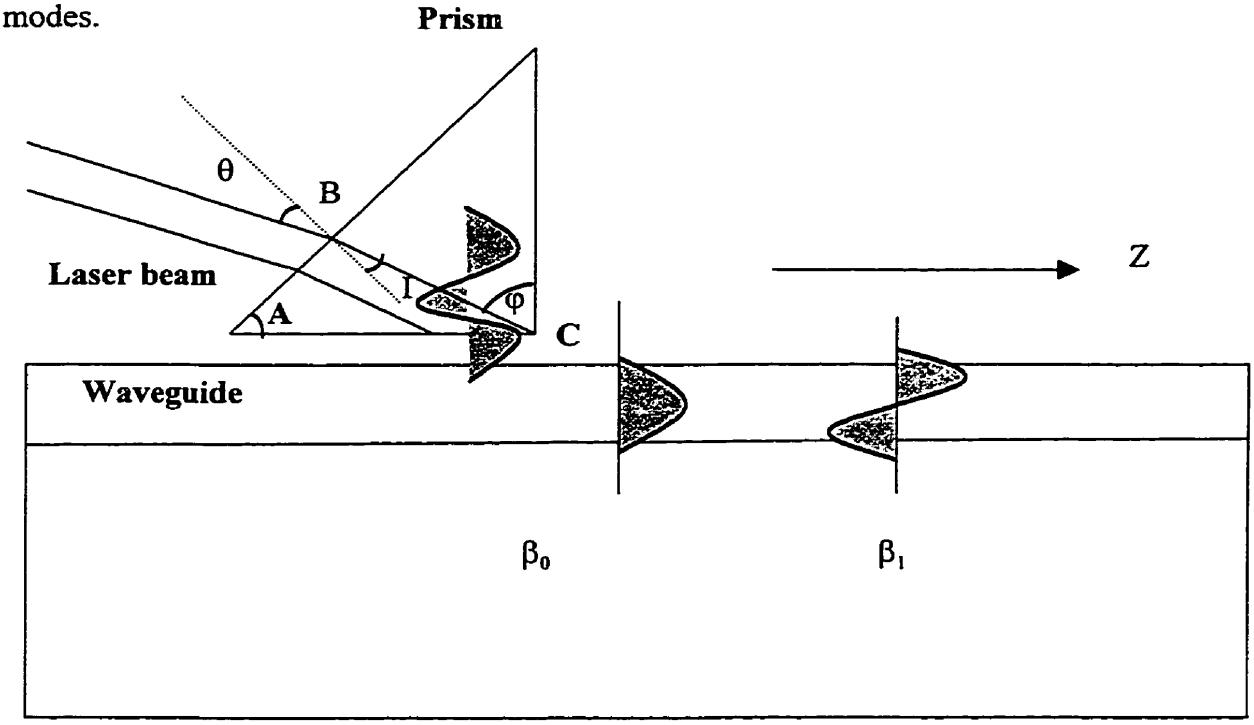

Figure App4-1 .Prism coupling method.

In addition, the maximum coupling from incident energy into a guided mode

requires that the right hand beam boundary in the prism intersects the prism corner, as shown in figure [App4-1] . By some simple manipulation, it is easy to relate the angles ϕ_m in [App4-2] to corresponding coupling angleθ_m, which are directly measurable. In the triangle ABC we have:

$[(\pi/2)-\phi)]+A+[(\pi/2)+I]=\pi$ [App4-3]

Therefore , $A+I=\varphi$ and finally using Snell laws for the Air-Prism interface we have ,

$\varphi=[A+\sin^{-1}(Sin\theta/n_p)]$ [App4-4]

From Measured θ_m the effective refractive indices for guided modes can be calculated by $N_m=n_p * Sin[A+Sin^{-1}(Sin\theta_m/n_p)]$ [App4-5]

where A is the base angle of the prism.

The experimental set-up for the measurement of coupling angles And the measurements are explained in chapter3 .